Computing atomic nuclei based on Chiral EFT and HALQCD interactions

Carlo Barbieri
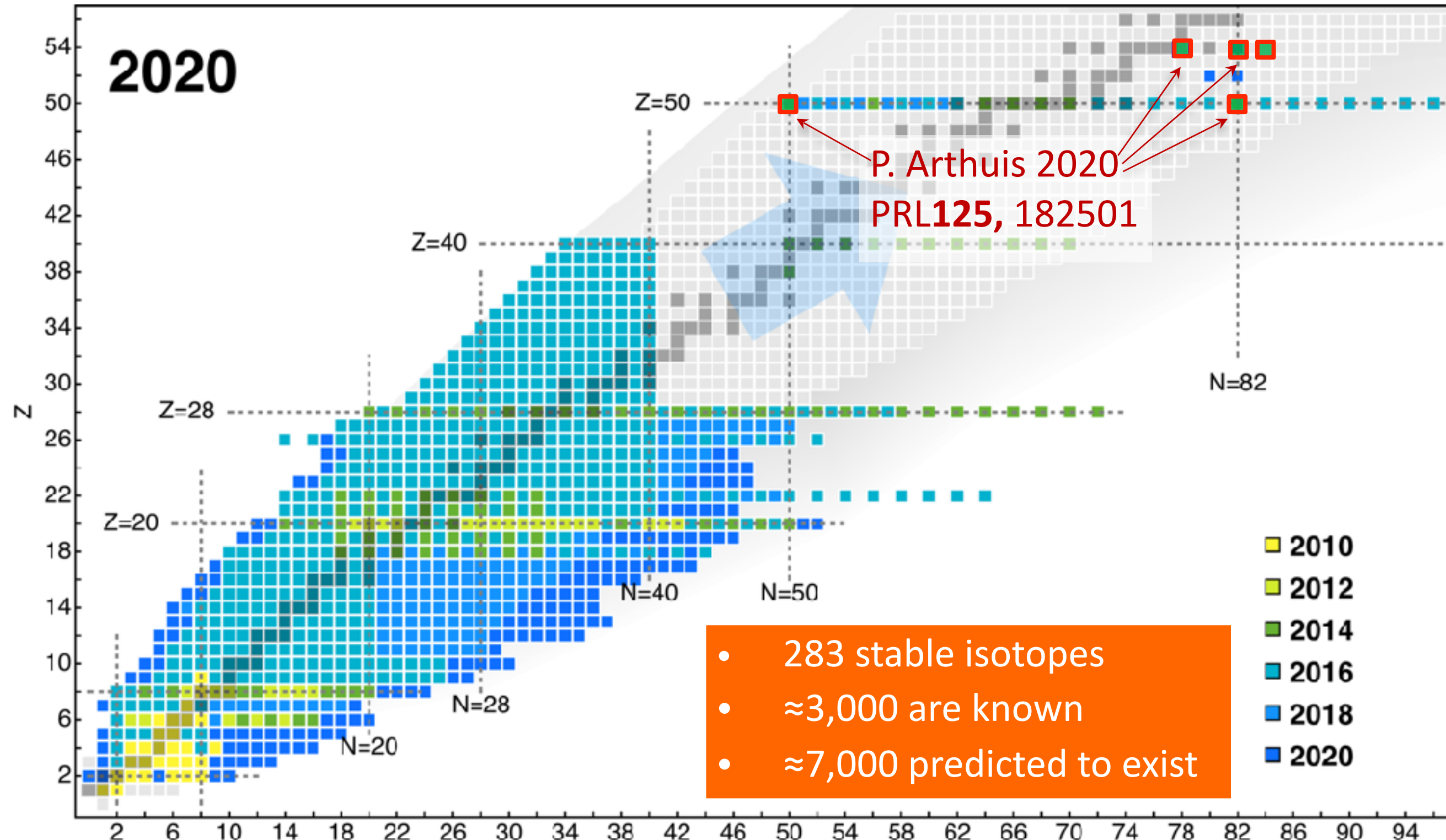
- HAL QCD and nuclei

- Results with ChEFT

- Diagrammatic Monte Carlo
  (for nuclei, eventually...)

The Nuclear Interaction: Post-Modern Developments   August 19-23, 2024
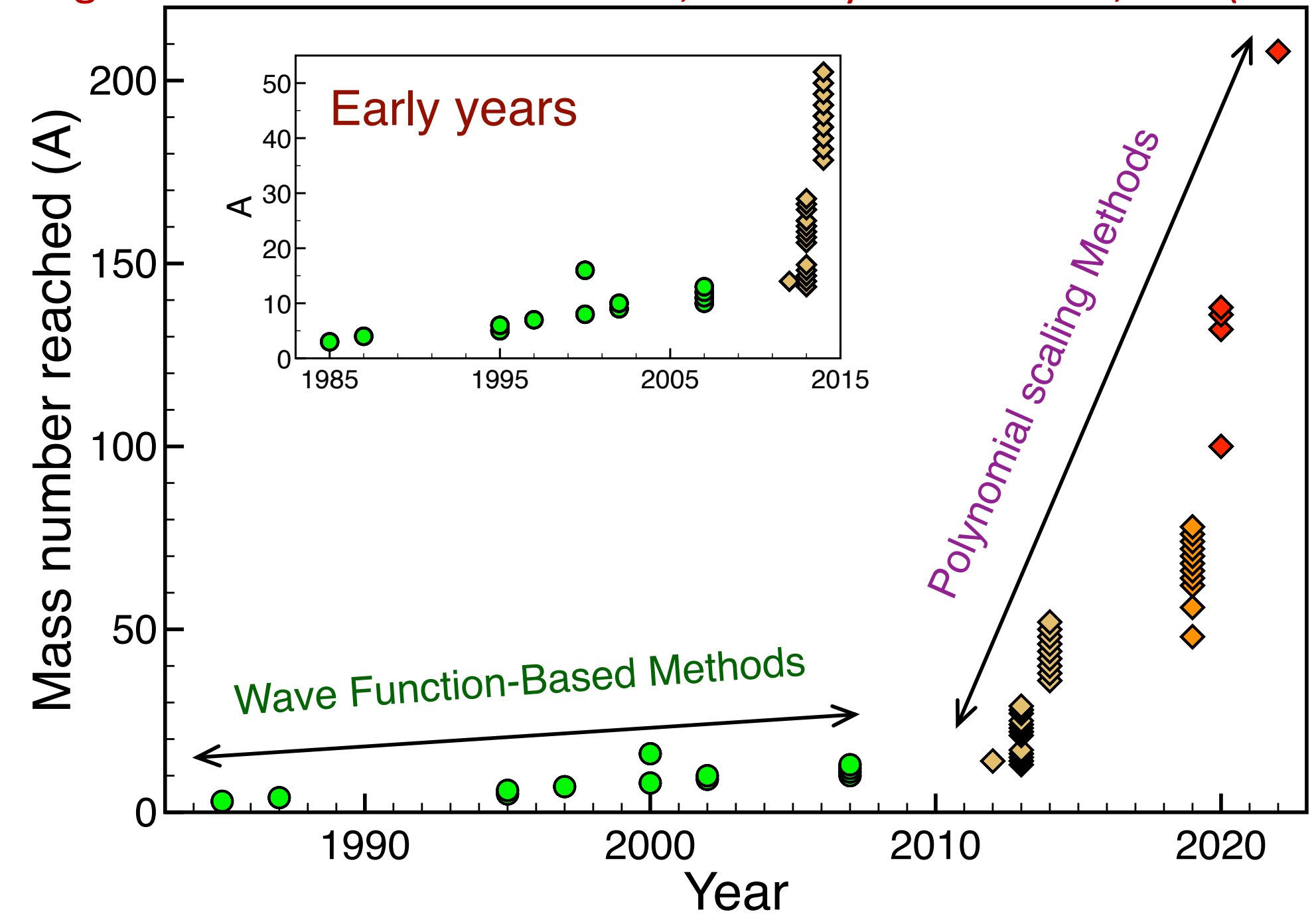
Reach of ab initio methods across the nuclear chart

Extension beyond few-nucleons thanks to:

- Soft (nearly perturbative) effective nuclear forces

- Diagrammatic many-body approaches

2020

P. Arthuis 2020
PRL**125,** 182501

Z=50
Z=40
Z=28
Z=20
N=82
N=50
N=40
N=28
N=20

- 283 stable isotopes
- ≈3,000 are known
- ≈7,000 predicted to exist

2010
2012
2014
2016
2018
2020

Mass number reached (A)

Early years

A

Polynomial scaling Methods

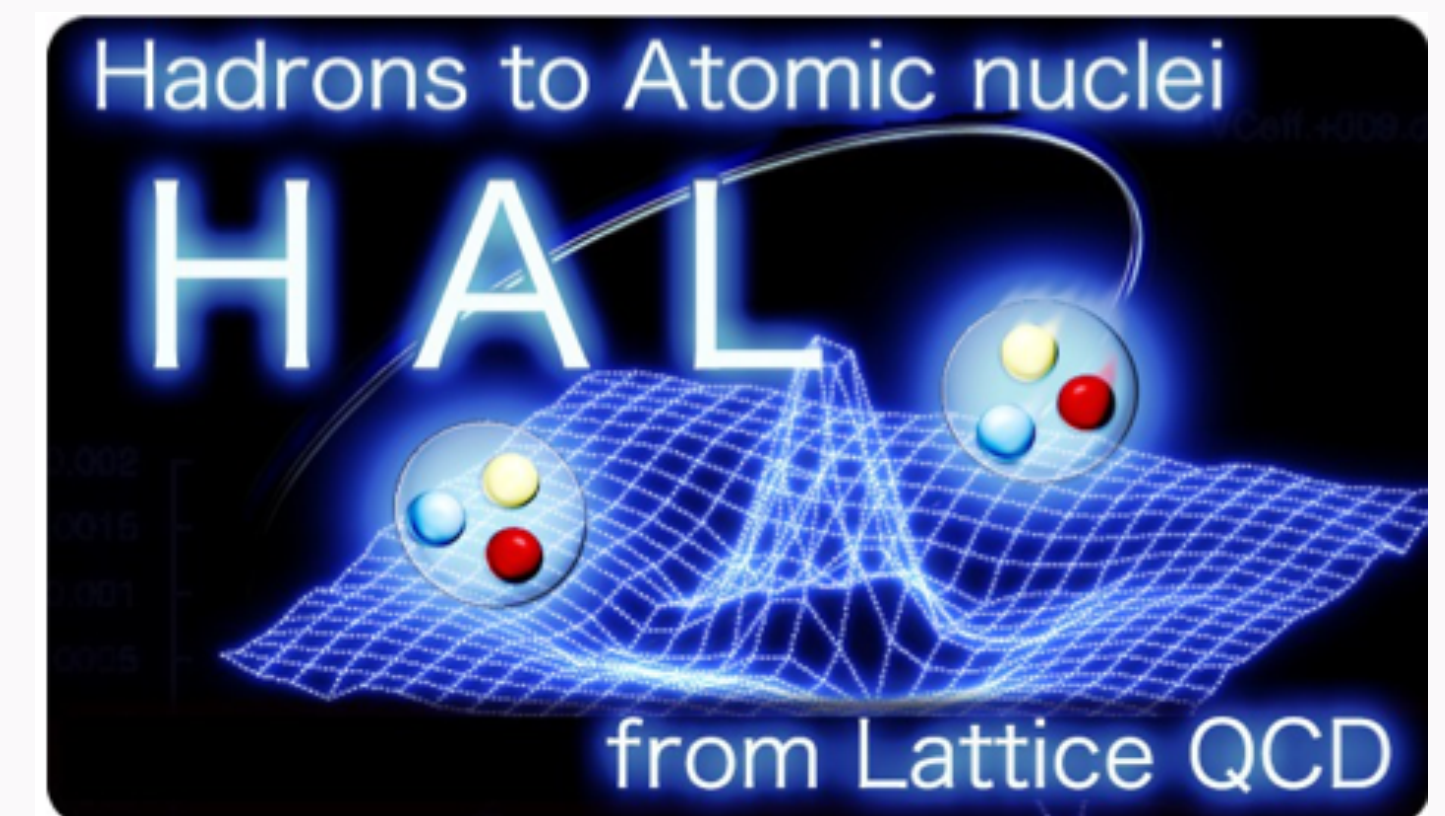Wave Function-Based Methods

Year

Open challenges:

- Accuracy (better theory of nuclear forces)

- Mass number limit (optimised model spaces)

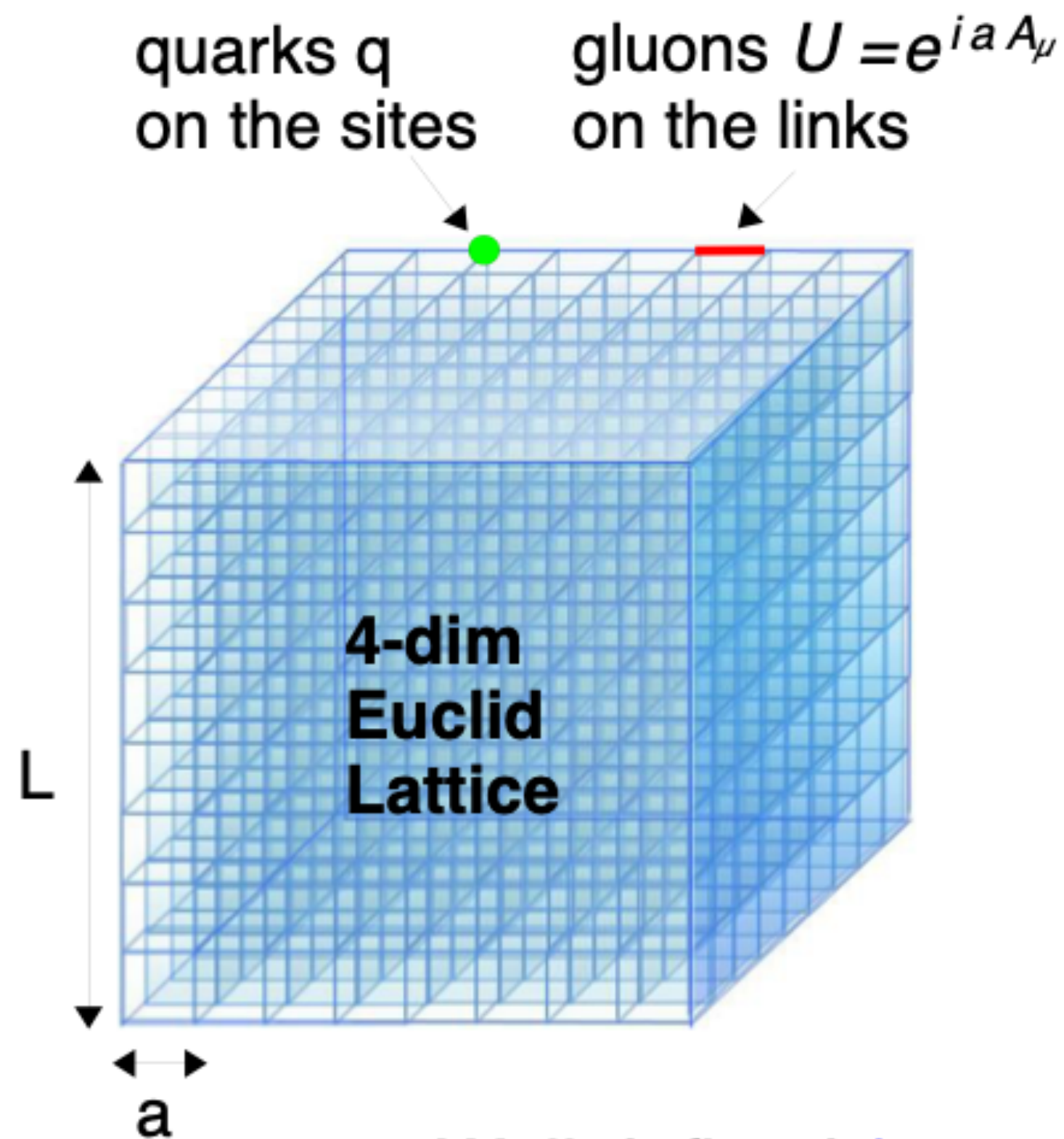- Precision & scattering (high-order diag. resummations)

H. Hergert, Frontiers in Phys **8**, 379 (2020)
L. Coraggio, S. Pastore, **CB**, Frontiers in Phys **8**, 626976 (2021)

INFN
MILANO

Nuclei with HAL QCD forces

C. McIlroy, CB et al. Phys. Rev. C**97**, 021303(R) (2018)
D. Lonardoni et al. - in preparation

In collaboration with:

UNIVERSITÀ DEGLI STUDI DI MILANO
DIPARTIMENTO DI FISICA

Lattice QCD

$$L = -\frac{1}{4}G^a_{\mu\nu}G^{\mu\nu}_a + \bar{q}\,\gamma^\mu\left(i\,\partial_\mu - g\,t^a\,A^a_\mu\right)q - \bar{m}\,q\,q$$

quarks q
on the sites

gluons $U = e^{i a A_\mu}$
on the links

4-dim Euclid Lattice

L

a

Vacuum expectation value

$$\langle O(q,q,U)\rangle$$

path integral

$$= \int dU\, d\bar{q}\, dq\; e^{-S(q,q,U)}\, O(q,q,U)$$

$$= \int dU\, \det D(U)\, e^{-S_U(U)}\, O(D^{-1}(U))$$

quark propagator

$$= \lim_{N\to\infty}\frac{1}{N}\sum_{i=1}^{N} O(D^{-1}(U_i))$$

{ U_i } : ensemble of gauge conf. U
generated w/ probability $\det D(U)\, e^{-S_U(U)}$

✸ Well defined (reguralized)   ✸ Fully non-perturvative
✸ Manifest gauge invariance   ✸ Highly predictive

Slide, courtesy of T. Inoue (YITP talk, Oct. 8th 2015)

The HAL-QCD Method

Define a general potential U(**r**,**r'**) which is and non-local but energy independent up to inelastic threshold, such that:

$$\frac{-\nabla^2}{2\mu}\varphi_{\vec{k}}(\vec{r}) + \int d\vec{r}' U(\vec{r},\vec{r}')\varphi_{\vec{k}}(\vec{r}') = E_{\vec{k}}\varphi_{\vec{k}}(\vec{r})$$

for the Nambu-Bethe-Salpeter (NBS) wave function, $\varphi_{\vec{k}}(\vec{r}) = \sum \langle 0|B_i(\vec{x}+\vec{r},t)B_j(\vec{x},t)|B=2,\vec{k}\rangle$

Operationally, measure the 4-pt function on the QCD Lattice

$$\psi(\vec{r},t) = \sum_{\vec{x}}\langle 0|B_i(\vec{x}+\vec{r},t)B_j(\vec{x},t)\,J(t_0)|0\rangle = \sum_{\vec{k}}A_{\vec{k}}\varphi_{\vec{k}}(\vec{r})e^{-W_{\vec{k}}(t-t_0)} + \dots$$

and extract U(**r**,**r'**) from:

$$\left\{2M_B - \frac{\nabla^2}{2\mu}\right\}\psi(\vec{r},t) + \int d\vec{r}' U(\vec{r},\vec{r}')\psi(\vec{r}',t) = -\frac{\partial}{\partial t}\psi(\vec{r},t)$$

A *local potential* V(**r**) is then obtained through a derivative expansion of U(**r**,**r'**), which *must give the same observables* of the LQCD simulation:

$$U(\vec{r},\vec{r}') = \delta(\vec{r}-\vec{r}')V(\vec{r},\nabla) = \delta(\vec{r}-\vec{r}')\left\{V(\vec{r}) + \mathcal{O}(\nabla) + \mathcal{O}(\nabla^2) + \dots\right\}$$

$$\rightarrow \quad V(\vec{r}) = \frac{1}{2\mu}\frac{\nabla^2\psi(\vec{r},t)}{\psi(\vec{r},t)} - \frac{\frac{\partial}{\partial t}\psi(\vec{r},t)}{\psi(\vec{r},t)} - 2M_B$$
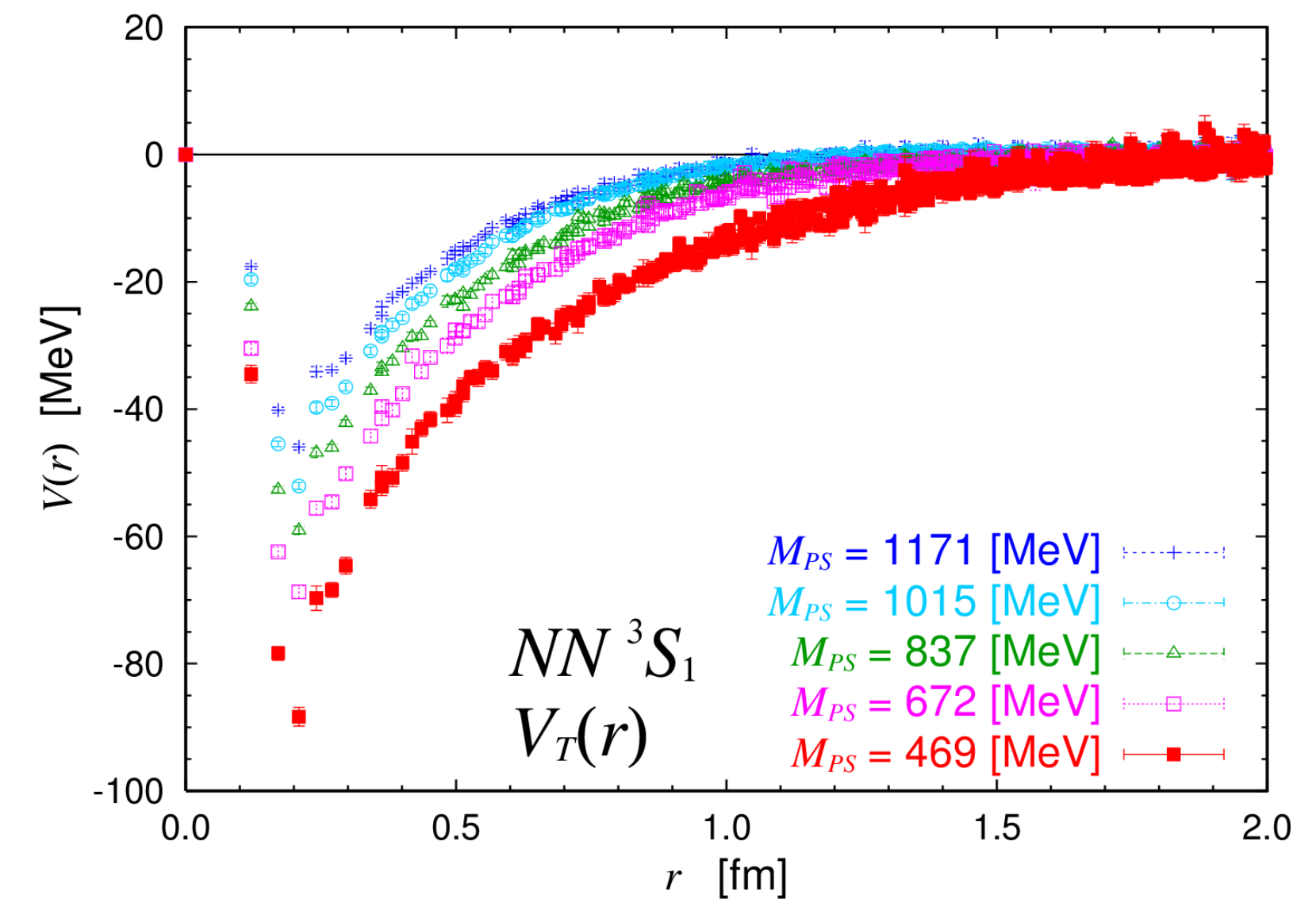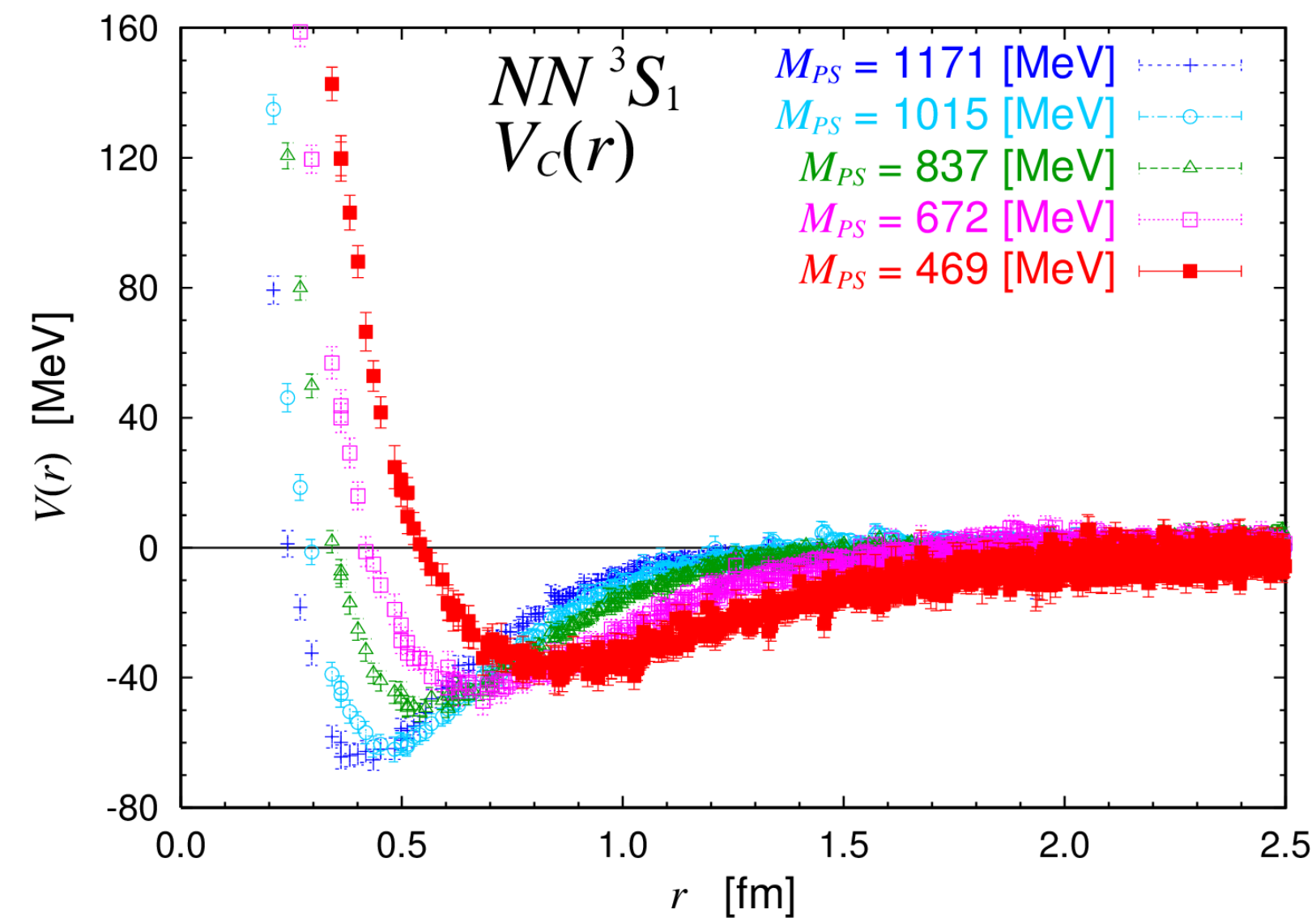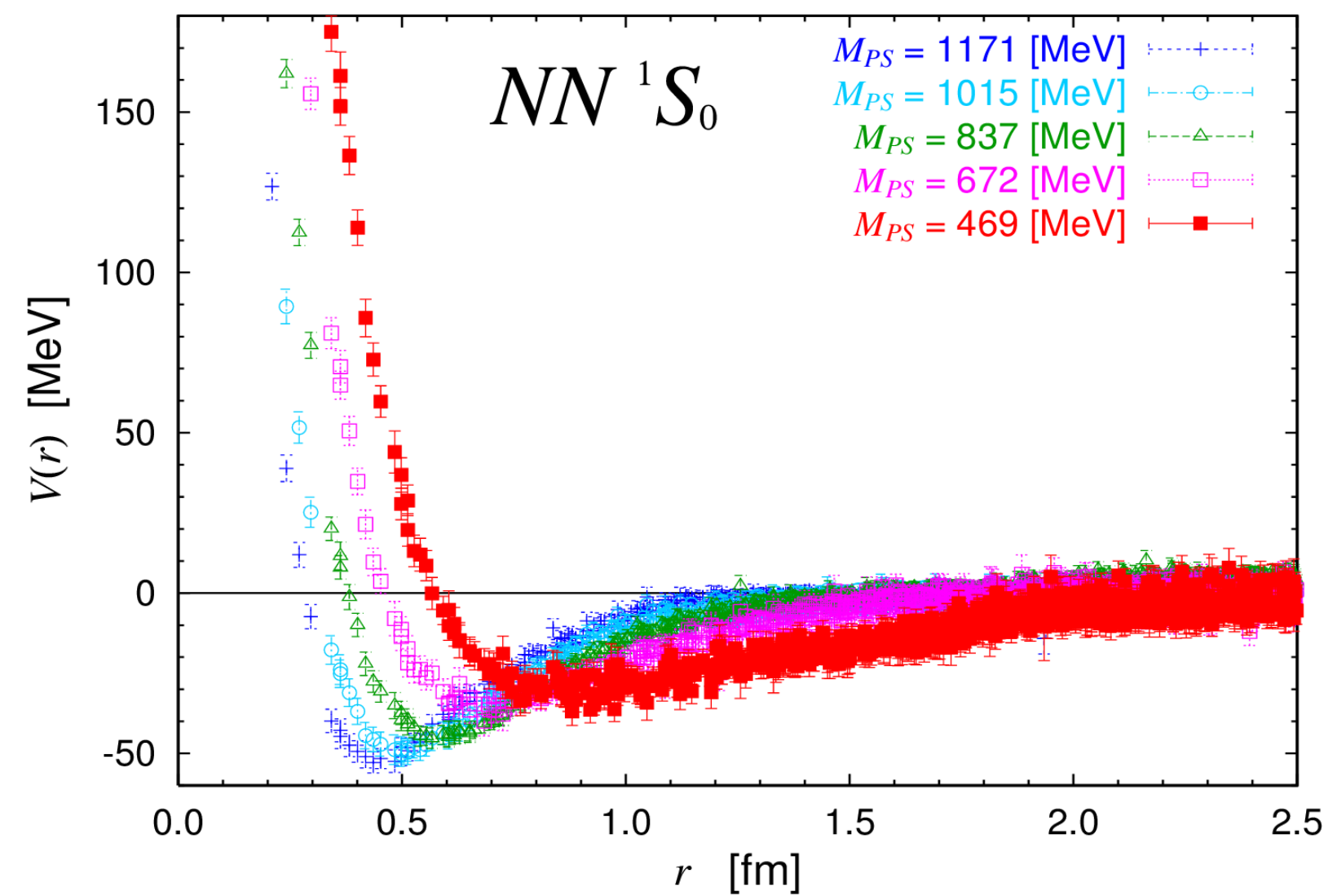
Tensor/Yukawa force in S-D

Spin-orbit force, P waves

Two-Nucleon HAL potentials in flavour SU(3) symm.

Quark mass dependence of $V(r)$ for NN partial wave ($^1S_0$, $^3S_1$, $^3S_1$-$^3D_1$)
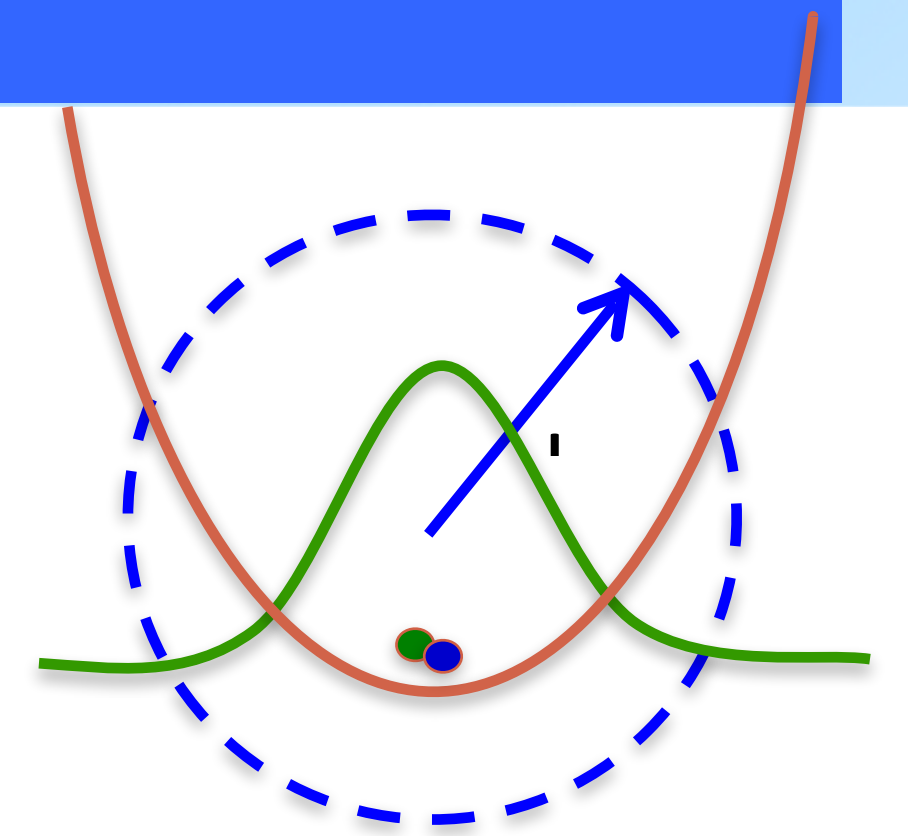
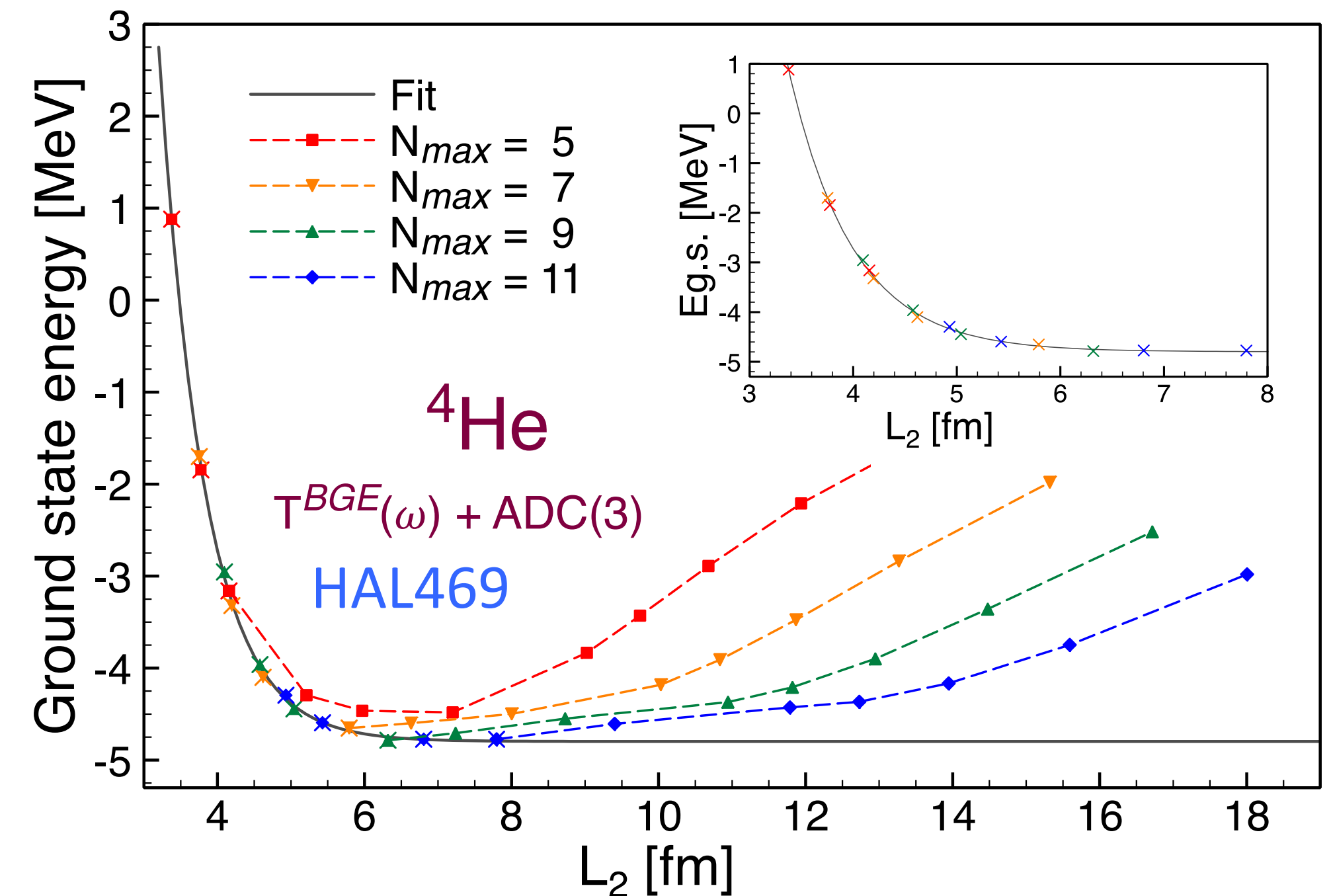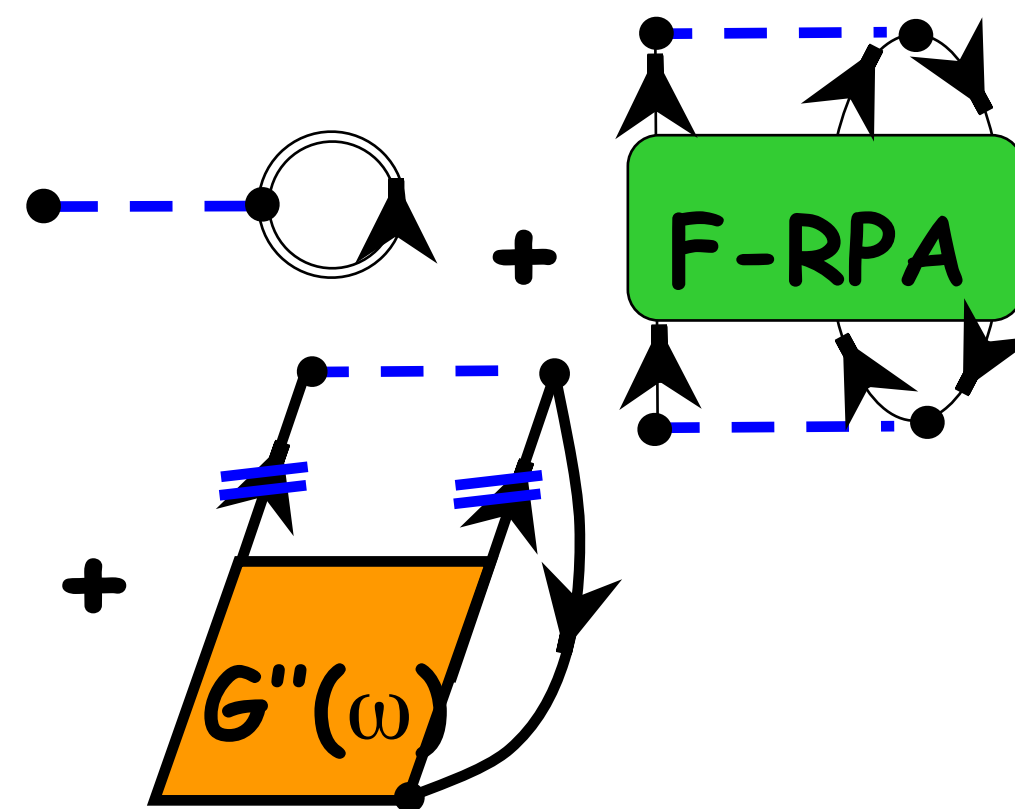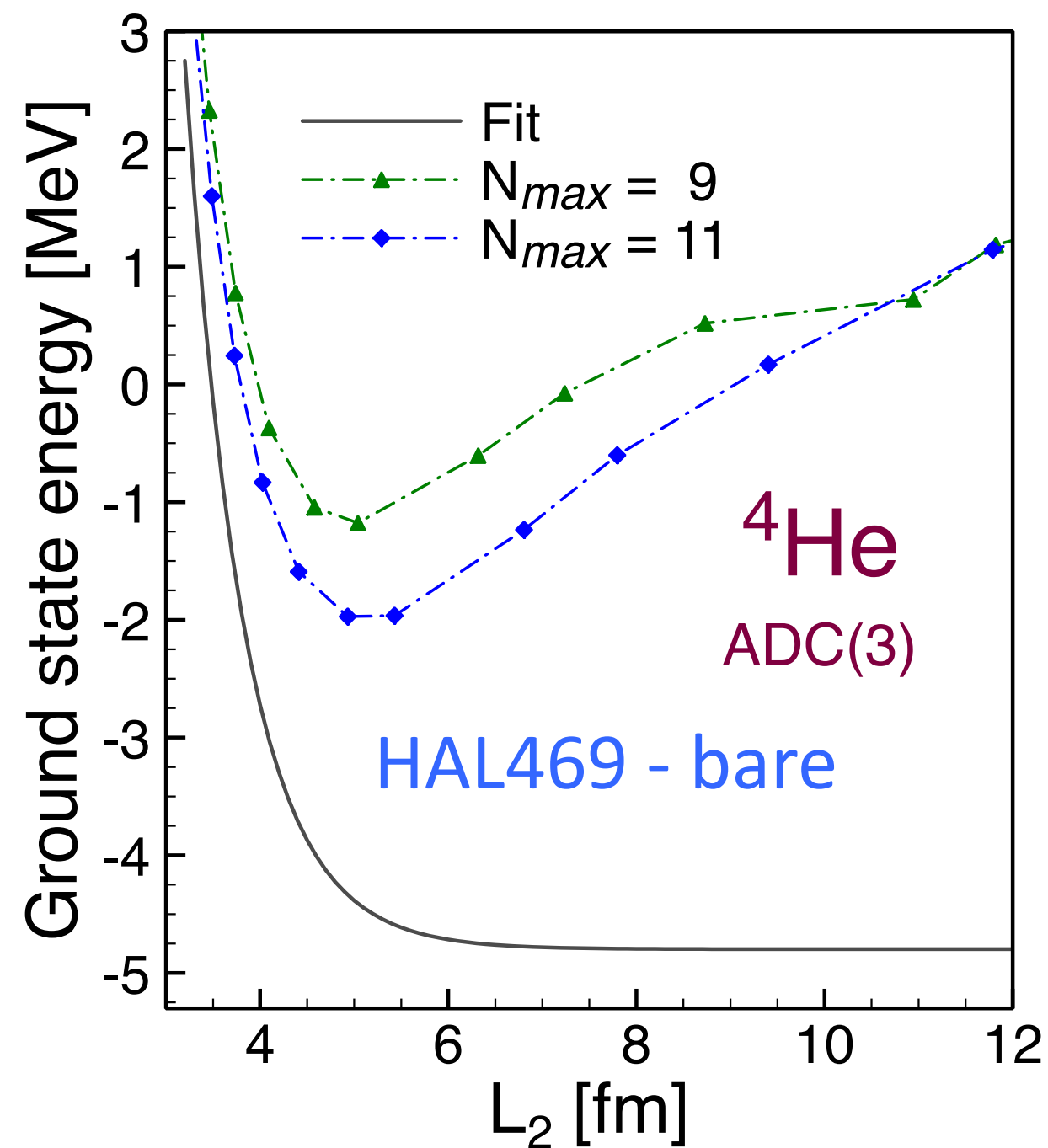➔ Potentials become stronger m_π as decreases.

Infrared convergence

Short-range repulsion in the HALQCD-type potentials
can be tamed correctly even for large nuclei.
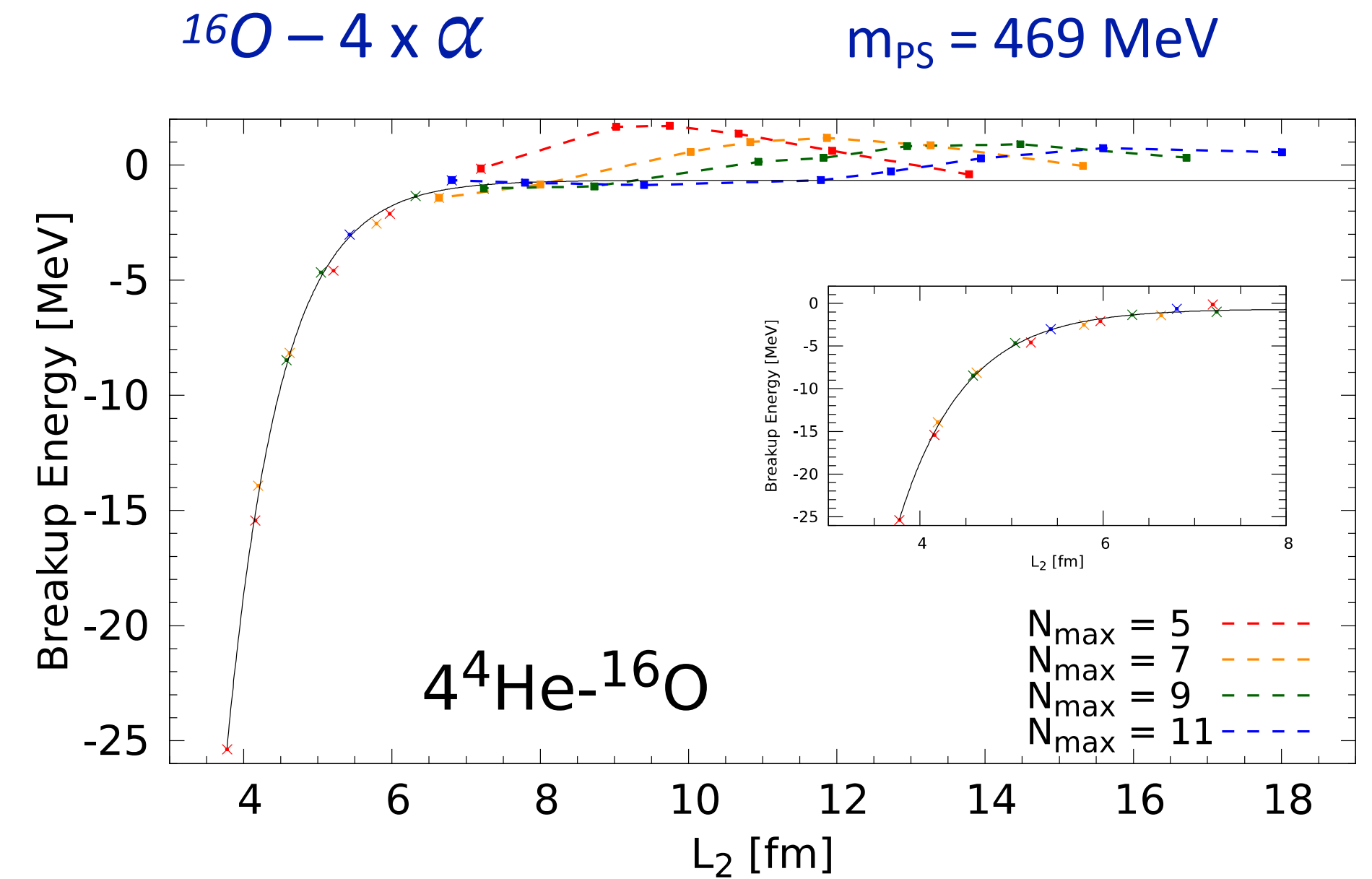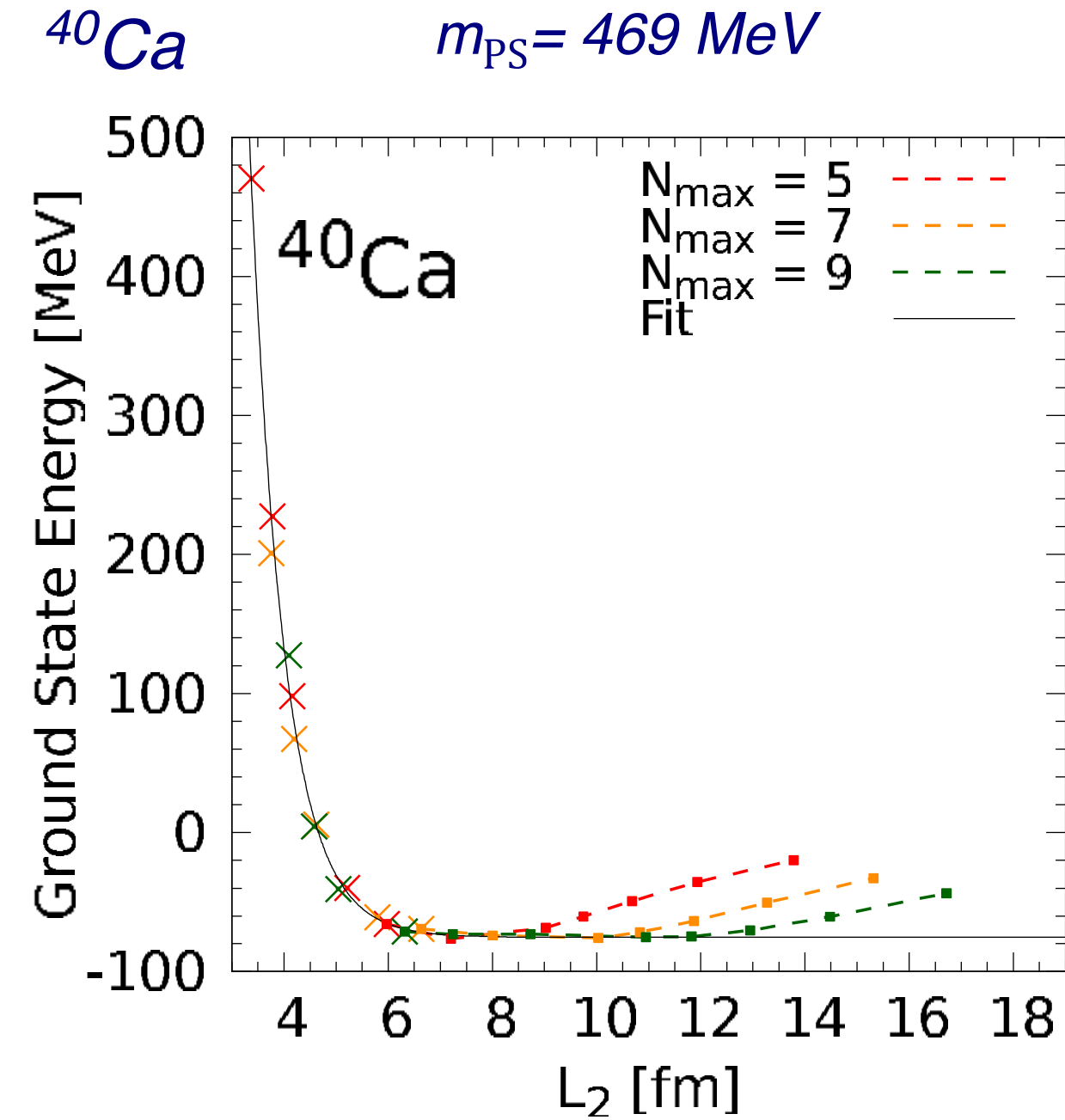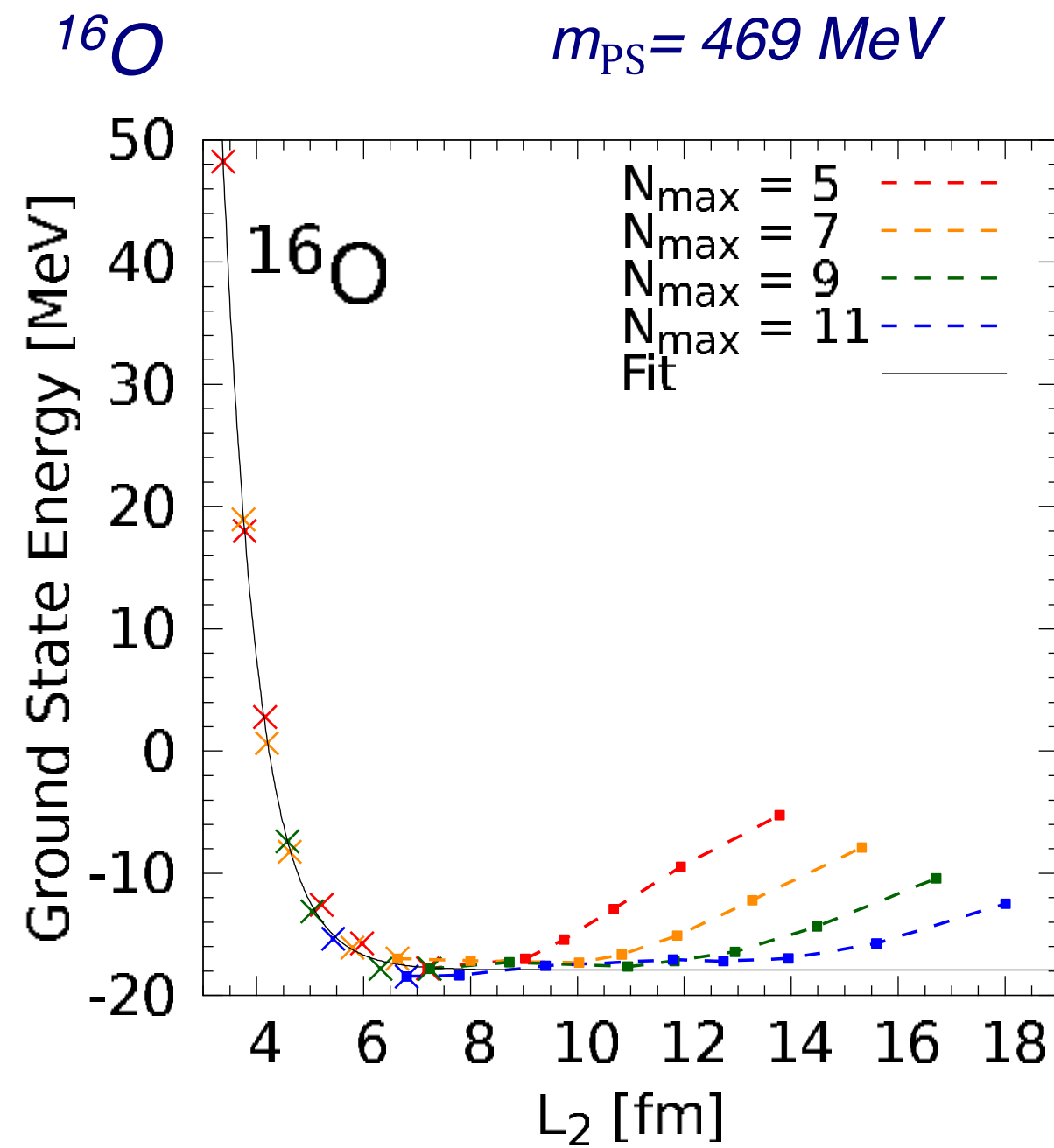C. McIlroy, CB, et al., Phys. Rev. **C97**, 021303(R) (2018)

$$L_2 = \sqrt{2(N + 3/2 + 2)}b$$

Left plot: Ground state energy [MeV] vs L_2 [fm], ^{4}He, ADC(3), HAL469 – bare. Legend: Fit, $N_{max} = 9$, $N_{max} = 11$.

Middle: Diagram: F-RPA + $G''(\omega)$

Right plot: Ground state energy [MeV] vs L_2 [fm], ^{4}He, $T^{BGE}(\omega)$ + ADC(3), HAL469. Legend: Fit, $N_{max} = 5$, $N_{max} = 7$, $N_{max} = 9$, $N_{max} = 11$. Inset: Eg.s. [MeV] vs L_2 [fm].

Binding of ^{16}O and ^{40}Ca:

^{16}O m_{PS} = 469 MeV

^{40}Ca m_{PS} = 469 MeV

$^{16}O - 4 \times \alpha$ m_{PS} = 469 MeV

$4^4He-^{16}O$

Binding energies are ~17 MeV ^{16}O and 70-75MeV for ^{40}Ca. Possibly being underestimated by 10%

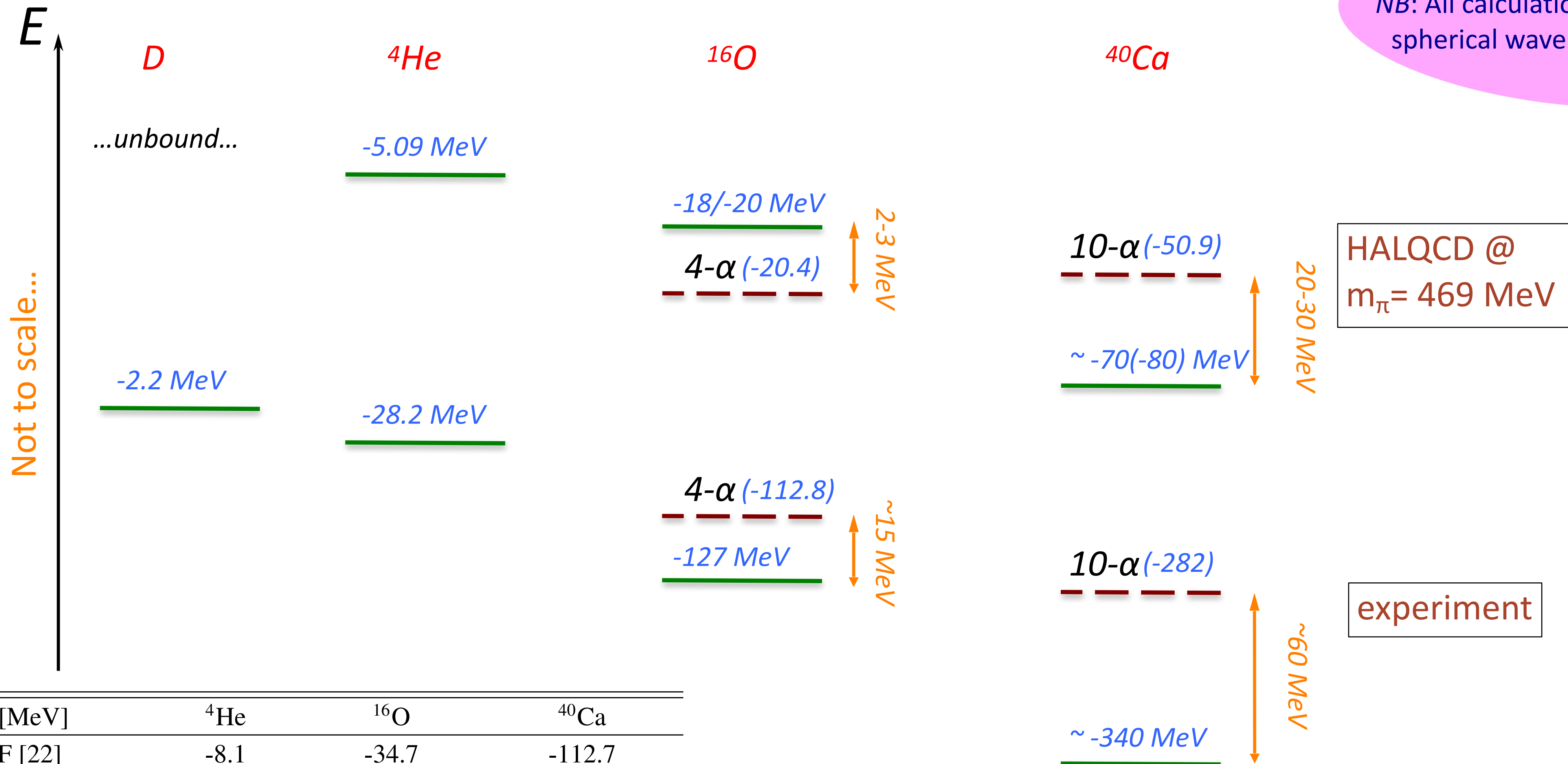➜ ^{16}O at $m_\pi \approx$ 470 MeV is unstable toward 4-α breakup!

C. McIlroy, CB, et al., Phys. Rev. C**97**, 021303(R) (2018)

E_0^A [MeV]	^4He	^{16}O	^{40}Ca
BHF [22]	-8.1	-34.7	-112.7
G(ω) + ADC(3)	-4.80(0.03)	-17.9 (0.3) (1.8)	-75.4 (6.7) (7.5)
Exact Result [51]	-5.09	–	–
Separation into ^4He clusters:		-2.46 (0.3) (1.8)	24.5 (6.7) (7.5)

UNIVERSITÀ DEGLI STUDI DI MILANO
DIPARTIMENTO DI FISICA

UNIVERSITY OF SURREY

NB: All calculations assuming spherical wave functions...

E

D ^4He ^{16}O ^{40}Ca

Not to scale...

...unbound...

-5.09 MeV

-18/-20 MeV

2-3 MeV

4-α (-20.4)

10-α (-50.9)

HALQCD @ m_π = 469 MeV

-2.2 MeV

-28.2 MeV

~ -70(-80) MeV

20-30 MeV

4-α (-112.8)

-127 MeV

~15 MeV

10-α (-282)

experiment

~ -340 MeV

~60 MeV

E_0^A [MeV]	^{4}He	^{16}O	^{40}Ca
BHF [22]	-8.1	-34.7	-112.7
G(ω) + ADC(3)	-4.80(0.03)	-17.9 (0.3) (1.8)	-75.4 (6.7) (7.5)
Exact Result [51]	-5.09	–	–
Separation into ^{4}He clusters:		-2.46 (0.3) (1.8)	24.5 (6.7) (7.5)

UNIVERSITÀ DEGLI STUDI DI MILANO
DIPARTIMENTO DI FISICA

C. McIlroy, CB, et al., Phys. Rev. **C97**, 021303(R) (2018)

UNIVERSITY OF SURREY

- Physical mass now under reach ($m_\pi \approx 145$ MeV) for hyperons

- Need to improve on statistic for the NN sector
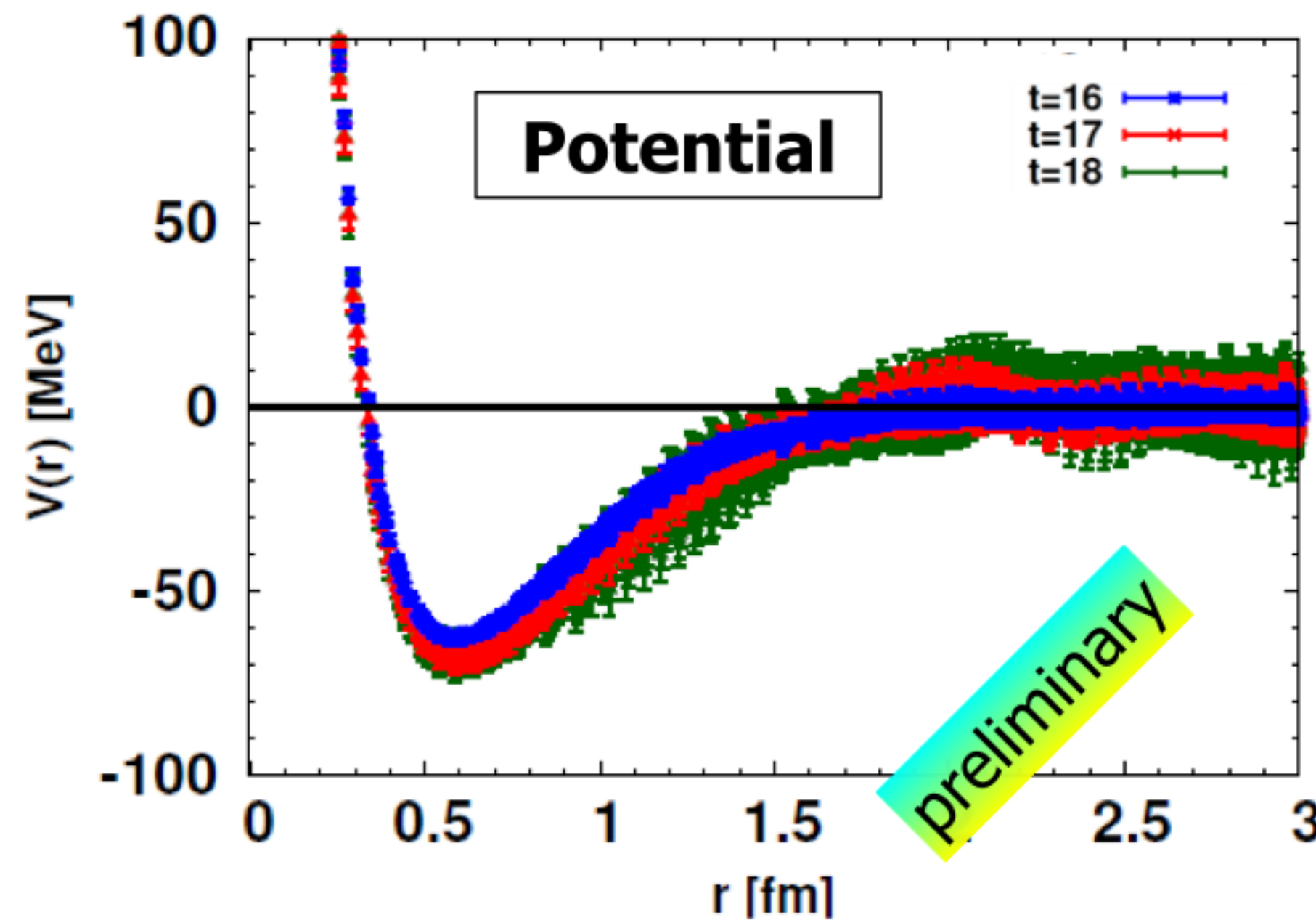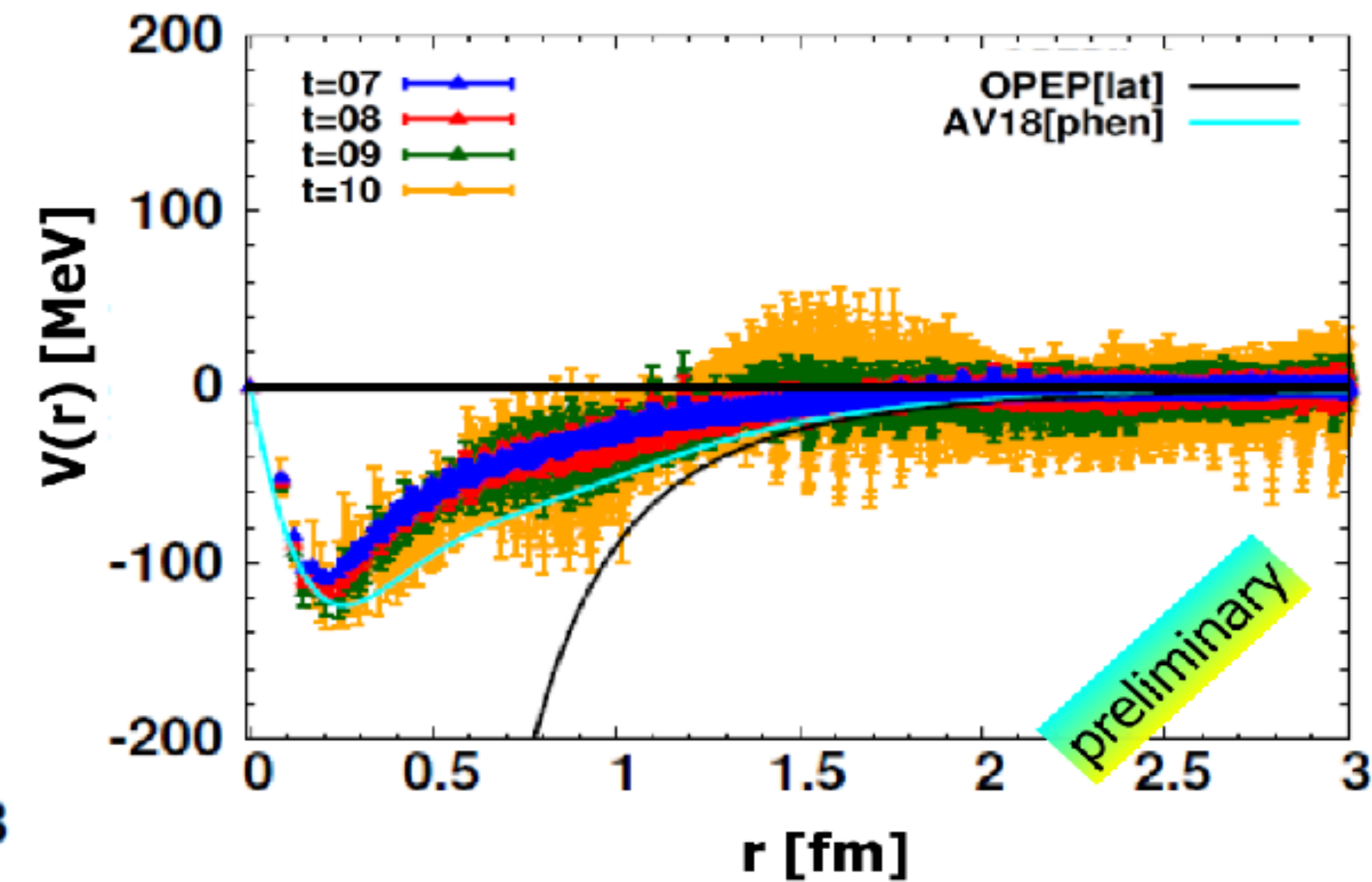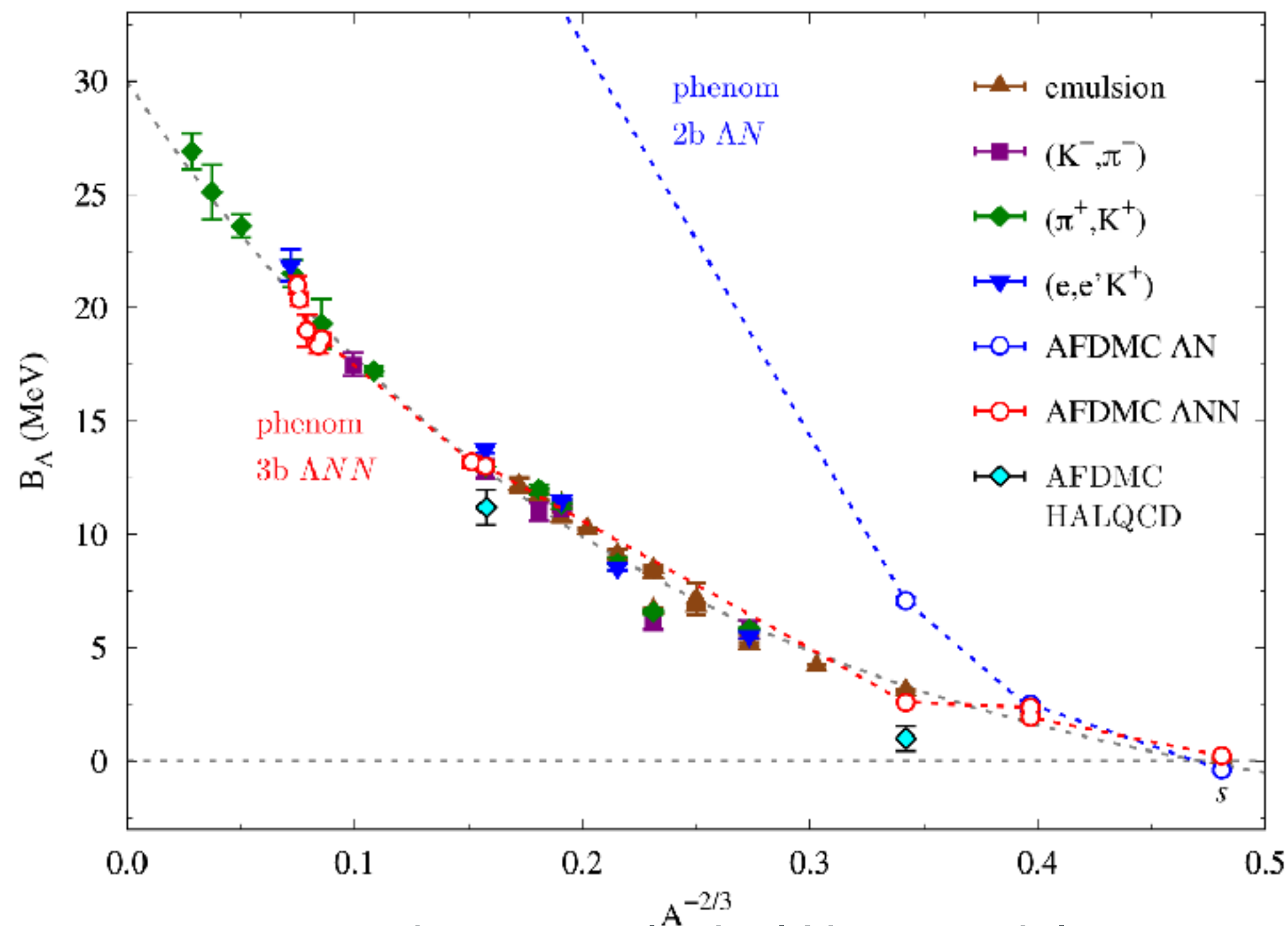

Slides from *S. Aoki* at Kavli institute, Oct. 2016

S. Aoki, T. Doi, Front. Phys. 8:307 (2020).

- AV4' + UIX with phenomenological hypernuclear forces requires large ΛNN 3-baryon force

- Physical mass now under reach ($m_\pi \approx 145$ MeV) for hyperons

- HALQCD ΛN 3-baryon force is already very close to experiment

$$H = -\frac{\hbar^2}{2m_N}\sum_i \nabla_i^2 + \sum_{i<j} v_{ij} + \sum_{i<j<k} V_{ijk} - \frac{\hbar^2}{2m_\Lambda}\nabla_\Lambda^2 + \sum_i v_{i\Lambda}$$

Argonne v_4' (AV4') nucleon-nucleon (NN) interaction $\quad v_{ij} = \sum_{p=1,4} v^p(r_{ij})\, O_{ij}^p$

central component of the Urbana IX (UIX$_c$) $\quad V_{ijk} = A_R \sum_{cyc} T^2(m_\pi r_{ij})\, T^2(m_\pi r_{ik})$

The hyperon-nucleon (YN) potential $\quad v_{i\Lambda} = \sum_{p=c,\sigma,t} v^p(r_{i\Lambda})\, O_{i\Lambda}^p$

Diffusion Monte Carlo:

$$\langle X|\Psi_T\rangle = \langle X|\left(\prod_{i<j<k} U_{ijk}\right)\left(\prod_{i<j} F_{ij}\right)\left(\prod_i F_{i\Lambda}\right)|\Phi_{J^\pi, J_z, T_z}\rangle, \qquad |\Psi_0\rangle = e^{-(H-E_0)\tau}|\Psi_T\rangle$$

AFDMC:

- - -○- - - : phenomenological NΛ potential

- - -○- - - : phenomenological NΛ + NNΛ potential

◆ : HALQCD NΛ potential

Future application for Ys in nuclei now possible

- AV4' + UIX requires very large with phenomenological hypernuclear forces requires large ΛNN 3-baryon force

- Physical mass now under reach ($m_\pi \approx$ 145 MeV) for hyperons

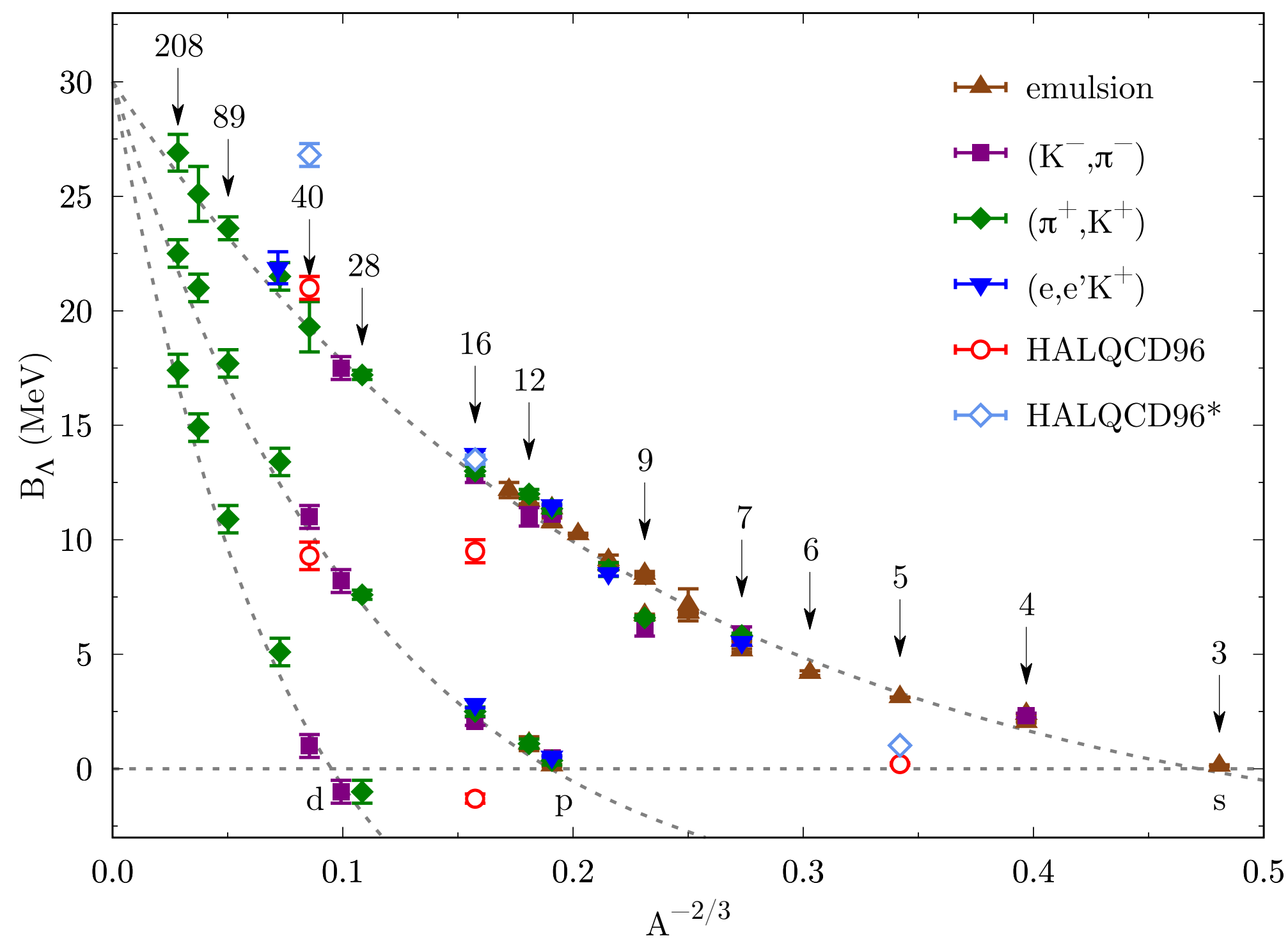- HALQCD ΛN 3-baryon force is already very close to experiment

Table 1: Λ separation energies (in MeV) for different hypernuclei with the hyperon in different single-particle states. Second column reports the AFDMC results using the original HALQCD96 ΛN potential. Third column shows the results for the modified HALQCD96 ΛN potential (see text for details). In the last column, the available experimental data [] are reported.

$^A_\Lambda Z$	J^π (state)	HALQCD96	HALQCD96*	Exp
$^5_\Lambda$He	$1/2^+$ (s)	0.21(5)	1.02(3)	3.12(2)
$^{16}_\Lambda$O	1^- (s)	9.5(5)	13.5(2)	13.4(4)
	2^+ (p)	$-1.3(2)$	0.5(1)	2.5(2)
$^{40}_\Lambda$Ca	2^+ (s)	21.0(5)	26.8(5)	19.3(1.1)
	3^- (p)	9.3(6)	13.7(6)	11.0(5)

UNIVERSITÀ DEGLI STUDI DI MILANO
DIPARTIMENTO DI FISICA
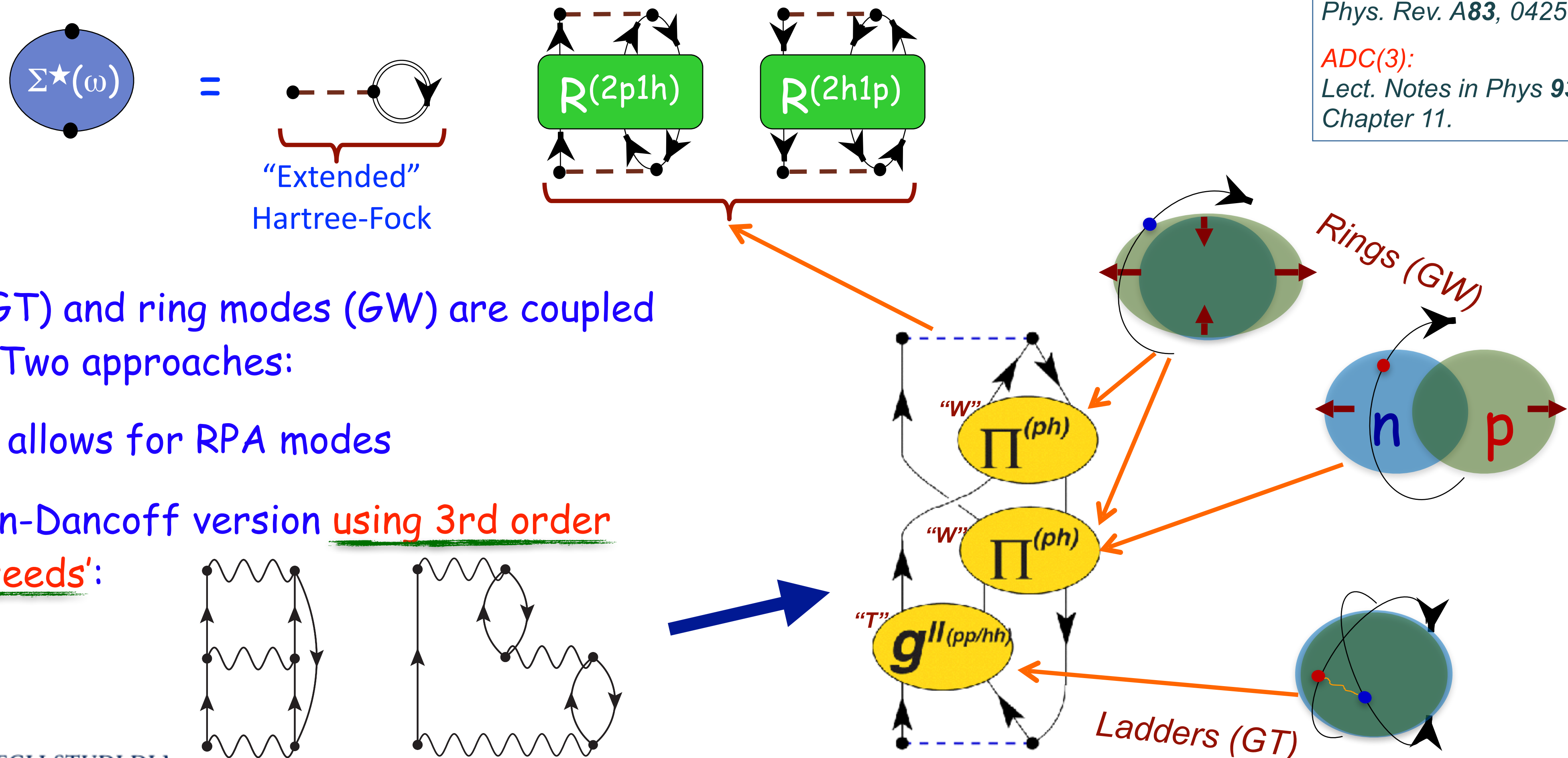
UNIVERSITY OF SURREY

Self-Consistent Green's function computations based
on Chiral EFT interactions (NN+3N forces)

The Faddev-RPA and ADC(3) methods in a few words

Compute the nuclear self energy to extract both scattering (optical potential) and spectroscopy.
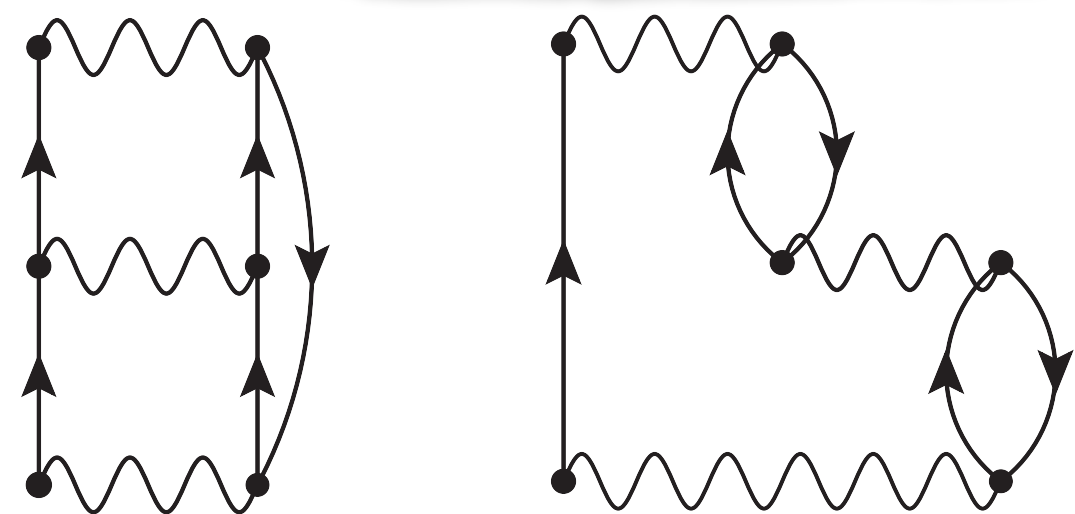Both ladders and rings are needed for atomi nuclei:

$\Sigma^{\star}(\omega)$ =

"Extended"
Hartree-Fock

$R^{(2p1h)}$ $R^{(2h1p)}$

All Ladders (GT) and ring modes (GW) are coupled
to all orders. Two approaches:

- Faddev-RPA allows for RPA modes

- ADC(3) Tamn-Dancoff version using 3rd order
diagrams as 'seeds':

Rings (GW)

"W" $\Pi^{(ph)}$

"W" $\Pi^{(ph)}$

n   p

"T" $g^{II}{}_{(pp/hh)}$

Ladders (GT)

The Self-Consistent Green's Function with Faddev-RPA

Binding energies
Oxygen drip line
[Phys Rev. Lett. **111**, 062501 (2013)]

$\hbar\omega$=24 MeV
λ_{SRG}=2.0 fm^{-1}

- *Dys*-ADC(3), NN+3N(ind)
- *Dys*-ADC(3), NN+3N(full)
- *Gorkov*-2nd, NN+3N(full)
- Exp

$E_{g.s.}$ [MeV]

^{14}O ^{16}O ^{18}O ^{20}O ^{22}O ^{24}O ^{26}O ^{28}O

Two-nucleon emission: $^{16}O(e,e'pn)^{14}N$
[Eur. Phys. J. A**43**, 137 (2010)]

(q,ω)

$d\sigma$

p_R(MeV/c)
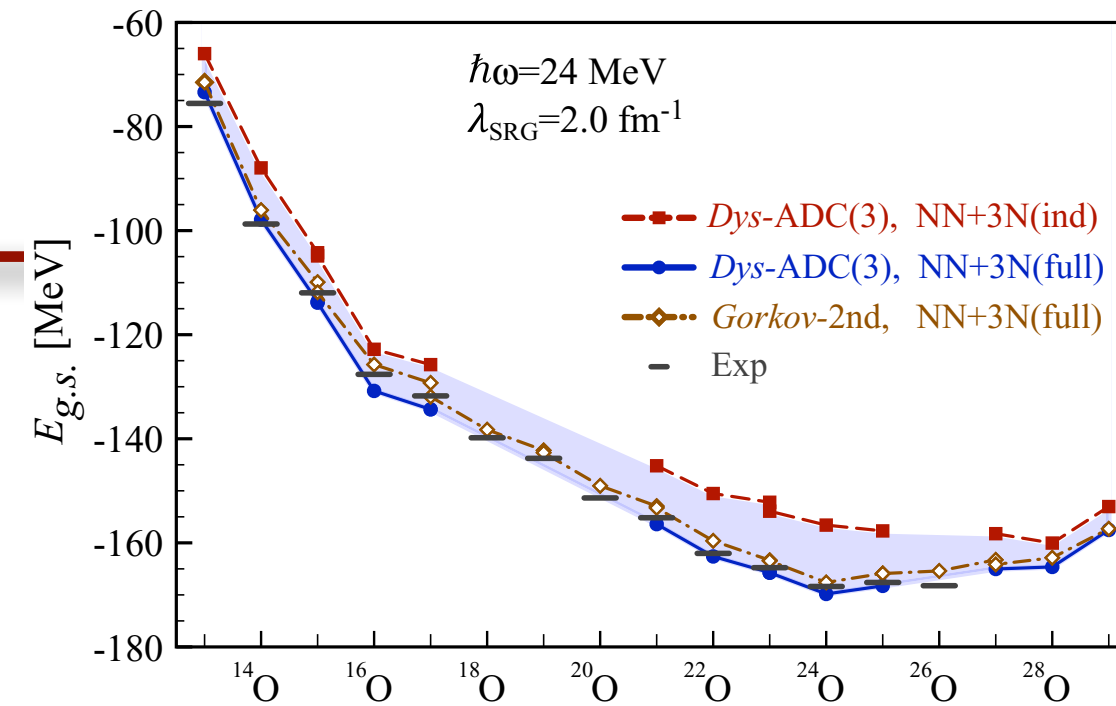
Charge & matter distribution
Neutron skins [Phys Rev. Lett. **125**, 182501 (2020)]
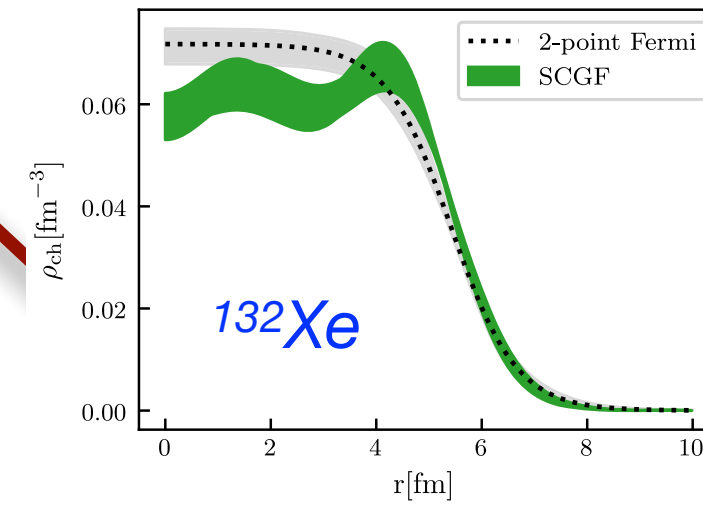
- 2-point Fermi
- SCGF

ρ_{ch}[fm^{-3}]

^{132}Xe

r[fm]

	SCGF	Exp.
^{100}Sn	4.525 – 4.707	
^{132}Sn	4.725 – 4.956	4.7093
^{132}Xe	4.700 – 4.948	4.7859
^{136}Xe	4.715 – 4.928	4.7964
^{138}Xe	4.724 – 4.941	4.8279

T$_{ladders}$

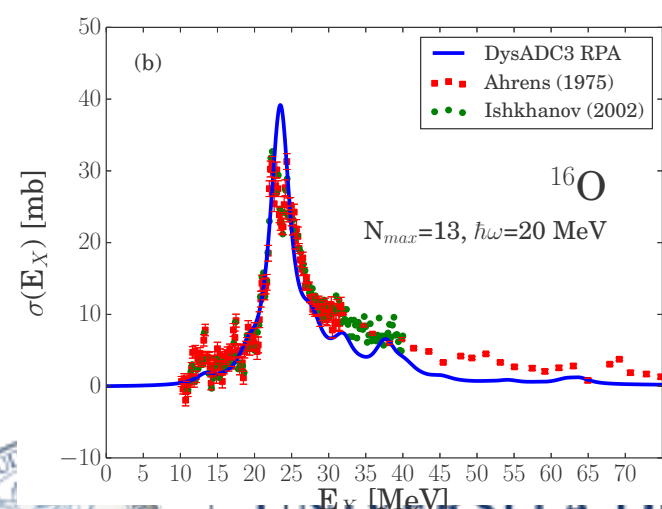## W$_{rings}$

T W W

Dyson Eq.
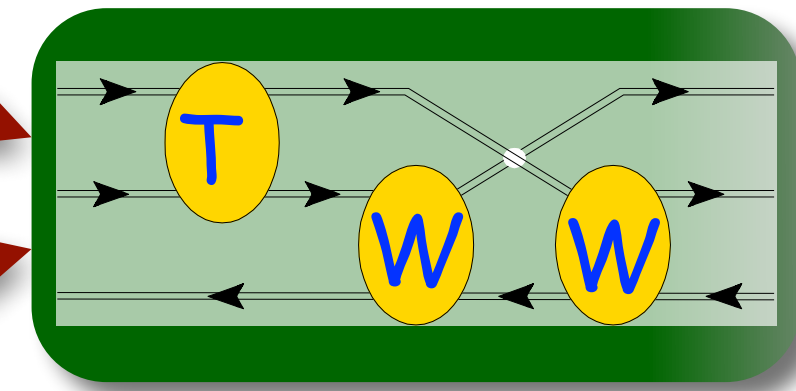
Spectroscopy
Ionisation energies and affinities for simple atoms and molecules
[Phys Rev. A. **83**, 042517 (2011); **85**, 012501 (2012)]

	Level	ADC(3)	FRPA	FRPA(c)	Expt.
HF					
	1π	16.48	16.05	16.35	16.05
	3σ	20.36	20.03	20.24	20.0
CO					
	5σ	13.94	14.37	13.69	14.01
	1π	16.98	16.95	16.84	16.91
	4σ	20.19	19.46	19.59	19.72
H_2O					
	$1b_1$	12.86	12.62	12.67	12.62
	$3a_1$	15.15	14.91	14.98	14.74
	$1b_2$	19.21	19.06	19.13	18.51
	$\bar{\Delta}$ (eV)	0.30(0.30)	0.25(0.23)	0.31(0.26)	
	Δ_{max} (eV)	0.70(0.70)	0.73(0.73)	0.88(0.62)	

Nuclear ELM response and dipole polarisability, a$_D$
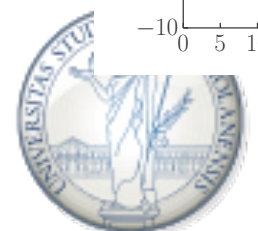[Phys Rev. C**99**, 054327 (2019)]

- DysADC3 RPA
- Ahrens (1975)
- Ishkhanov (2002)

$\sigma(E_X)$ [mb]

^{16}O
N$_{max}$=13, $\hbar\omega$=20 MeV

Ex [MeV]

^{68}Ni:

	SCGF	Exp
E_{PDR} (MeV)	10.68 10.92	9.55(17)
E_{GDR} (MeV)	18.1	17.1(2)
α_D (fm^3)	3.60	3.40(23) 3.88(31)

Optical potential
Elastic neutron scattering [Phys Rev. Lett. **123**, 092501 (2013)]

δ (deg)

- $3/2^+$ — $5/2^+$
- $1/2^+$
- $3/2^-$ — $1/2^-$
- $5/2^-$ — $7/2^-$

$E_{c.m.}$ (MeV)

$d\sigma$/dΩ (b/sr)

^{16}O

^{40}Ca

θ (deg)

^{56}Ni

f$_{7/2}$

p$_{3/2}$

p$_{1/2}$,$_{5/2}$

$S_{56Ni}^{(n)}(r,\omega)$

r [fm]

ω [MeV]

E_F
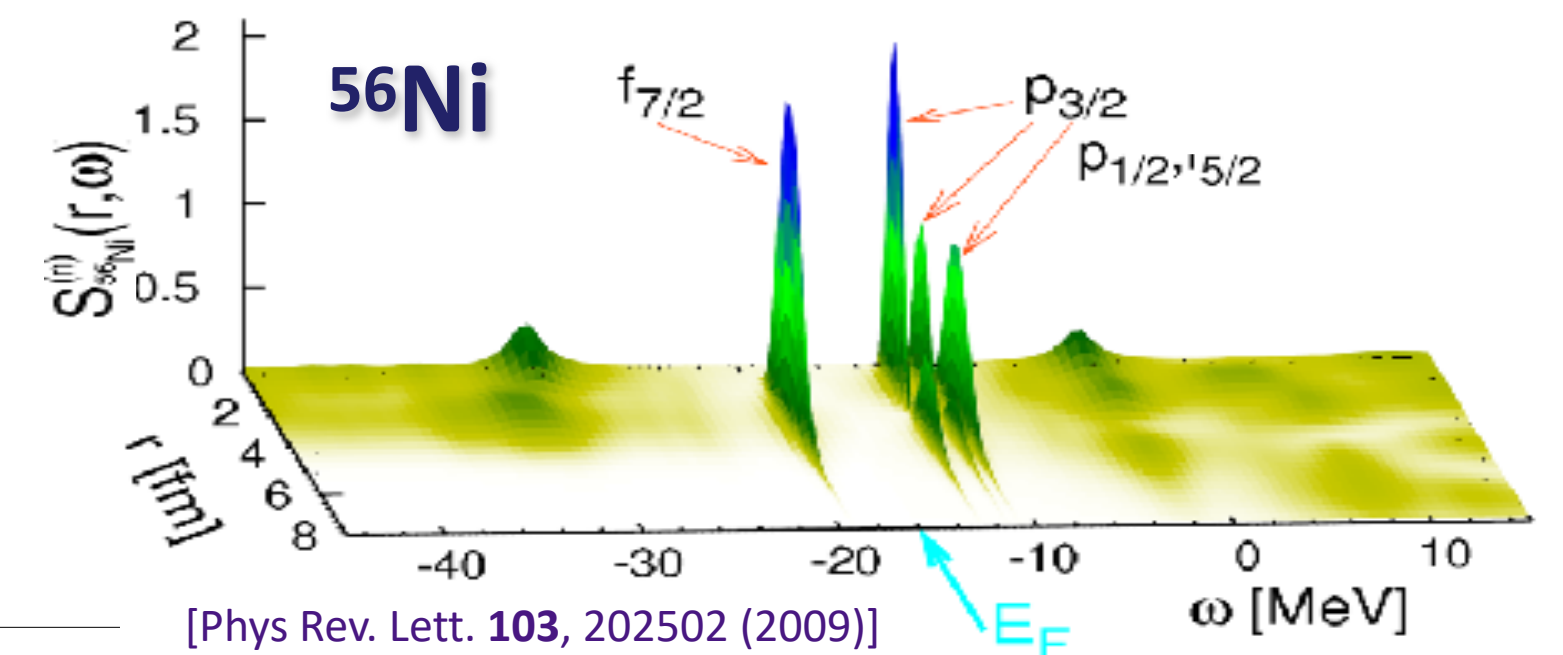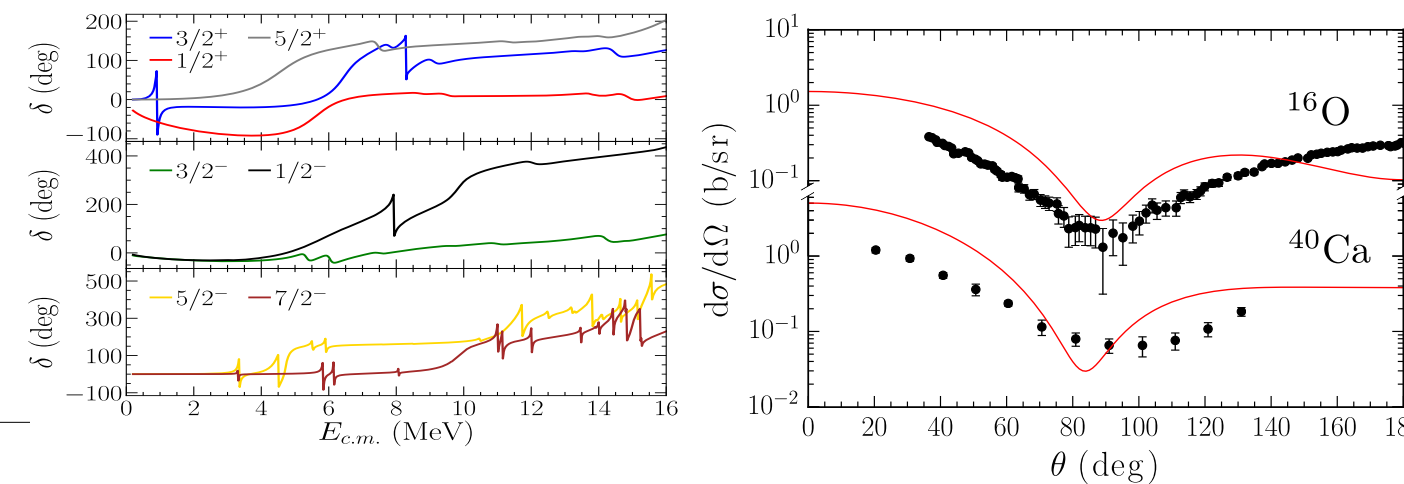
[Phys Rev. Lett. **103**, 202502 (2009)]

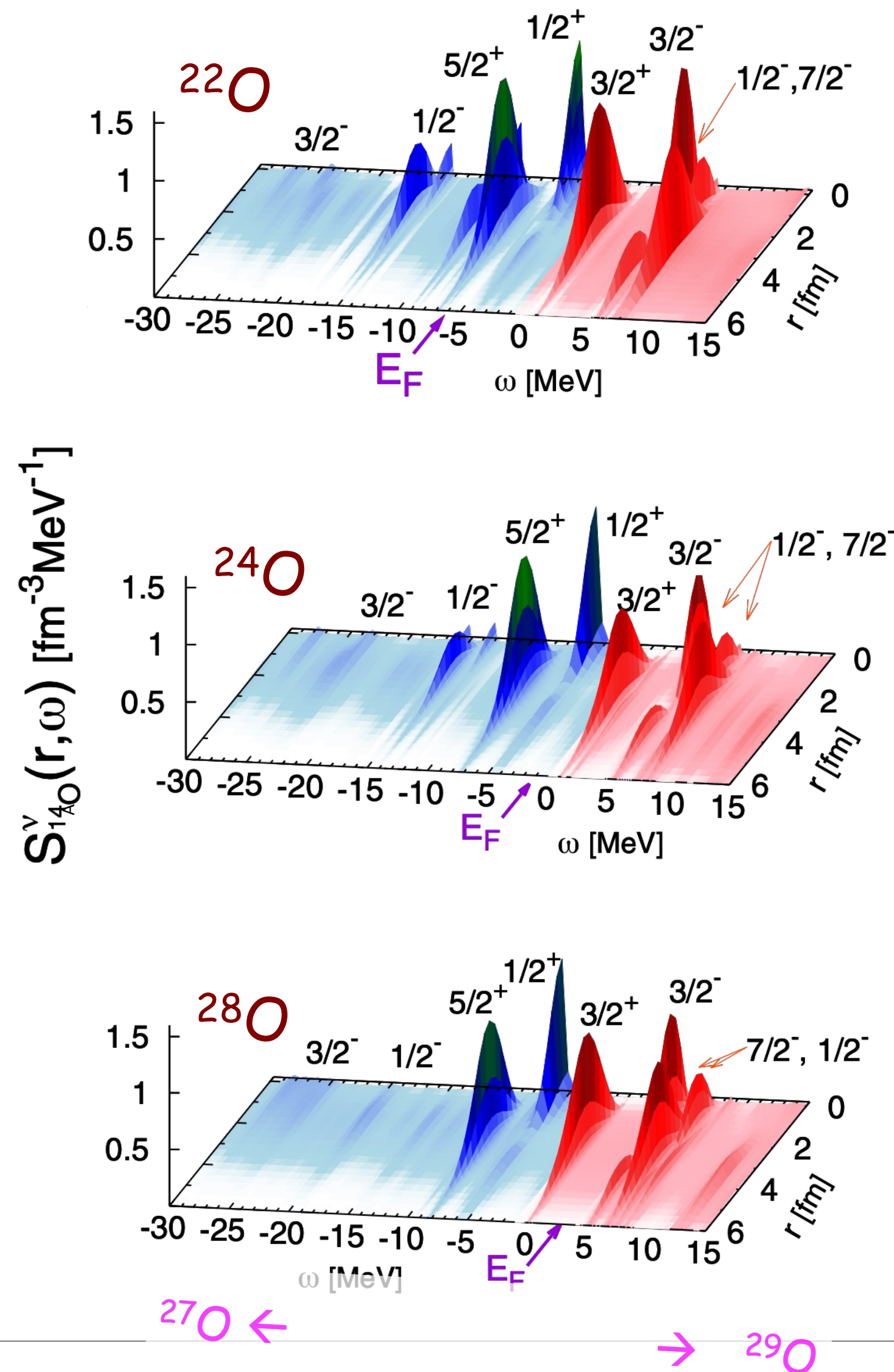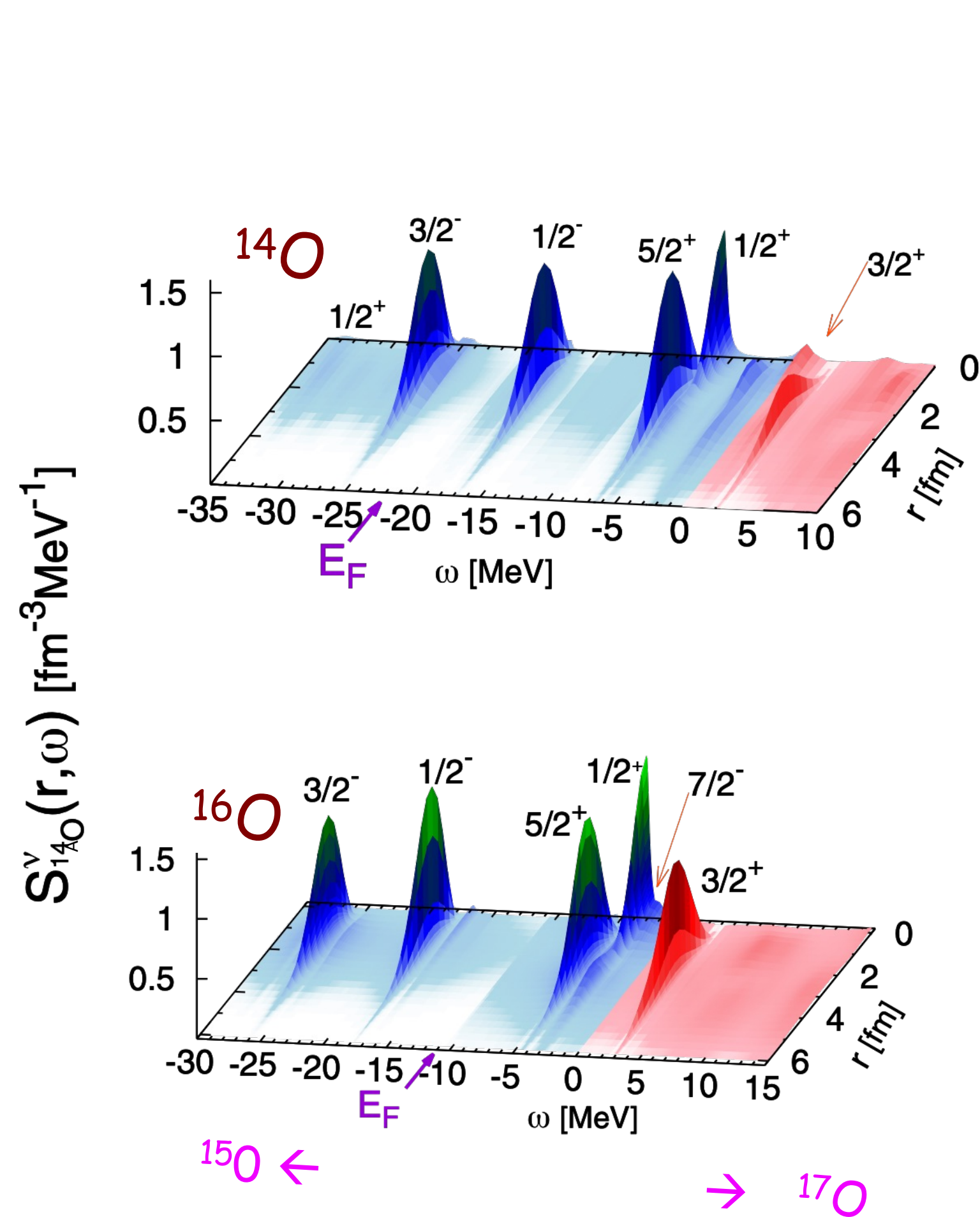→ 3NF crucial for reproducing binding energies and driplines around oxygen

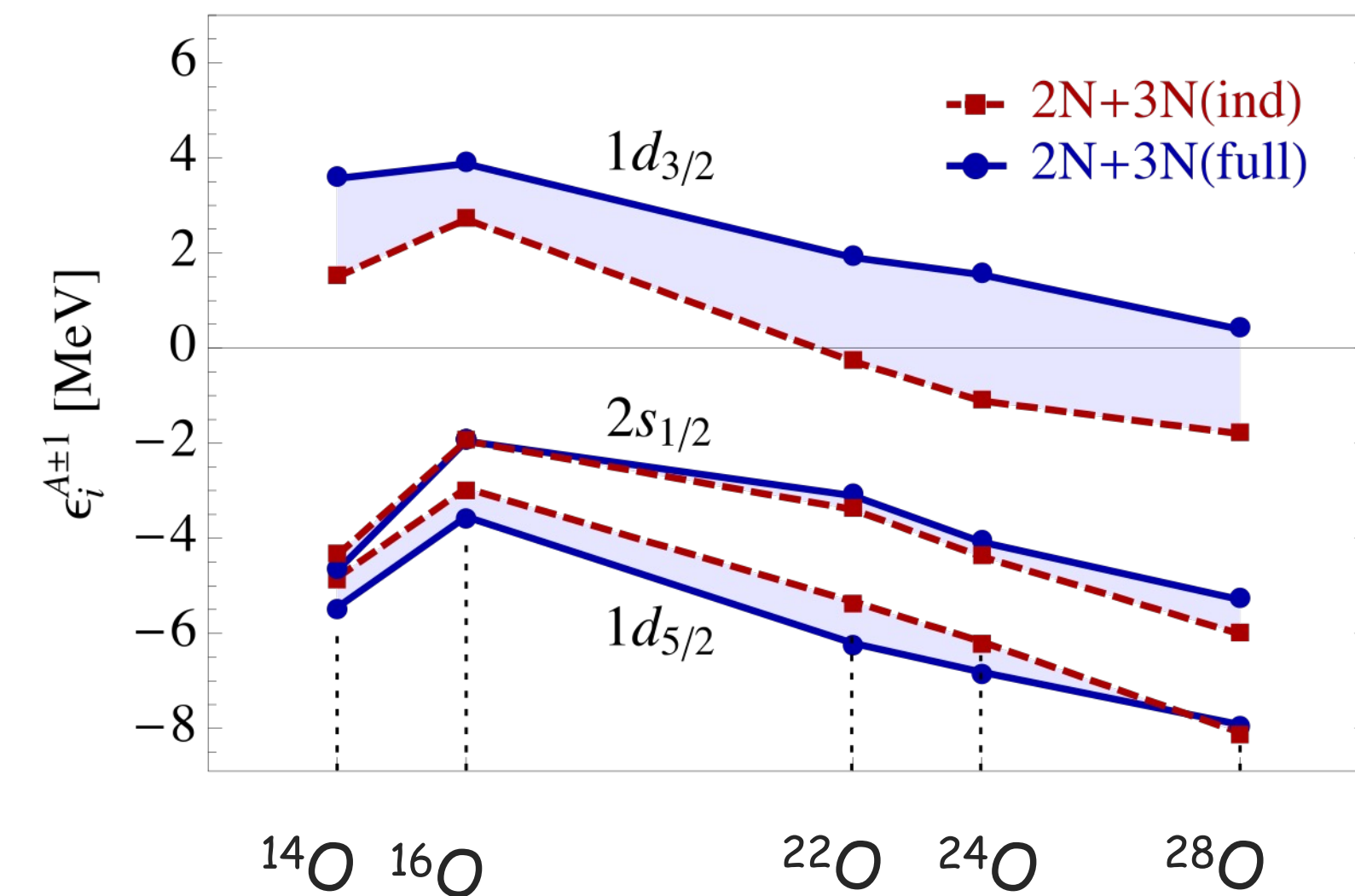→ cf. microscopic shell model [Otsuka et al, PRL**105**, 032501 (2010).]

N3LO (Λ = 500Mev/c) chiral NN interaction evolved to 2N + 3N forces (2.0fm^{-1})
N2LO (Λ = 400Mev/c) chiral 3N interaction evolved (2.0fm^{-1})

Neutron spectral function of Oxygens

N3LO(500) + nln 3NF

SCGF – Gorkov-ADC(2)
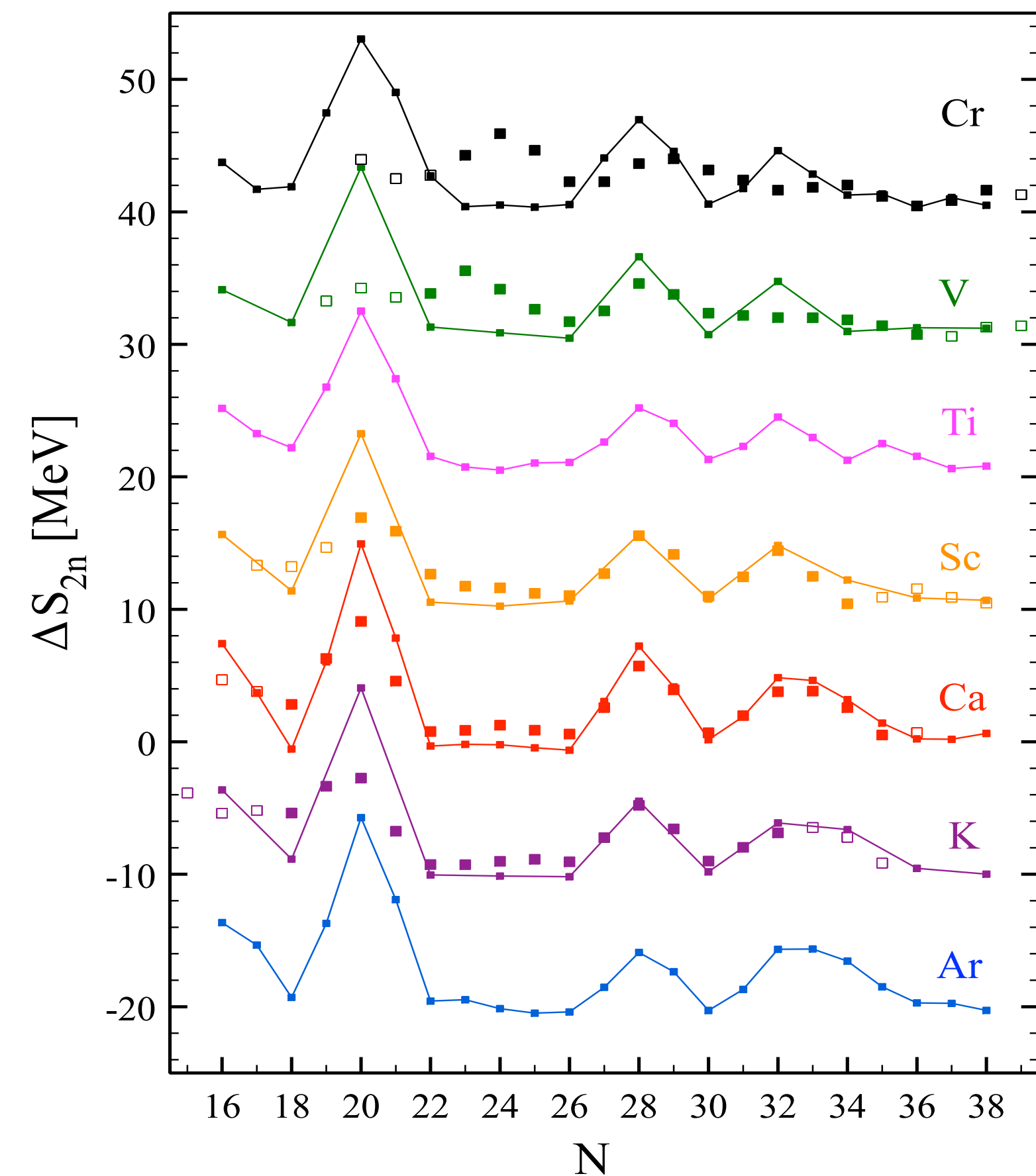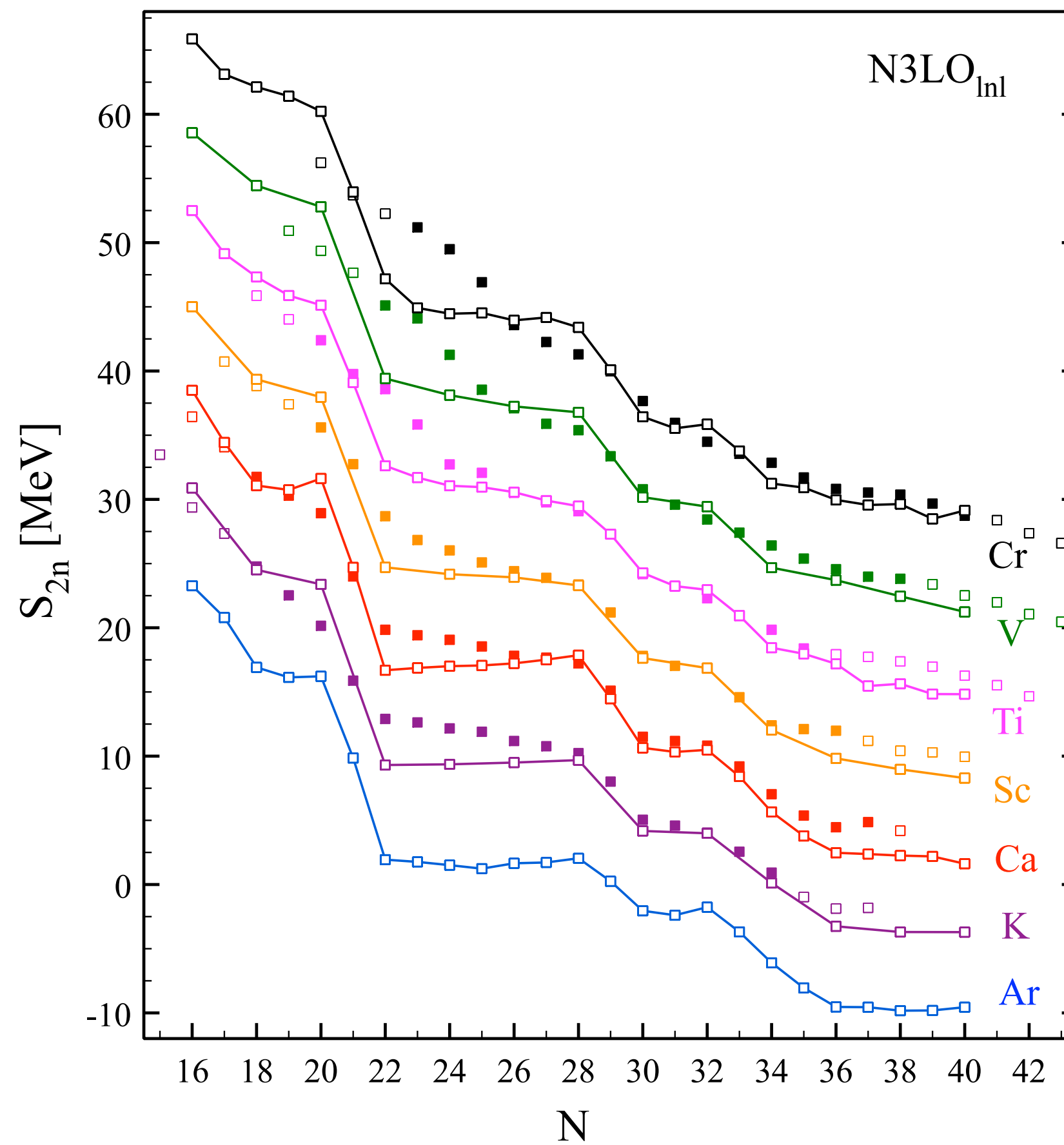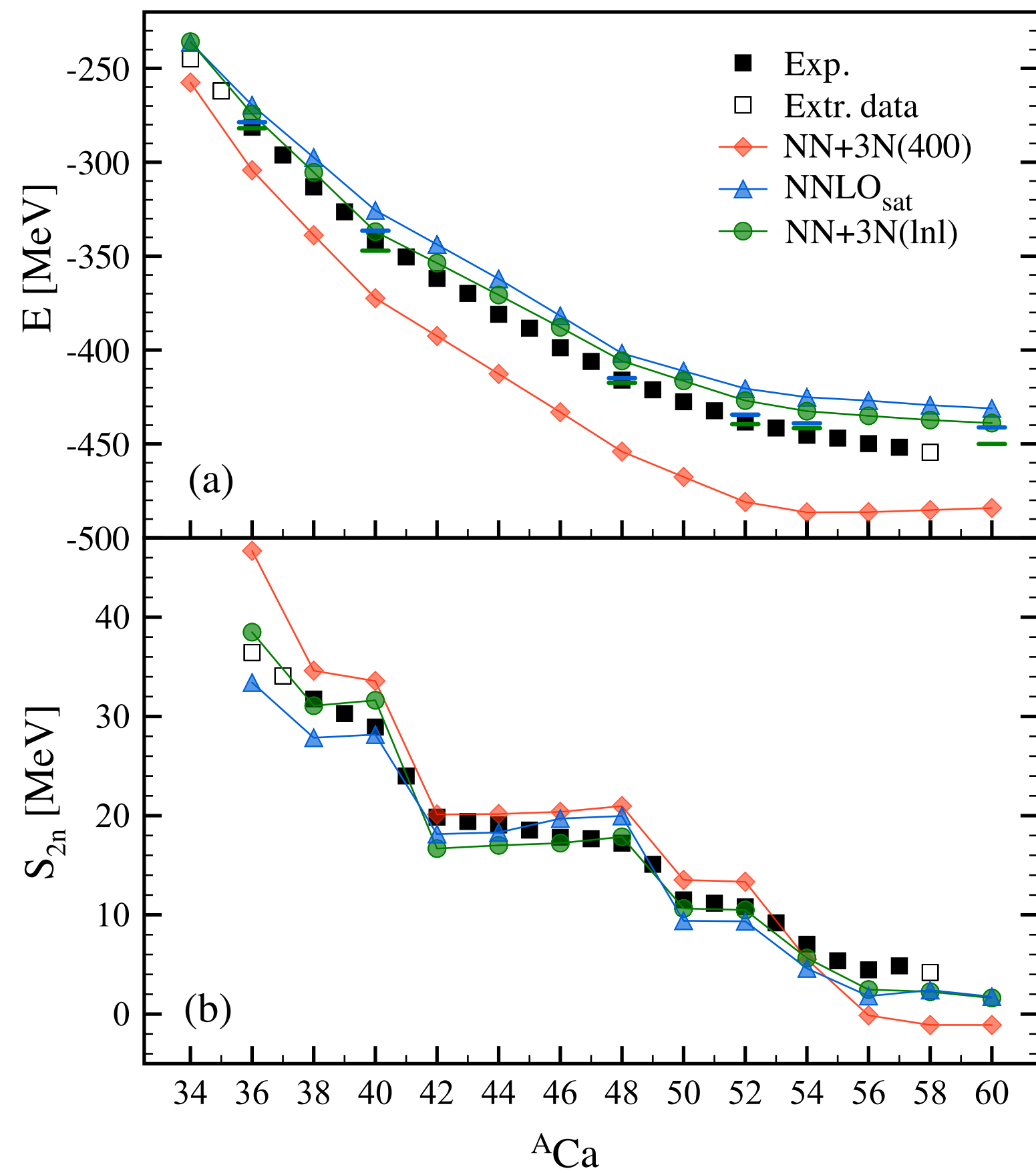
Bubble nuclei...   ³⁴Si prediction

Bubble nuclei...   ³⁴Si prediction
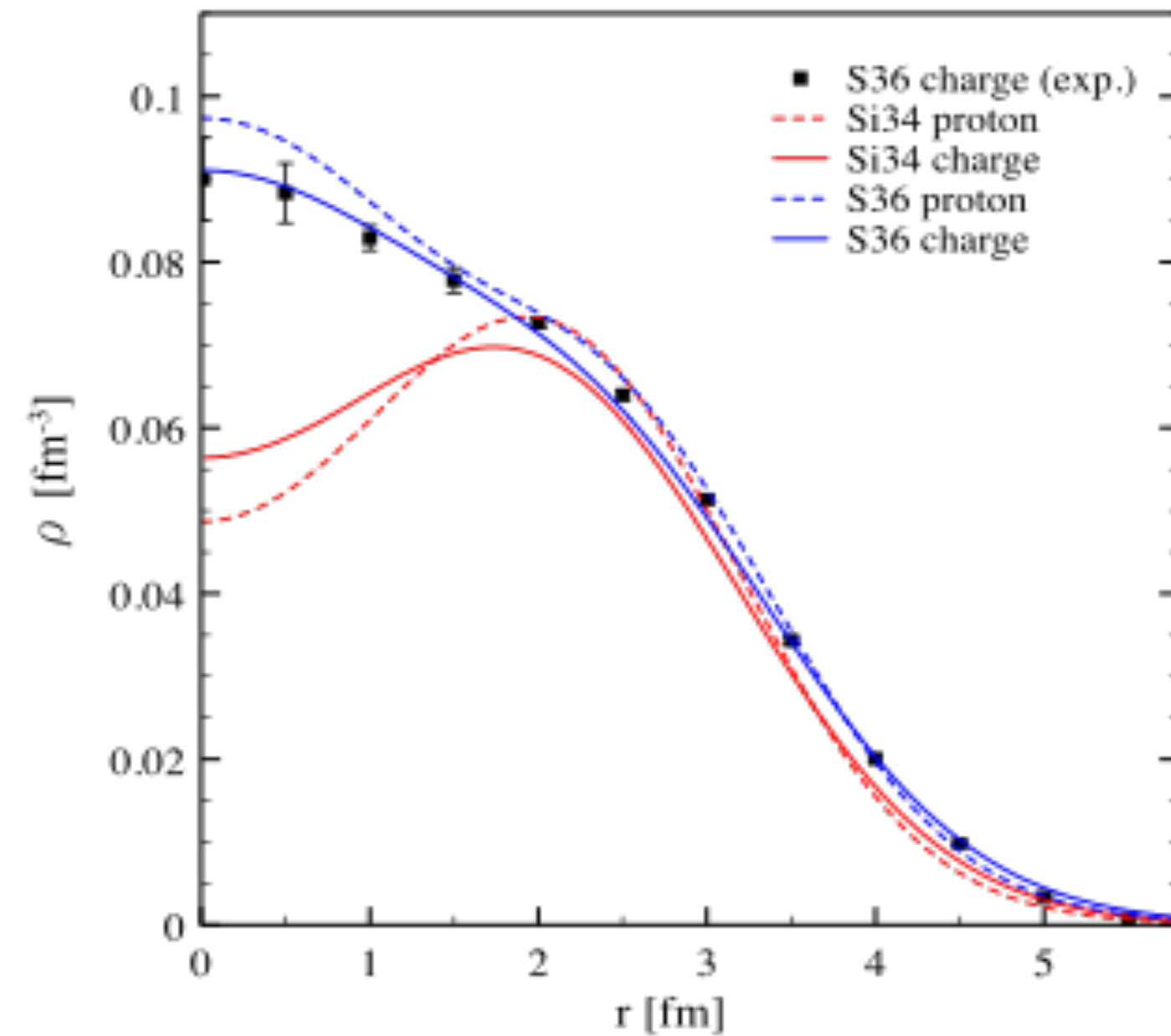
Duguet, Somà, Lecuse, CB, Navrátil,
Phys.Rev. C**95**, 034319 (2017)

- ³⁴Si is unstable, charge distribution is still unknown

- Suggested central depletion from mean-field simulations

-   Ab-initio theory confirms predictions

-   Other theoretical and experimental evidence:
    *Phys. Rev. **C 79**, 034318 (2009),*
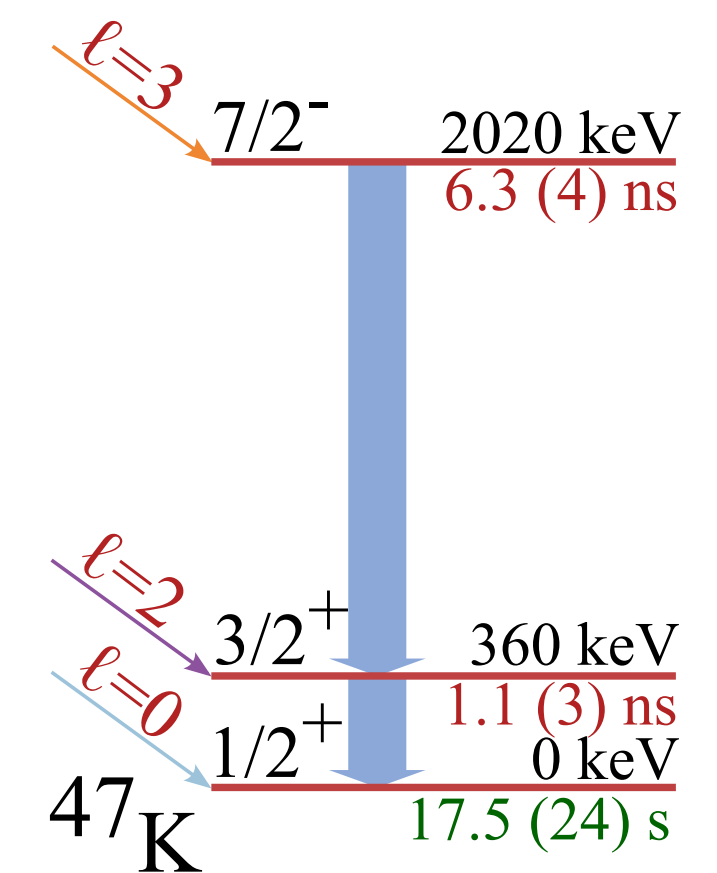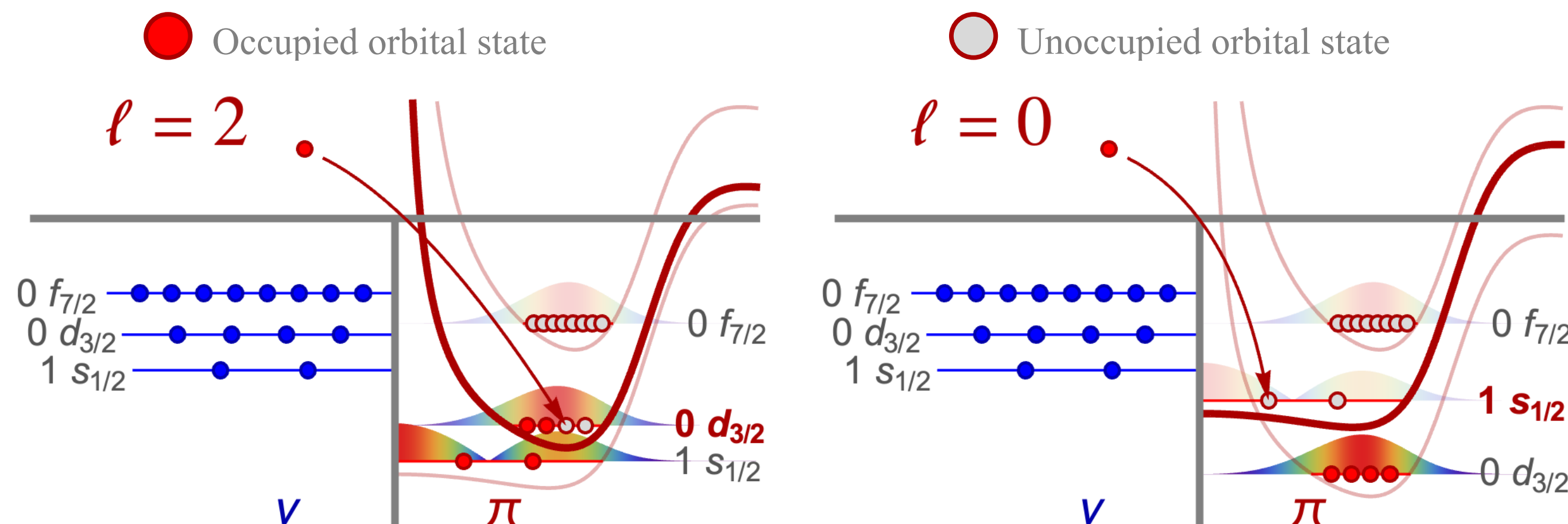   *Nature Physics **13**, 152–156 (2017).*

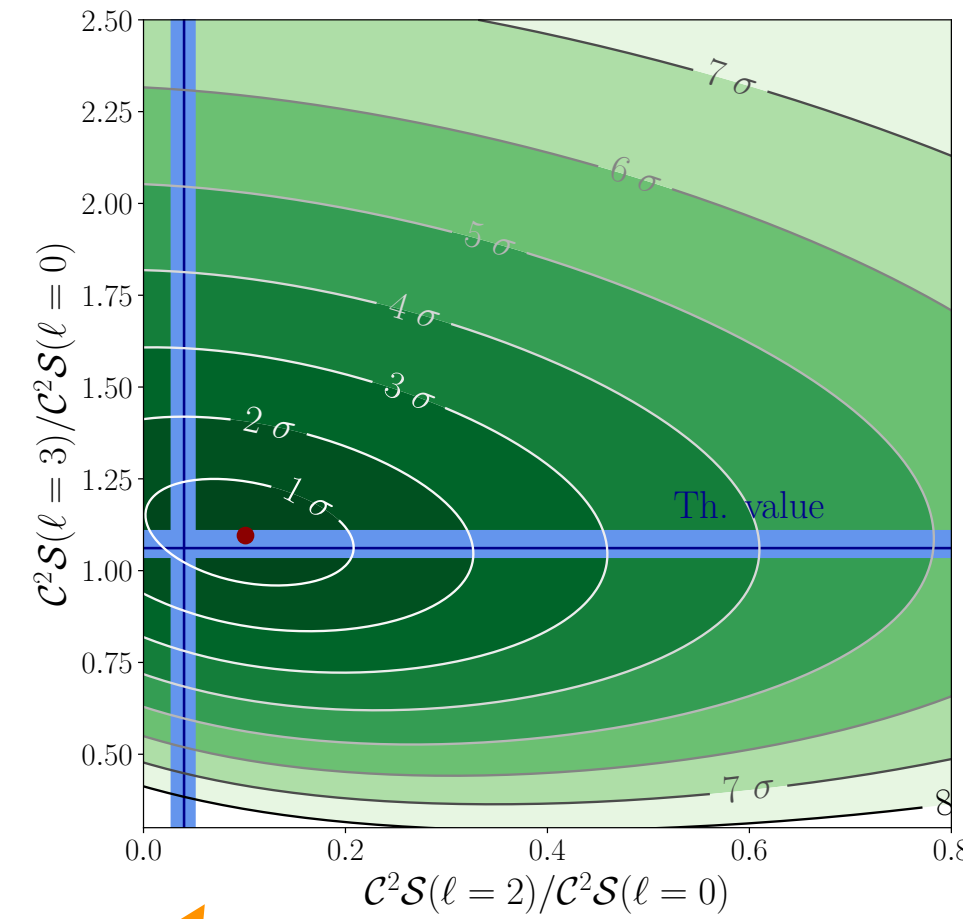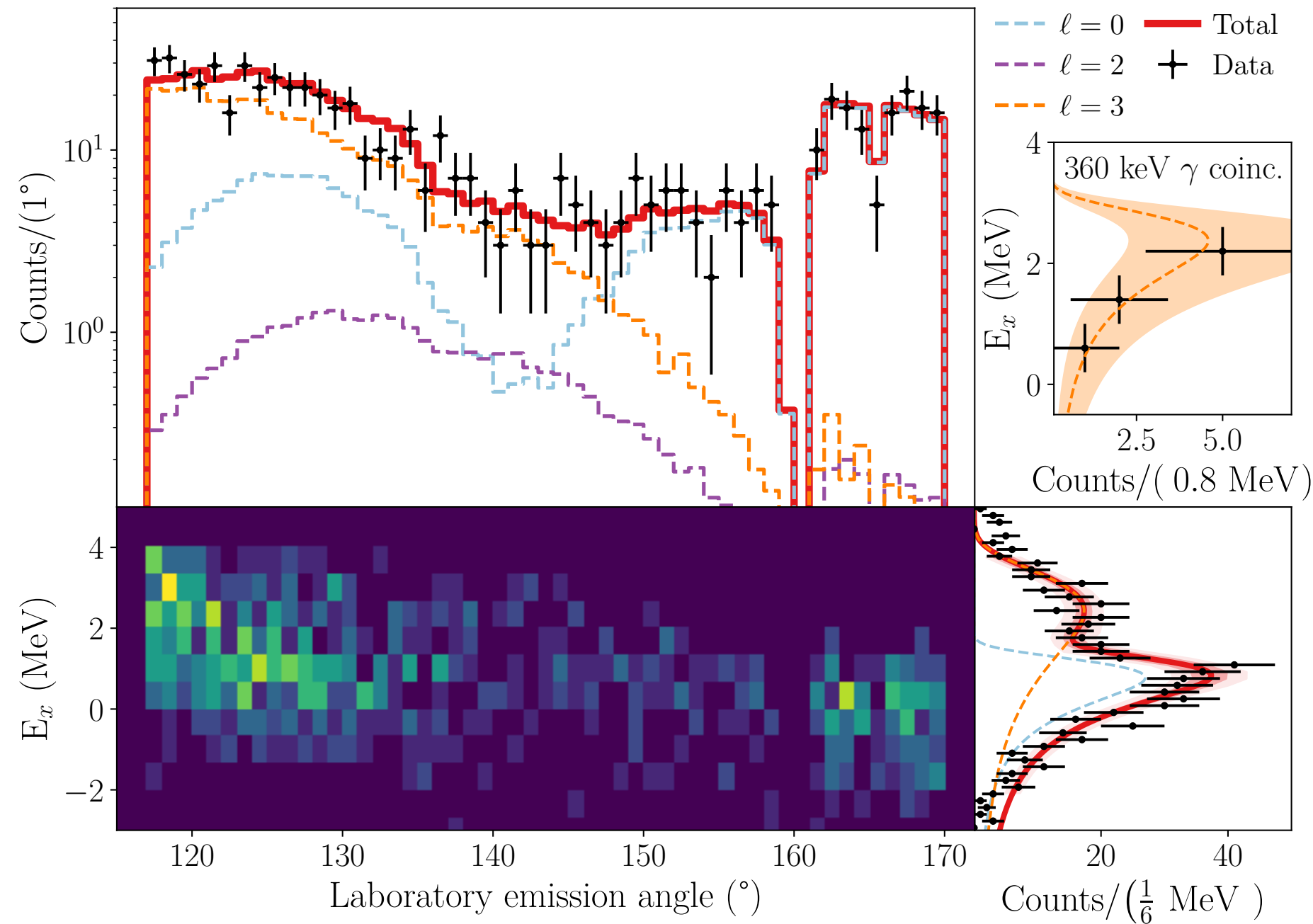Validated by charge distributions and neutron quasiparticle spectra:
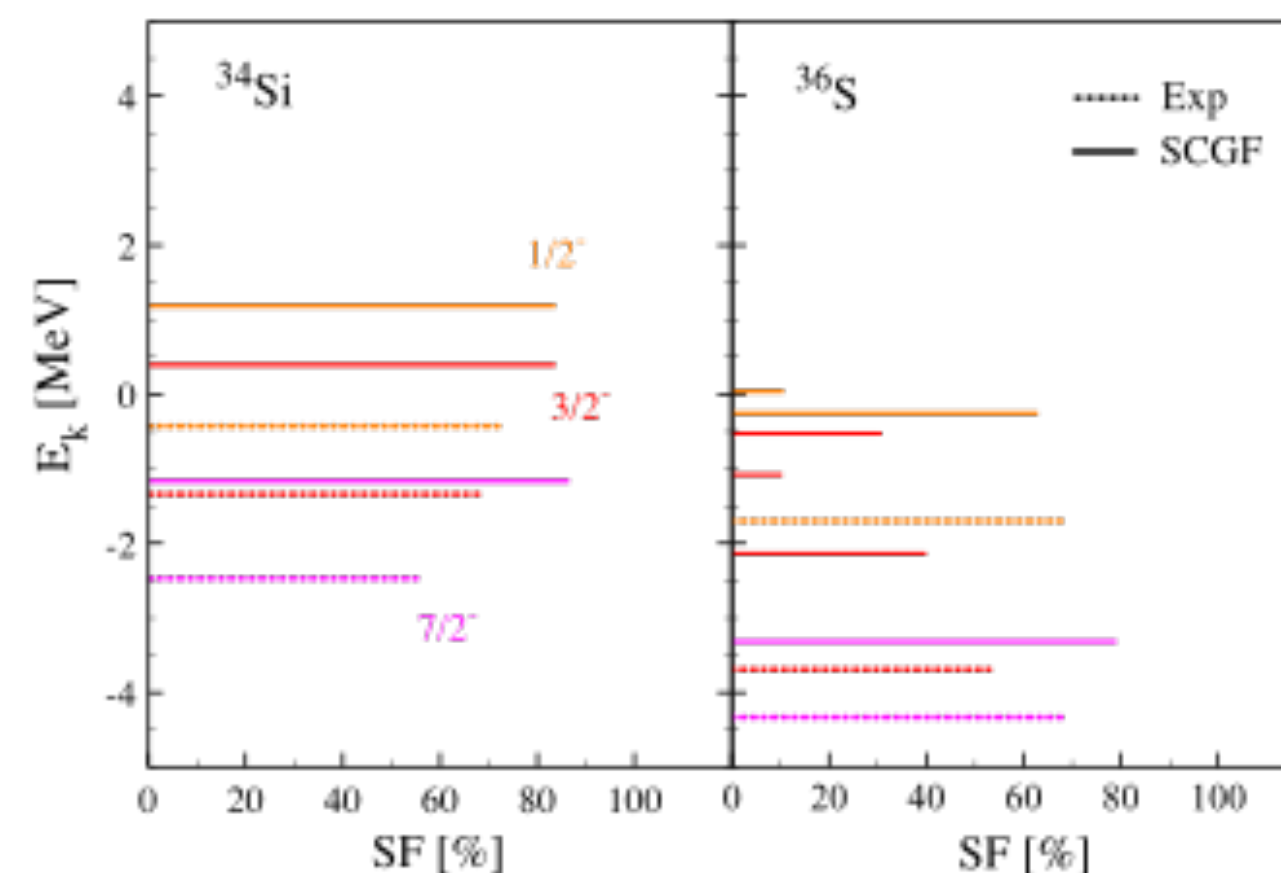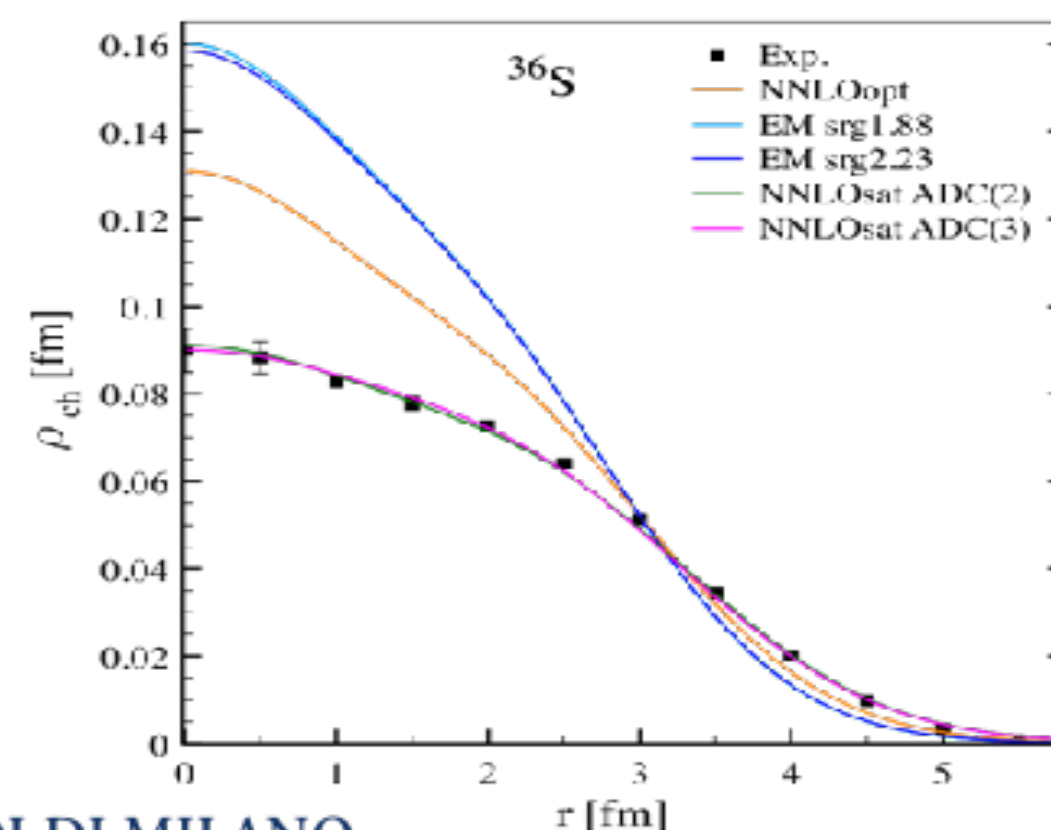
^{46}Ar(^{3}He,d)^{47}K at GANIL
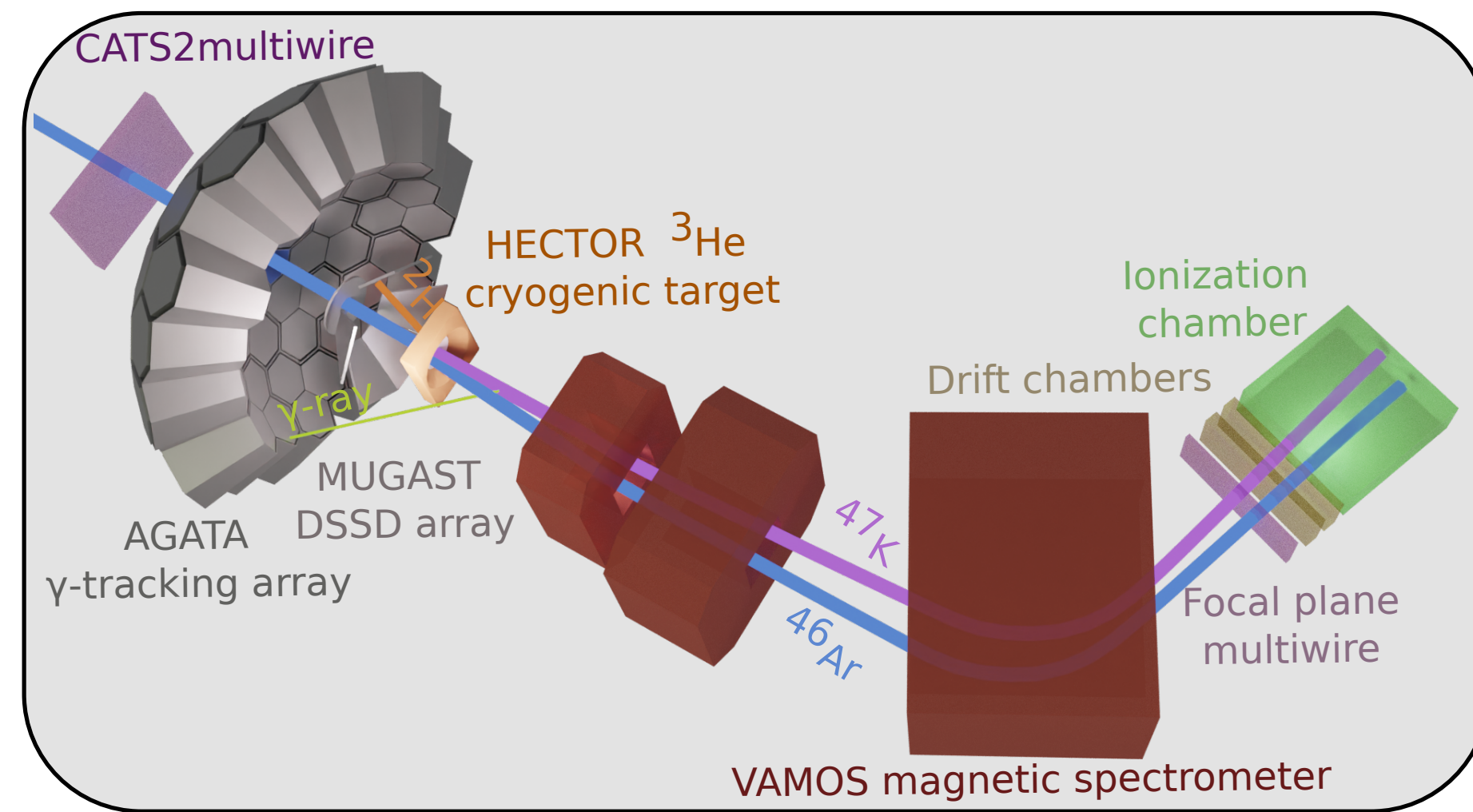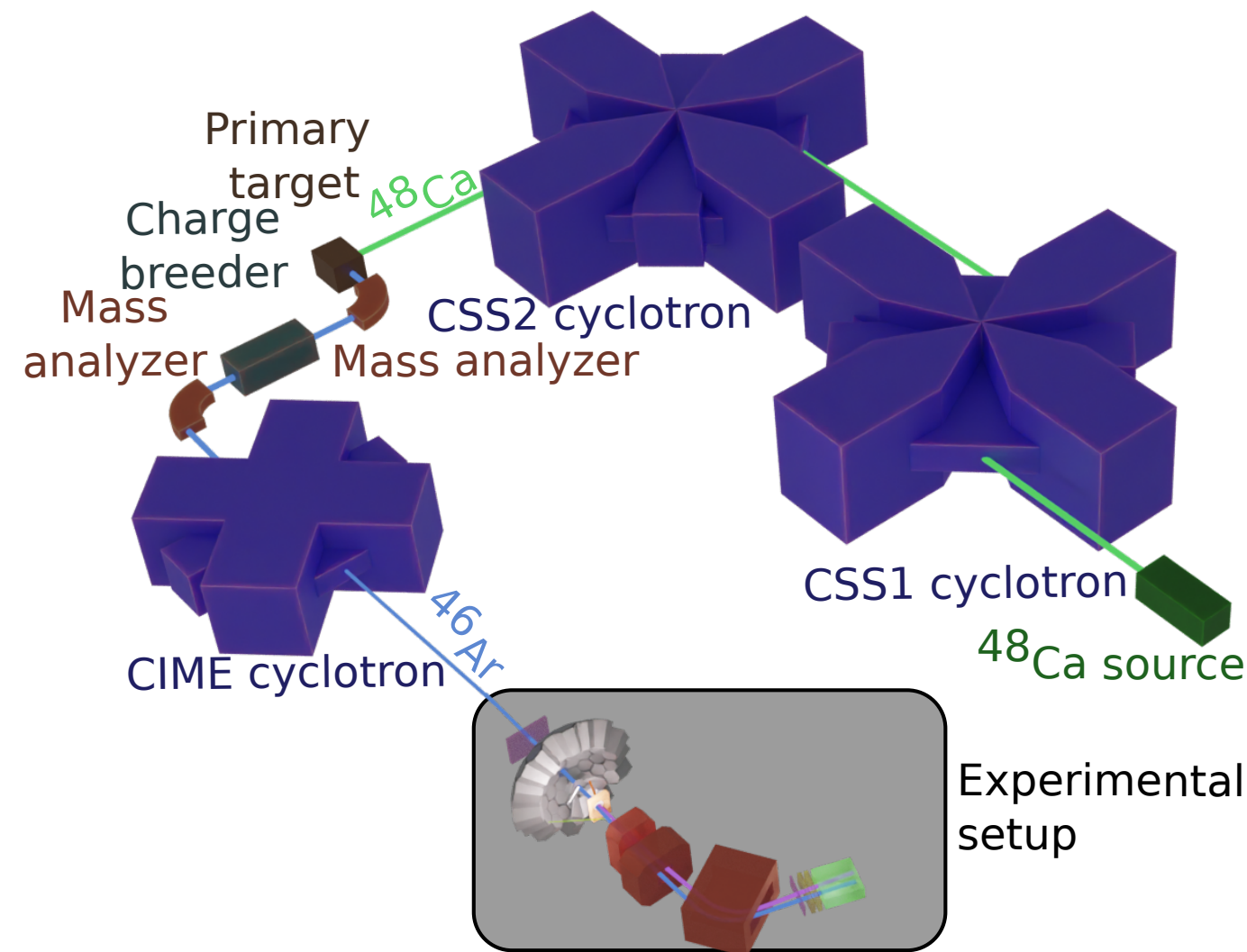
d3/2 - s1/2 inversion revisited from adding protons to ^{46}Ar

D. Brugnara, A. Gottardo, CB et al…

$$\frac{d\sigma}{d\Omega} = \sum_k g_k \, \mathcal{C}^2\mathcal{S}_k \, \frac{d\sigma_k^{SP}}{d\Omega}$$
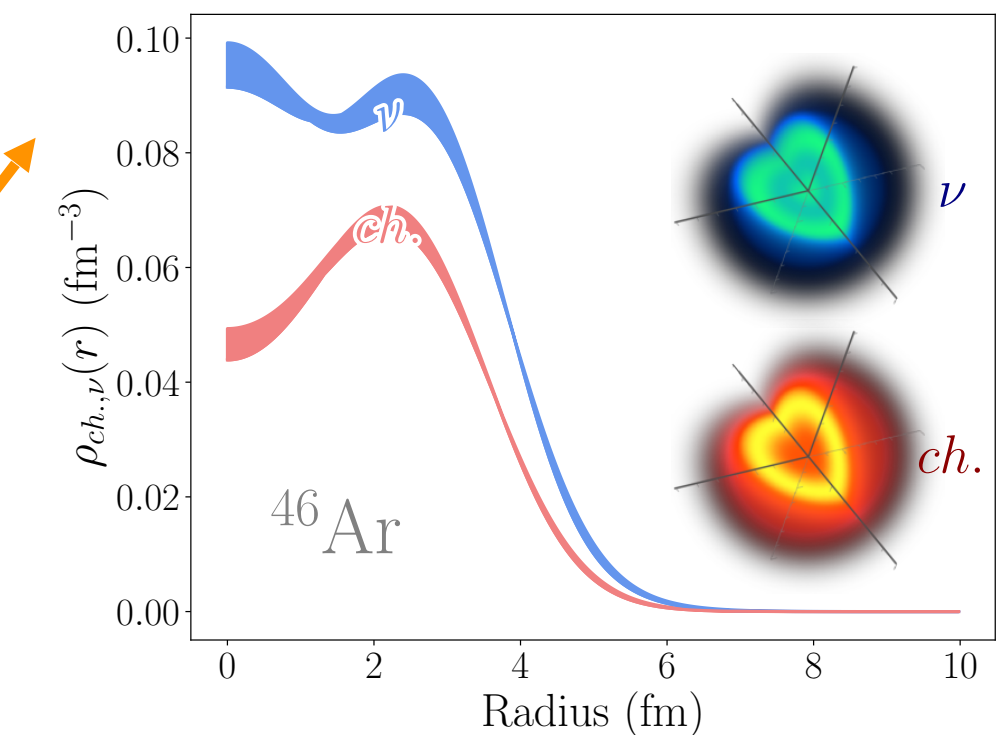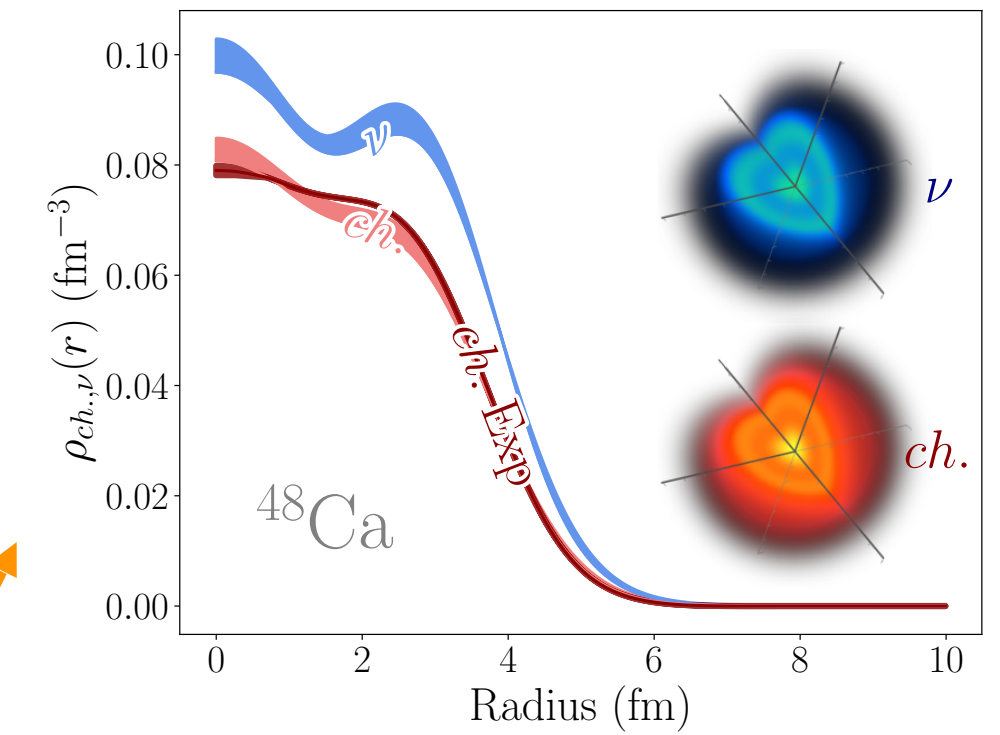
d3/2 - s1/2 inversion revisited from adding protons to ^{46}Ar

Theory & experiment for relative SFs agree within 1 sigma and confirms charge depletion in ^{46}Ar

Theory bands are a combination of NNLOsat, Δ-full DN²LO(394) and DN²LO(450), as well as Darmstadt's new saturating "magic force" 1.8/2.0 —all of these have constrained LECs using the ^{16}O radius and few other mid-mass nuclei data.
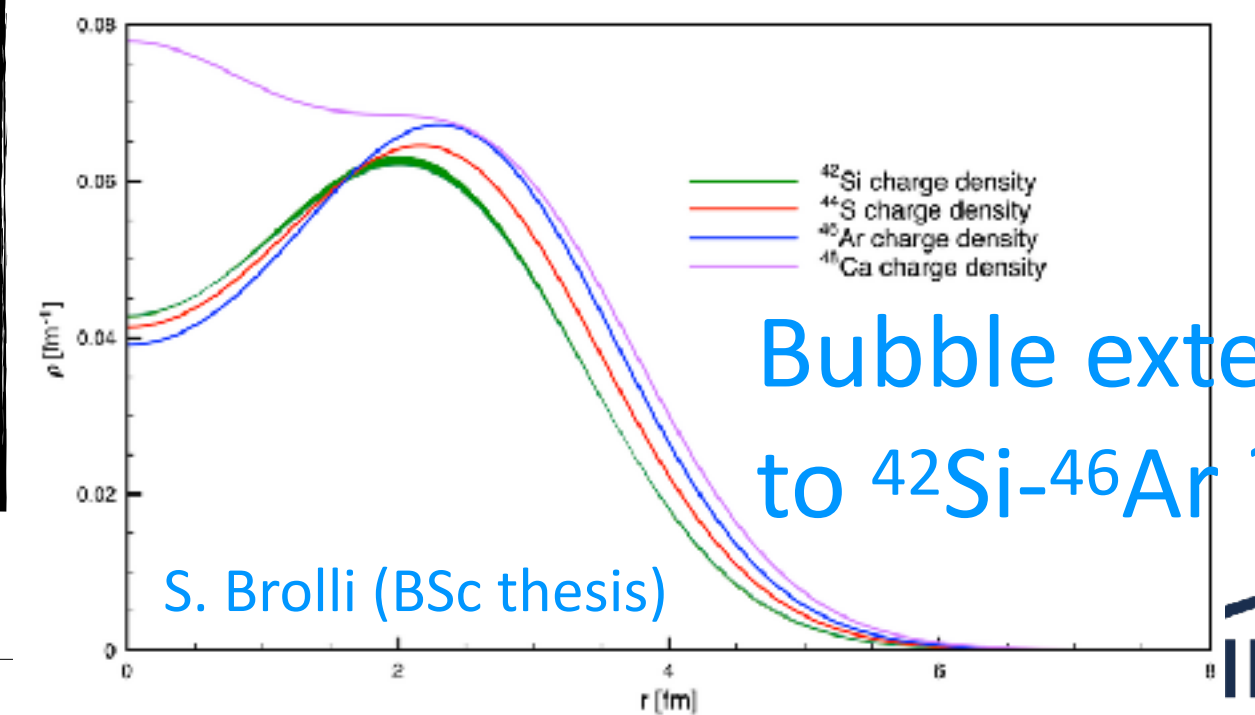
Bubble extends to ^{42}Si-^{46}Ar ??

S. Brolli (BSc thesis)

UNIVERSITÀ DEGLI STUDI DI MILANO
DIPARTIMENTO DI FISICA

D. Brugnara, A. Gottardo, CB et al... to be publishsed

INFN MILANO
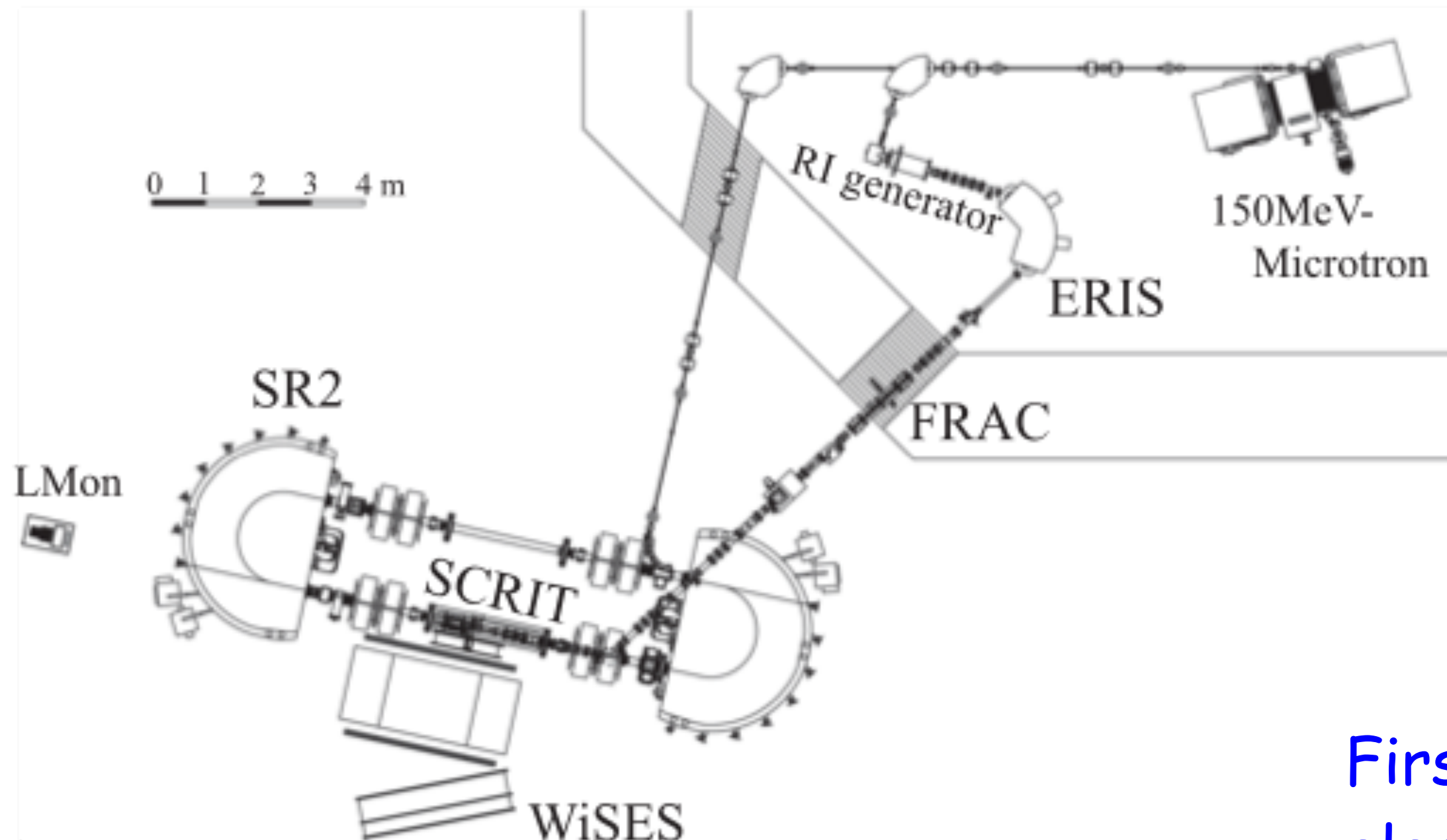
FIG. 1. Overview of the SCRIT electron scattering facility.
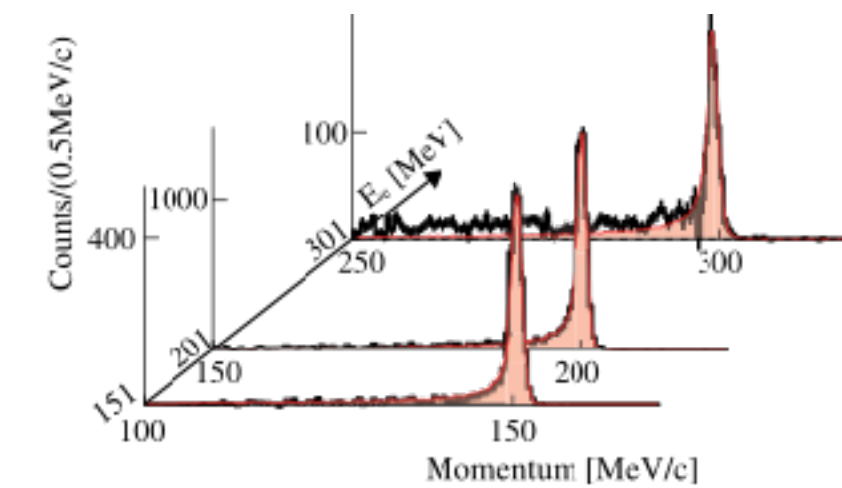
FIG. 3. Reconstructed momentum spectra of ^{132}Xe target after background subtraction. Red shaded lines are the simulated radiation tails following the elastic peaks.
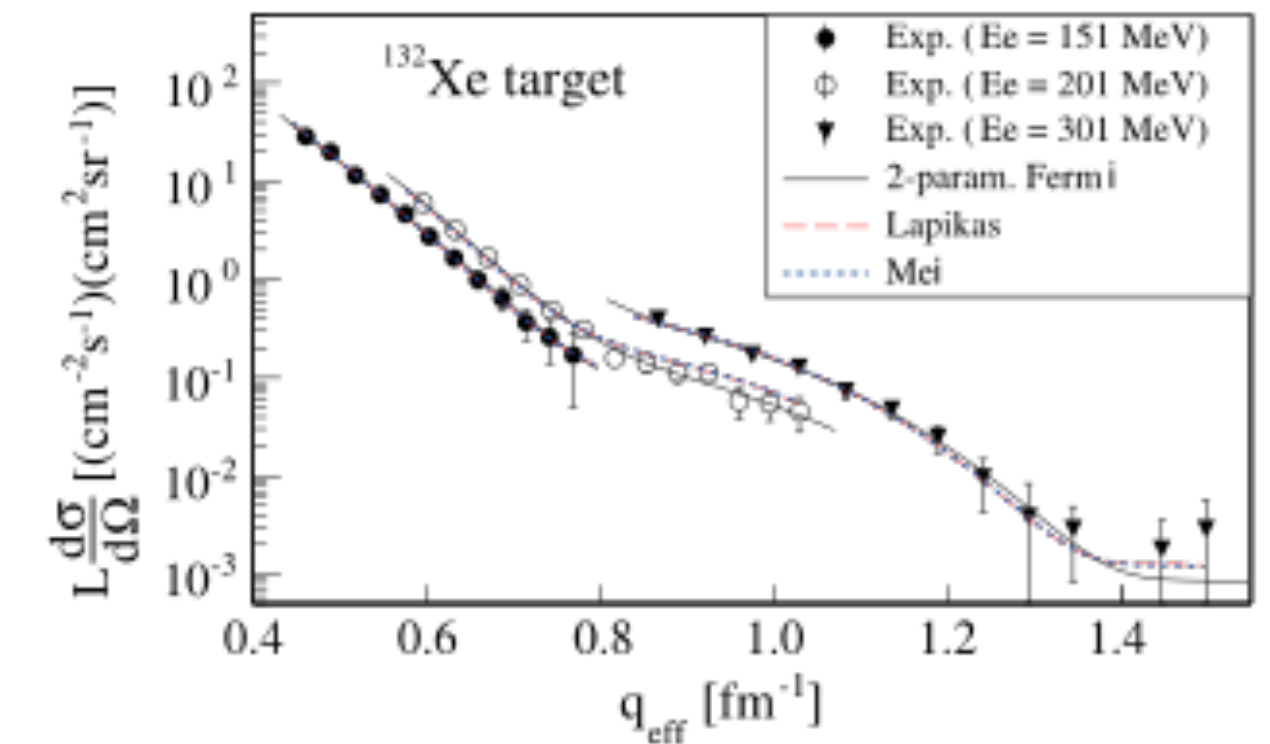
First ever measurement of charge radii through electron scattering with and ion trap setting that can be used on radioactive isotopes !!

K. Tsukada *et al.*, Phy rev Lett **118**, 262501 (2017)

Charge density for Sn and Xe isotopes

P. Arthuis (Surrey,
now @ TU Darmstadt,
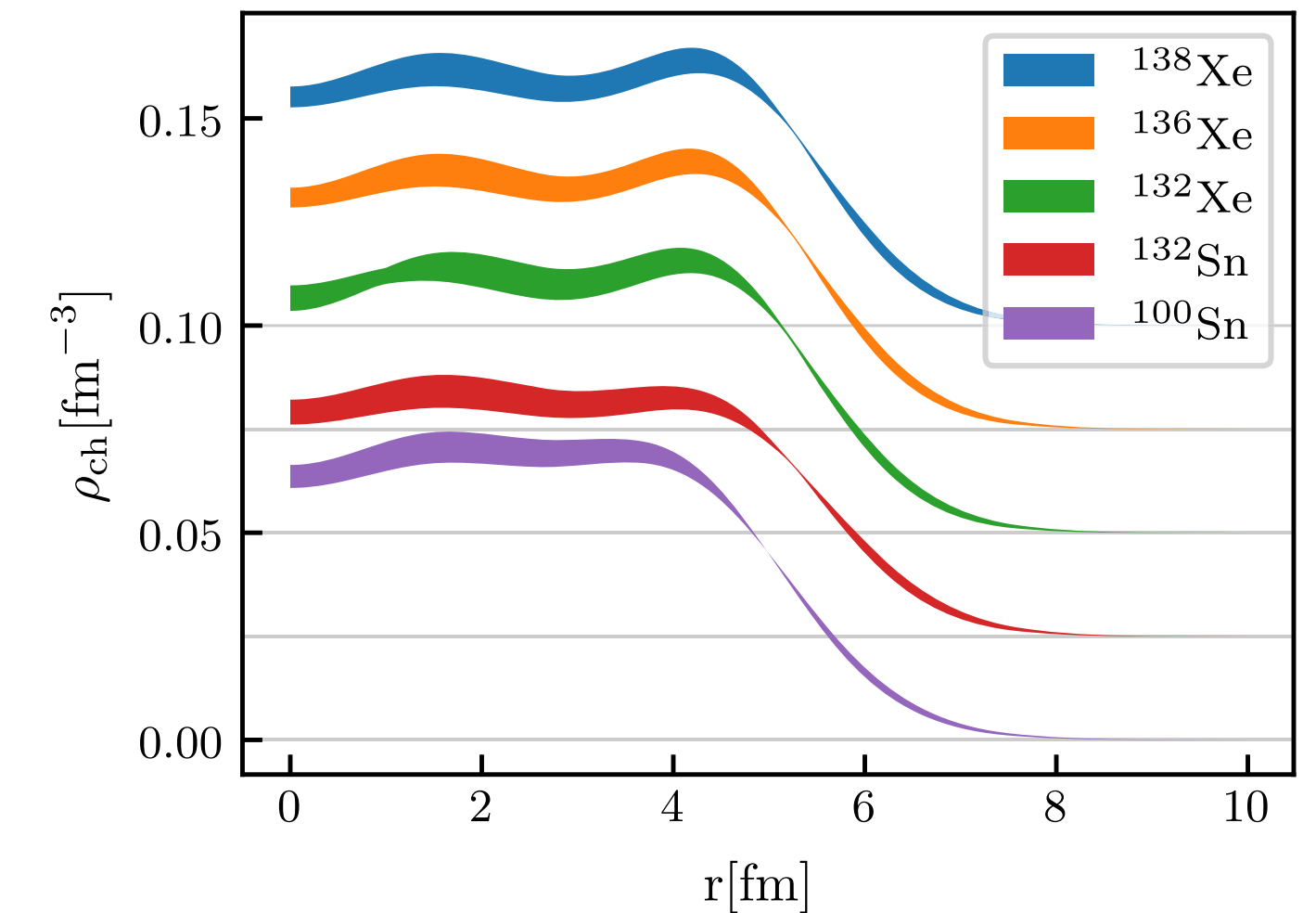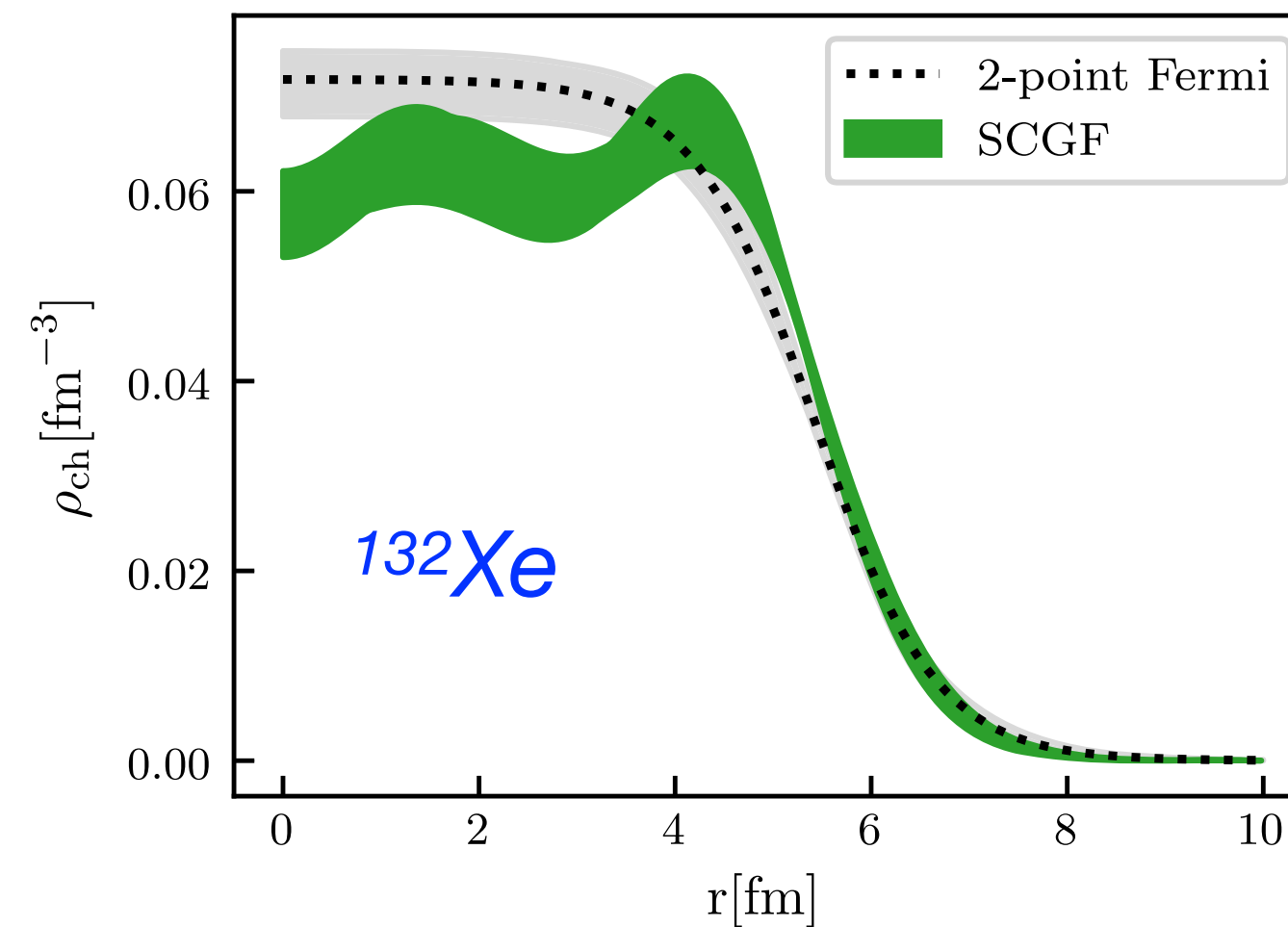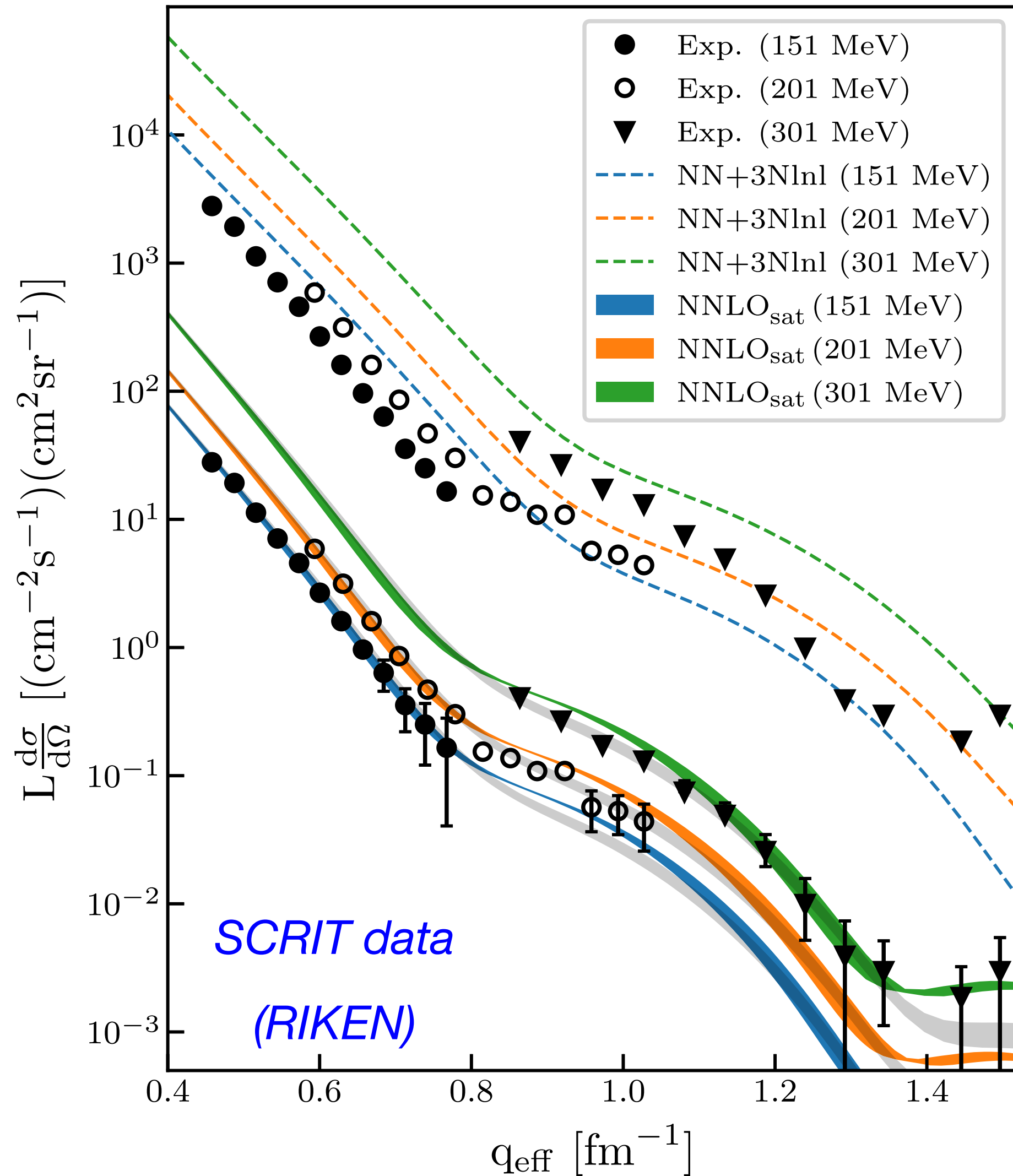
^{132}Xe

	SCGF	Exp.
^{100}Sn	$4.525 - 4.707$	
^{132}Sn	$4.725 - 4.956$	4.7093
^{132}Xe	$4.700 - 4.948$	4.7859
^{136}Xe	$4.715 - 4.928$	4.7964
^{138}Xe	$4.724 - 4.941$	4.8279

UNIVERSITÀ DEGLI STUDI DI MILANO
DIPARTIMENTO DI FISICA

Gorkov ADC(2) and Dyson ADC(3)   with N3LO-lnl and NNLOsat Hamiltonians

INFN MILANO

Ab initio optical potentials from propagator theory

Relation to Fesbach theory:
Mahaux & Sartor, Adv. Nucl. Phys. 20 (1991)
Escher & Jennings Phys. Rev. C**66**, 034313 (2002)

Previous SCGF work:
CB, B. Jennings, Phys. Rev. C**72**, 014613 (2005)
S. Waldecker, CB, W. Dickhoff, Phys. Rev. C**84**, 034616 (2011)
A. Idini, CB, P. Navrátil, Phys. Rv. Lett. **123**, 092501 (2019)
M. Vorabbi, CB, et al., Phys. Rev. C **109**, 034613 (2024)

Optical potentials for the rare-isotope beam era

C Hebborn[1,2], F M Nunes[1,3], G Potel[2], W H Dickhoff[4],
J W Holt[5], M C Atkinson[2,6], R B Baker[7], C Barbieri[8,9],
G Blanchon[10,11], M Burrows[12], R Capote[13],
P Danielewicz[1,3], M Dupuis[10,11], Ch Elster[7],
J E Escher[2], L Hlophe[2], A Idini[14], H Jayatissa[15],
B P Kay[15], K Kravvaris[2], J J Manfredi[16], A Mercenne[17],
B Morillon[10,11], G Perdikakis[18], C D Pruitt[2],
T R Whitehead[1], I J Thompson[2], M Vorabbi[19,20] and

[1] Facility for Rare Isotope Beams, East Lansing, MI 48824, United States of America

Microscopic optical potential

Nuclear self-energy $\Sigma^{\star}(\mathbf{r}, \mathbf{r}'; \varepsilon)$:

- contains *both particle* and *hole* props.

- it is proven to be a Feshbach opt. pot → in general it is *non-local !*

$$\Sigma^{\star}_{\alpha\beta}(\omega) = \Sigma^{(\infty)}_{\alpha\beta} + \sum_{i,j} \mathbf{M}^{\dagger}_{\alpha,i} \left(\frac{1}{E - (\mathbf{K}^{>} + \mathbf{C}) + i\Gamma} \right)_{i,j} \mathbf{M}_{j,\beta}$$

$$+ \sum_{r,s} \mathbf{N}_{\alpha,r} \left(\frac{1}{E - (\mathbf{K}^{<} + \mathbf{D}) - i\Gamma} \right)_{r,s} \mathbf{N}^{\dagger}_{s,\beta}$$

mean-field

Particle-vibration couplings:
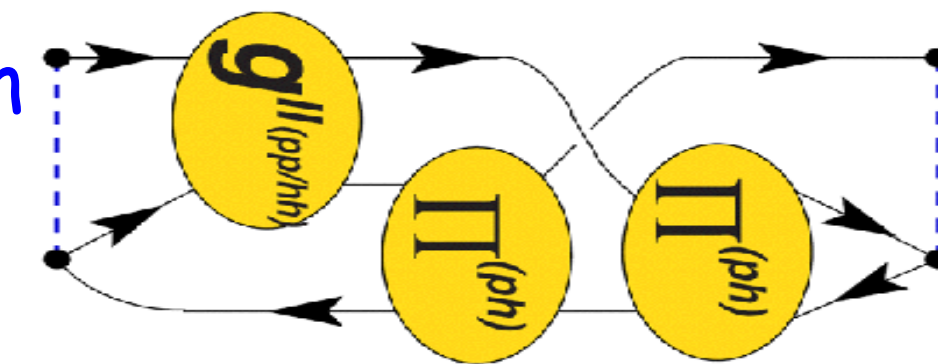

Solve scattering and overlap functions directly in momentum space:

$$\Sigma^{\star\, l,j}(k, k'; E) = \sum_{n, n'} R_{n\,l}(k)\, \Sigma^{\star\, l,j}_{n,\, n'}\, R_{n\,l}(k')$$

$$\frac{k^2}{2\mu} \psi_{l,j}(k) + \int \mathrm{d}k'\, k'^2\, \Sigma^{\star l,j}(k, k'; E_{c.m.}) \psi_{l,j}(k') = E_{c.m.} \psi_{l,j}(k)$$
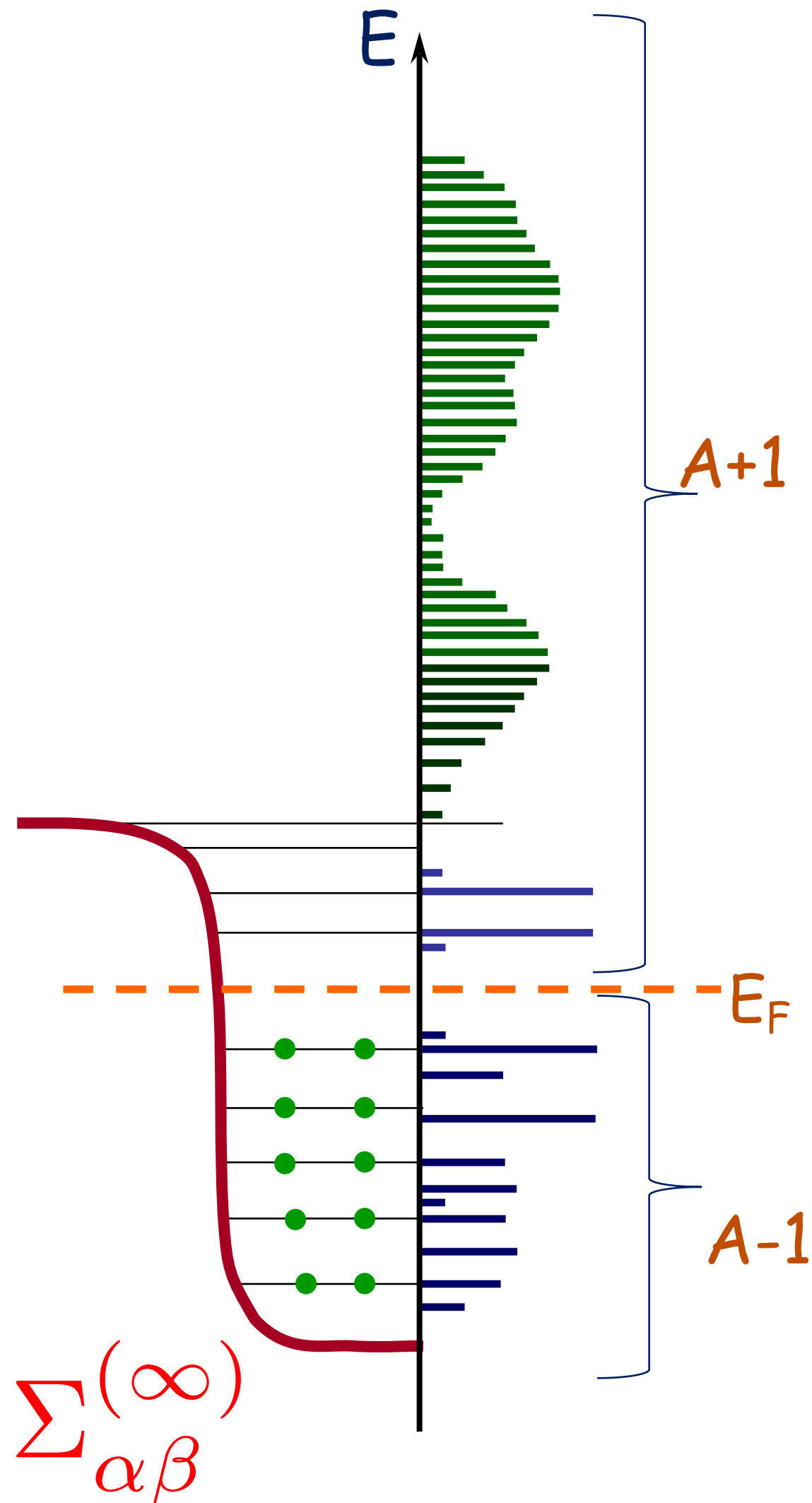
$\Sigma^{(\infty)}_{\alpha\beta}$

E

A+1

E_F

A-1

[A. Idini, CB, Navratil,
Phys. Rev. Lett. **123**, 092501 (2019)]

Benchmark with NCSM-based scattering.

Scattering from mean-field only:

- - - - - - NCSM/RGM [**without** core excitations]

EM500: NN-SRG λ_{SRG}= 2.66 fm^{-1}, Nmax=18 (IT)

[PR**C82**, 034609 (2010)]

NNLOsat: Nmax=8 (IT-NCSM)

———————

SCGF [$\Sigma^{(\infty)}$ only], always Nmax=13

${}^{16}O(n,n')^{16}O$

[A. Idini, CB, Navratil,
Phys. Rev. Lett. **123**, 092501 (2019)]

Benchmark with NCSM-based scattering.

Scattering from mean-field only:
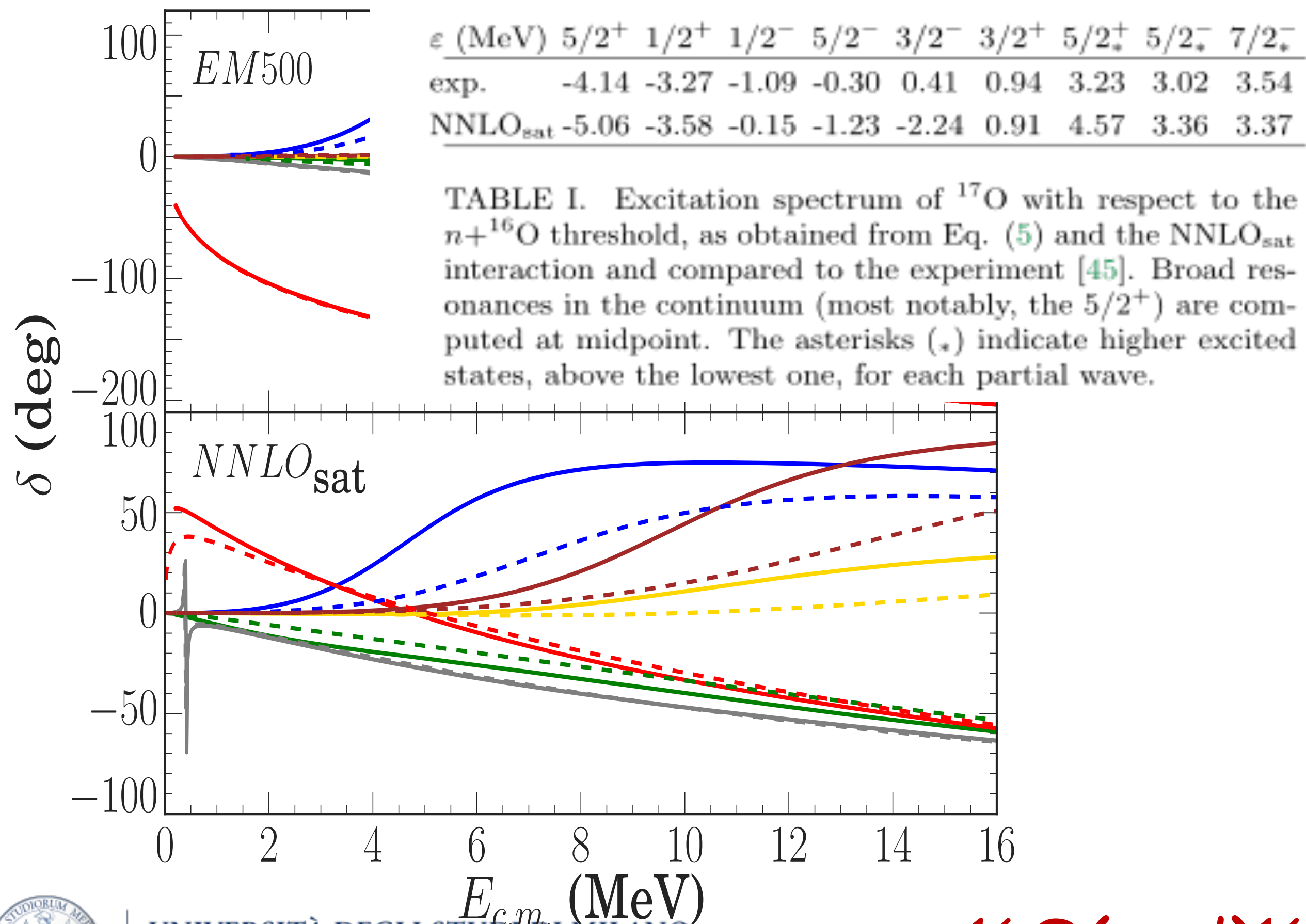
Full self-energy from SCGF:

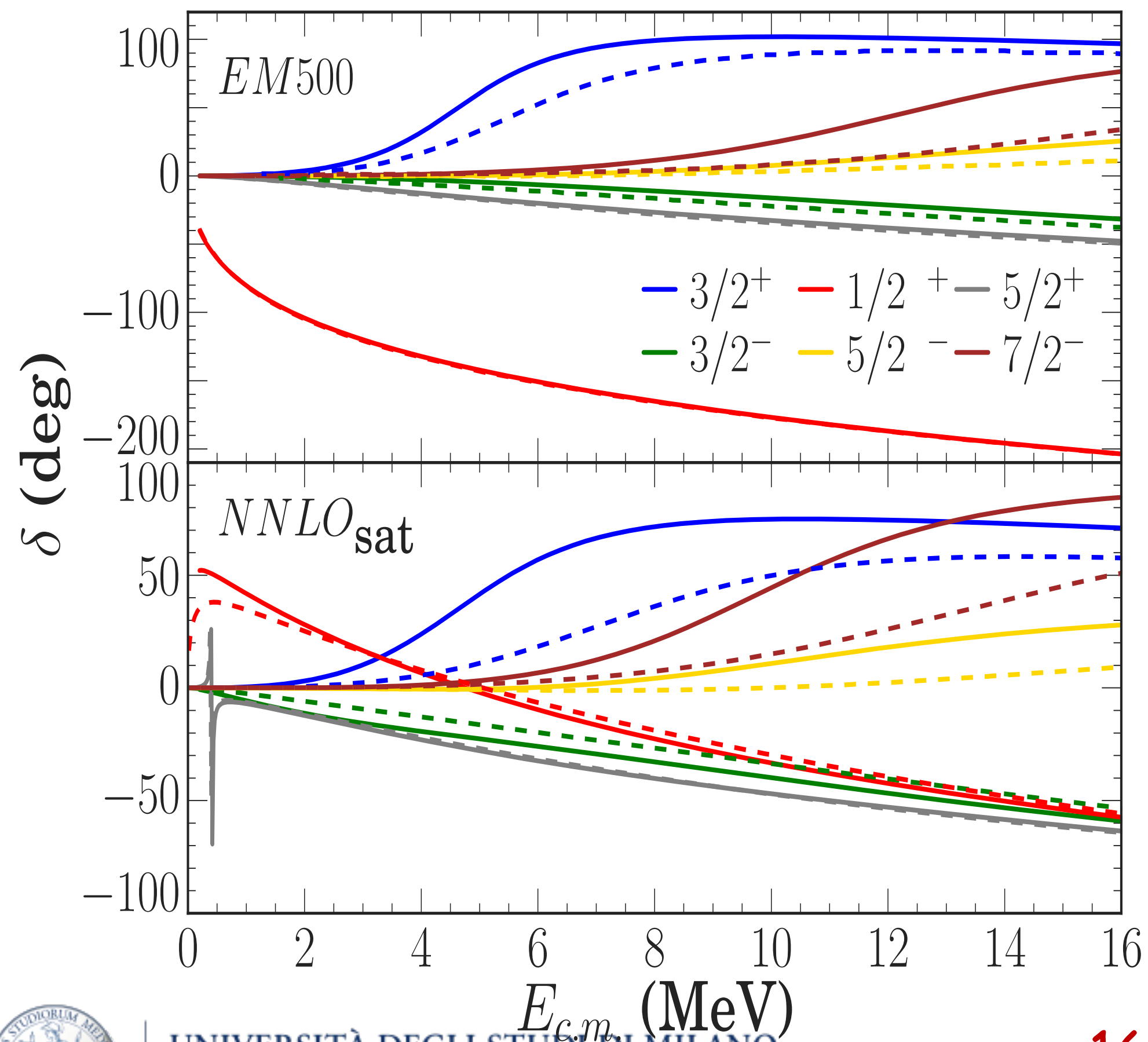ε (MeV) table:

ε (MeV)	$5/2^+$	$1/2^+$	$1/2^-$	$5/2^-$	$3/2^-$	$3/2^+$	$5/2^+_*$	$5/2^-_*$	$7/2^-_*$
exp.	−4.14	−3.27	−1.09	−0.30	0.41	0.94	3.23	3.02	3.54
NNLO$_{sat}$	−5.06	−3.58	−0.15	−1.23	−2.24	0.91	4.57	3.36	3.37

TABLE I. Excitation spectrum of ^{17}O with respect to the $n+^{16}$O threshold, as obtained from Eq. (5) and the NNLO$_{sat}$ interaction and compared to the experiment [45]. Broad resonances in the continuum (most notably, the $5/2^+$) are computed at midpoint. The asterisks ($_*$) indicate higher excited states, above the lowest one, for each partial wave.

$^{16}O(n,n')^{16}O$

Role of intermediate state configurations (ISCs)

n-^{16}O, total elastic cross section

Only $\Sigma_{\alpha\beta}^{(\infty)}$

50% of 2p1h/2h1p poles suppressed

Full $\Sigma_{\alpha\beta}^{\star}(\omega)$ (all ISCs included)

High order configurations, or ADC(n>>3), to be critical for fully ab initio optical potentials

$$\Sigma_{\alpha\beta}^{\star}(\omega) = \Sigma_{\alpha\beta}^{(\infty)} + \sum_{i,j} \mathbf{M}_{\alpha,i}^{\dagger} \left(\frac{1}{E - (\mathbf{K}^{>} + \mathbf{C}) + i\Gamma} \right)_{i,j} \mathbf{M}_{j,\beta} + \sum_{r,s} \mathbf{N}_{\alpha,r} \left(\frac{1}{E - (\mathbf{K}^{<} + \mathbf{D}) - i\Gamma} \right)_{r,s} \mathbf{N}_{s,\beta}^{\dagger}$$

2p1h   2h1p

UNIVERSITÀ DEGLI STUDI DI MILANO
DIPARTIMENTO DI FISICA

INFN
MILANO
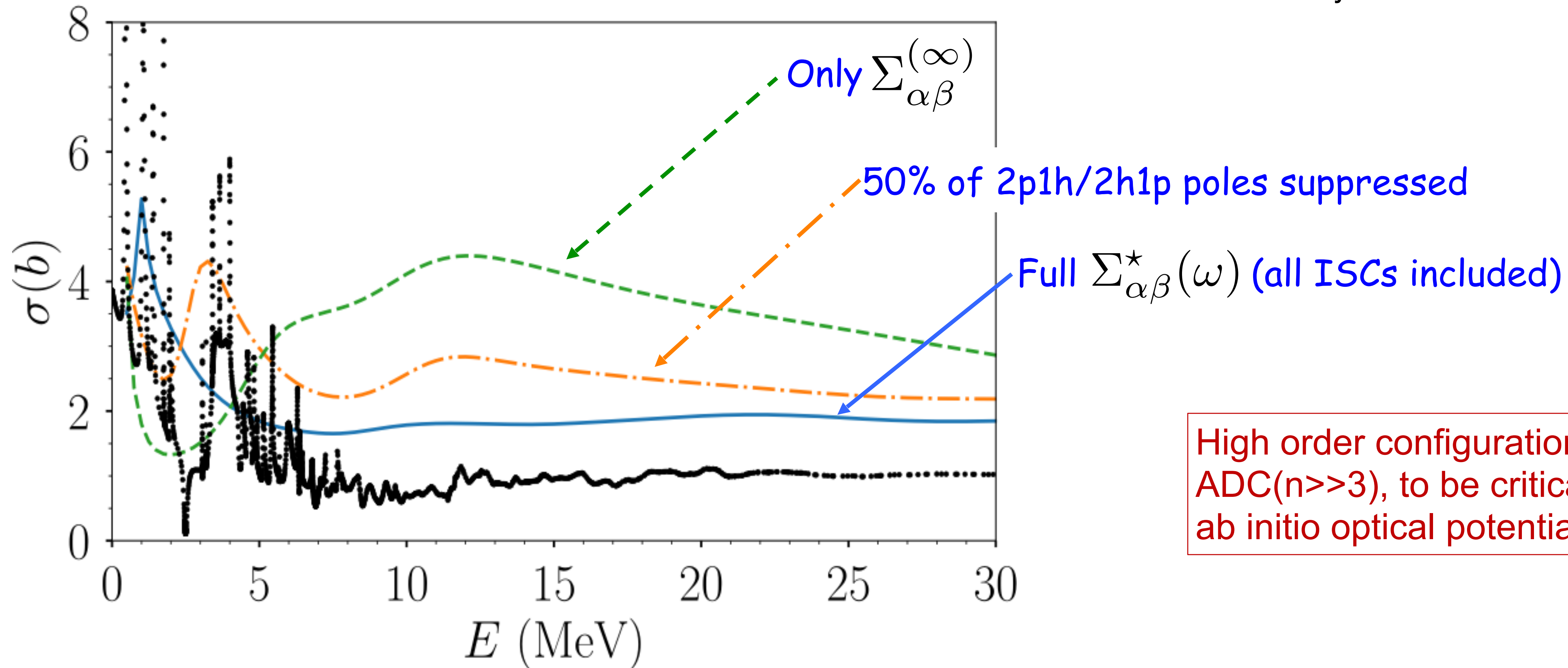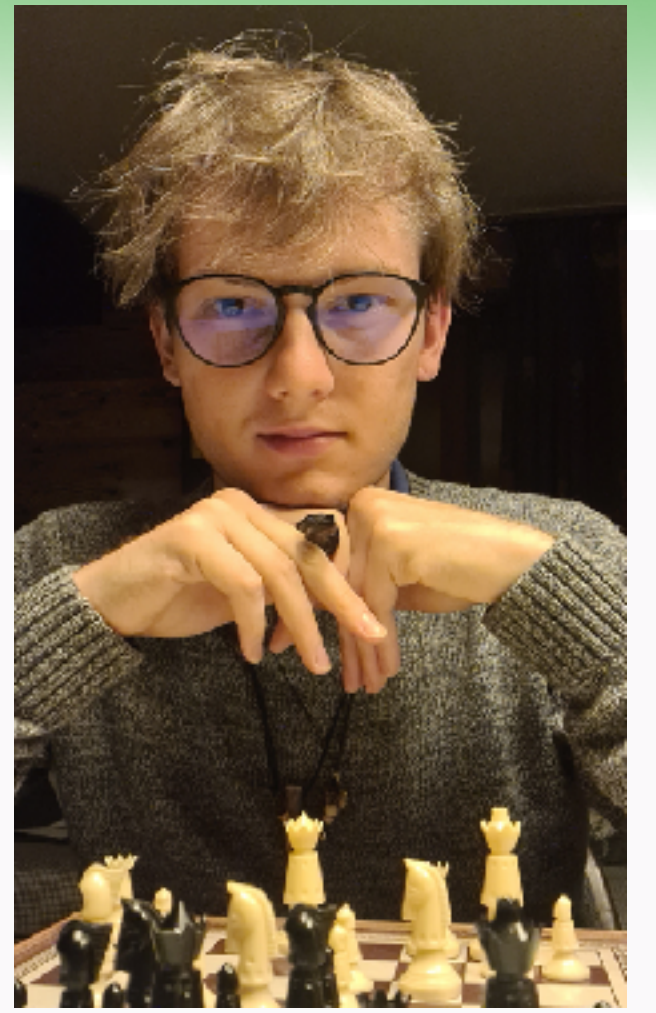
(Toward)
Diagrammatic Monte Carlo (DiagMC)
in finite systems

S. Brolli
(Masters thesis)
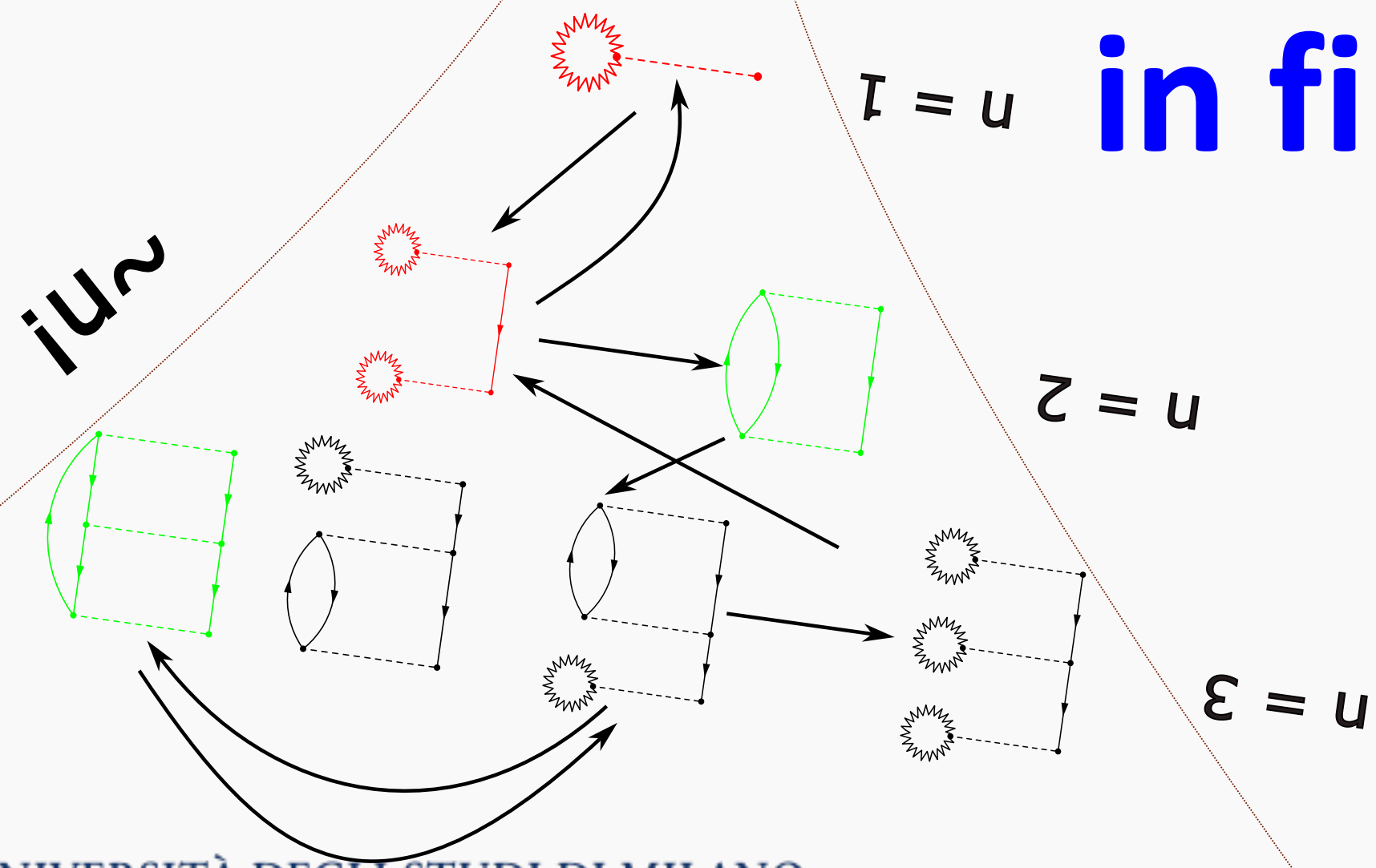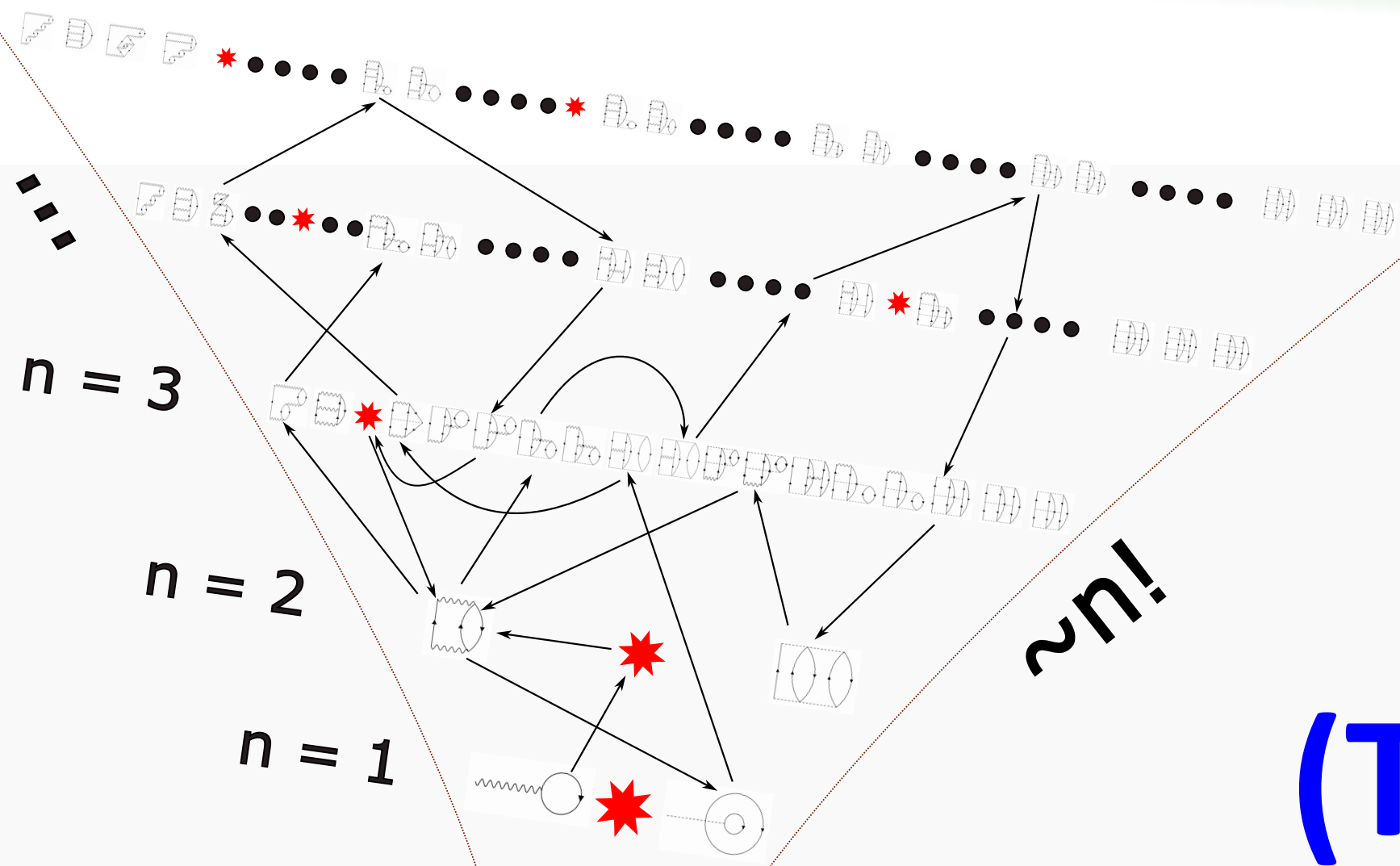
Green's function theory beyond ADC(3)?

The Green's function is found as the exact solution of the Dyson equation:

$$G_{\alpha\beta}(\omega) = G^{(0)}_{\alpha\beta}(\omega) + \sum_{\gamma\delta} G^{(0)}_{\alpha\gamma}(\omega) \Sigma^{\star}_{\gamma\delta}(\omega) G_{\delta\beta}(\omega)$$

It requires knowing the self-energy which is the sum of an *infinite series* of Feynman diagrams:
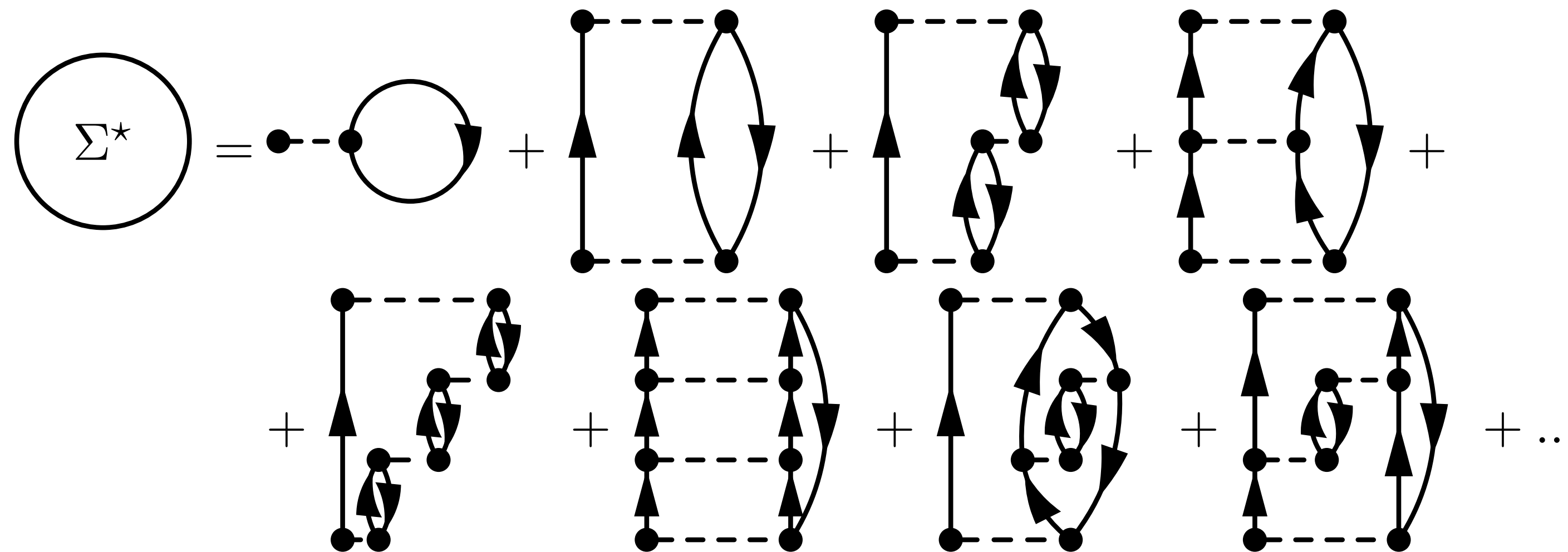
The number of required diagrams explodes (factorially!) with the order of the approximation…

Diagrams grow factorially (more than exponentially) with the order

A direct calculation of all diagrams beyond order three is unfeasible.

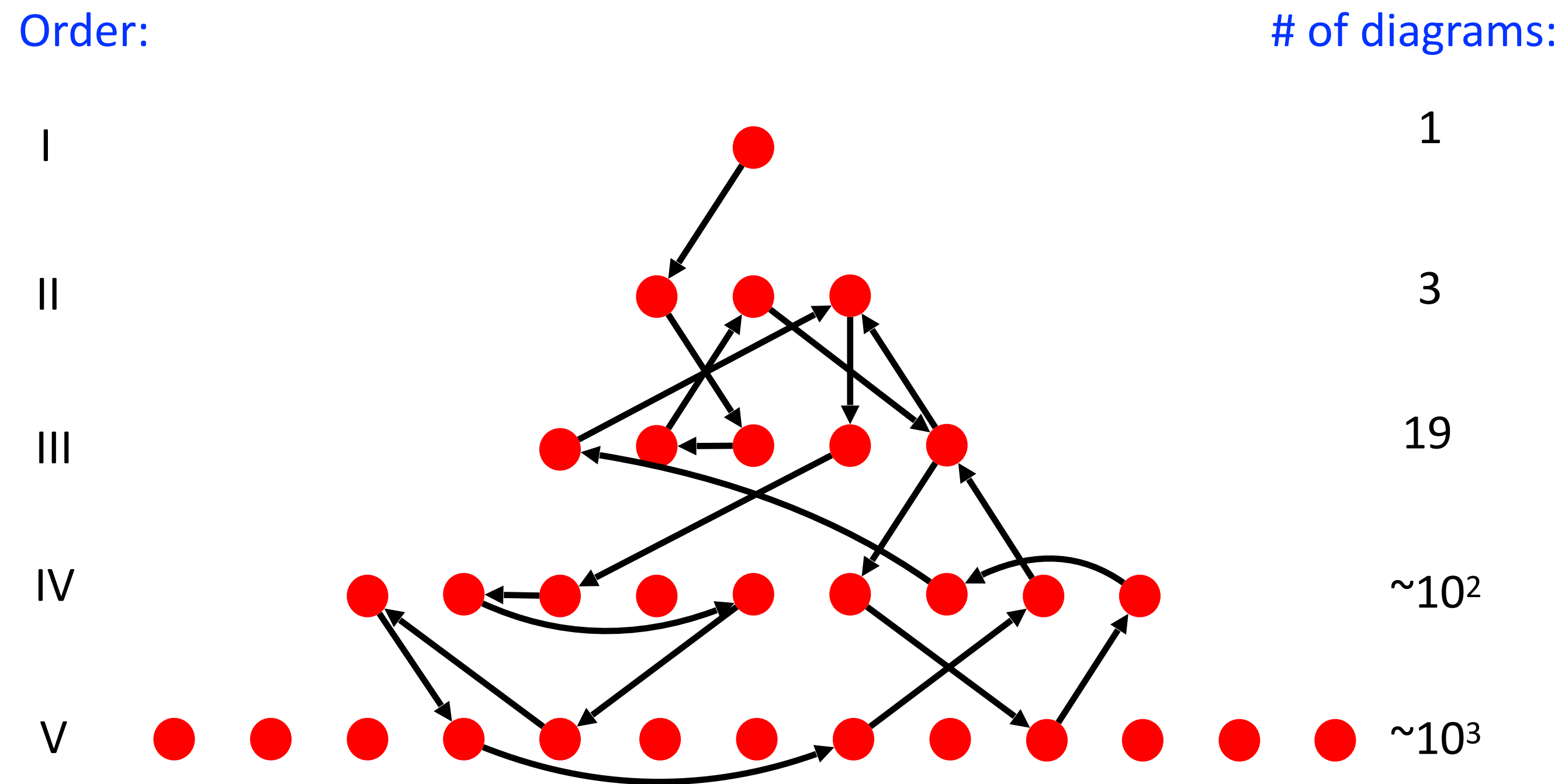Order: # of diagrams:

I   1

II   3

III   19

IV   ~10^2

V   ~10^3

Diagrammatic Monte Carlo (DiagMC) *samples diagrams in their topological space* using a Markov chain.

Diagrammatic Monte Carlo: overview

S. Brolli (Masters thesis)

$$\Sigma^{\star}_{\alpha\beta}(\omega) = \sum_{\mathcal{T}} \sum_{\gamma_1...\gamma_n} \int d\omega_1...d\omega_m \, \mathcal{D}^{\omega}_{\alpha\beta}(\mathcal{T};\gamma_1...\gamma_n;\omega_1...\omega_m) \, 1_{\mathcal{T} \in \mathcal{S}_{\Sigma^{\star}}}$$

We define $\mathcal{C} := (\mathcal{T};\gamma_1...\gamma_n;\omega_1...\omega_m)$

$$\Sigma^{\star}_{\alpha\beta}(\omega) = \int d\mathcal{C} \, |\mathcal{D}^{\omega}_{\alpha\beta}(\mathcal{C})| e^{i\arg[\mathcal{D}^{\omega}_{\alpha\beta}(\mathcal{C})]} 1_{\mathcal{T} \in \mathcal{S}_{\Sigma^{\star}}}$$

$$\Sigma^{\star}_{\alpha\beta}(\omega) = \mathcal{Z}^{\omega}_{\alpha\beta} \int d\mathcal{C} \, \frac{|\mathcal{D}^{\omega}_{\alpha\beta}(\mathcal{C})|W_o(N)}{\mathcal{Z}^{\omega}_{\alpha\beta}} \frac{e^{i\arg[\mathcal{D}^{\omega}_{\alpha\beta}(\mathcal{C})]}}{W_o(N)} 1_{\mathcal{T} \in \mathcal{S}_{\Sigma^{\star}}}$$
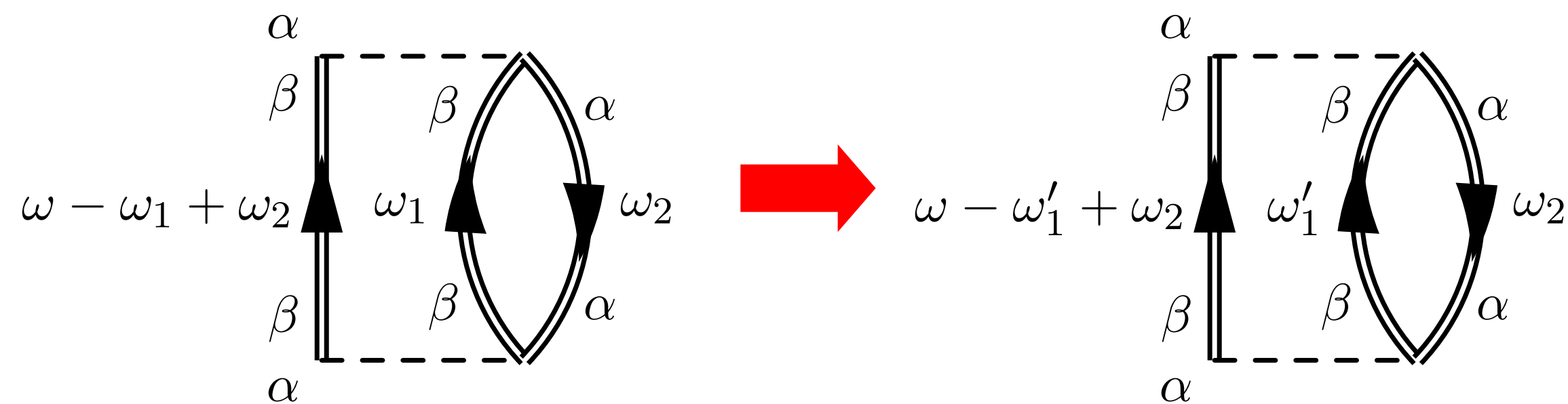
- $W_o(N)$ is an order dependent reweighting factor

- $\mathcal{Z}^{\omega}_{\alpha\beta} = \int d\mathcal{C} \, |\mathcal{D}^{\omega}_{\alpha\beta}(\mathcal{C})|W_o(N)$ is a normalization factor

- $w^{\omega}_{\alpha\beta}(\mathcal{C}) := \frac{|\mathcal{D}^{\omega}_{\alpha\beta}(\mathcal{C})|W_o(N)}{\mathcal{Z}^{\omega}_{\alpha\beta}}$ is a probability distribution function
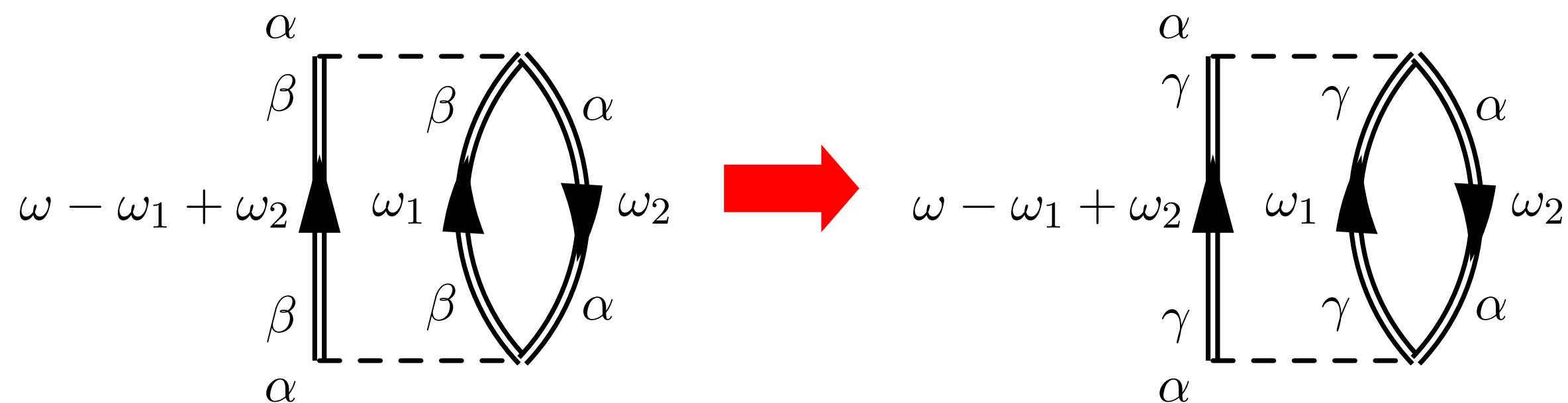
The updates

① *Change Frequency*

② *Change Single-Particle Quantum Numbers*

Standard Monte Carlo

Change Frequency:
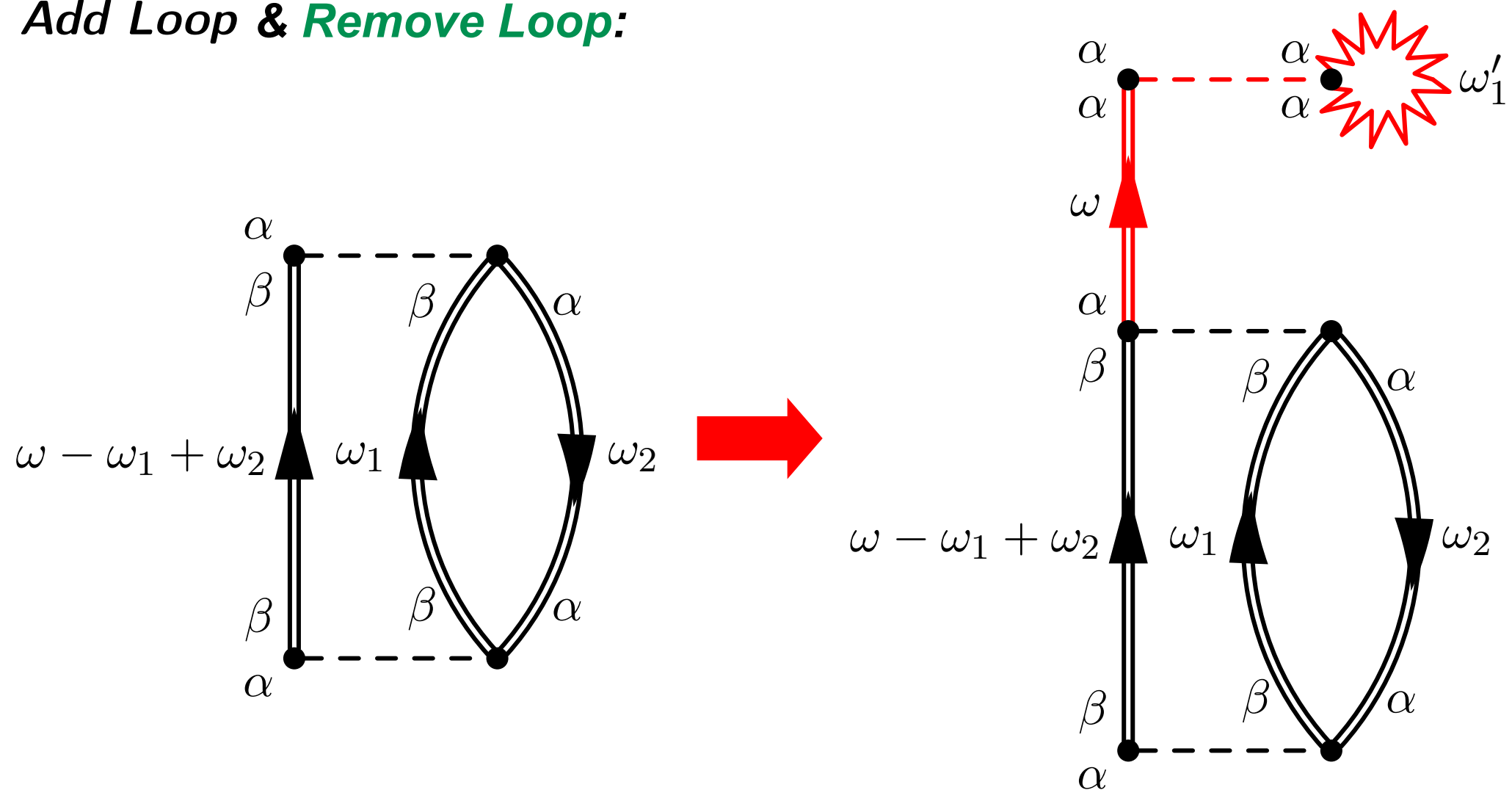

Change Single-Particle Quantum Numbers:

UNIVERSITÀ DEGLI STUDI DI MILANO
DIPARTIMENTO DI FISICA

INFN
MILANO

The updates

③ *Add Loop*

④ *Remove Loop* } Monte Carlo on the topology

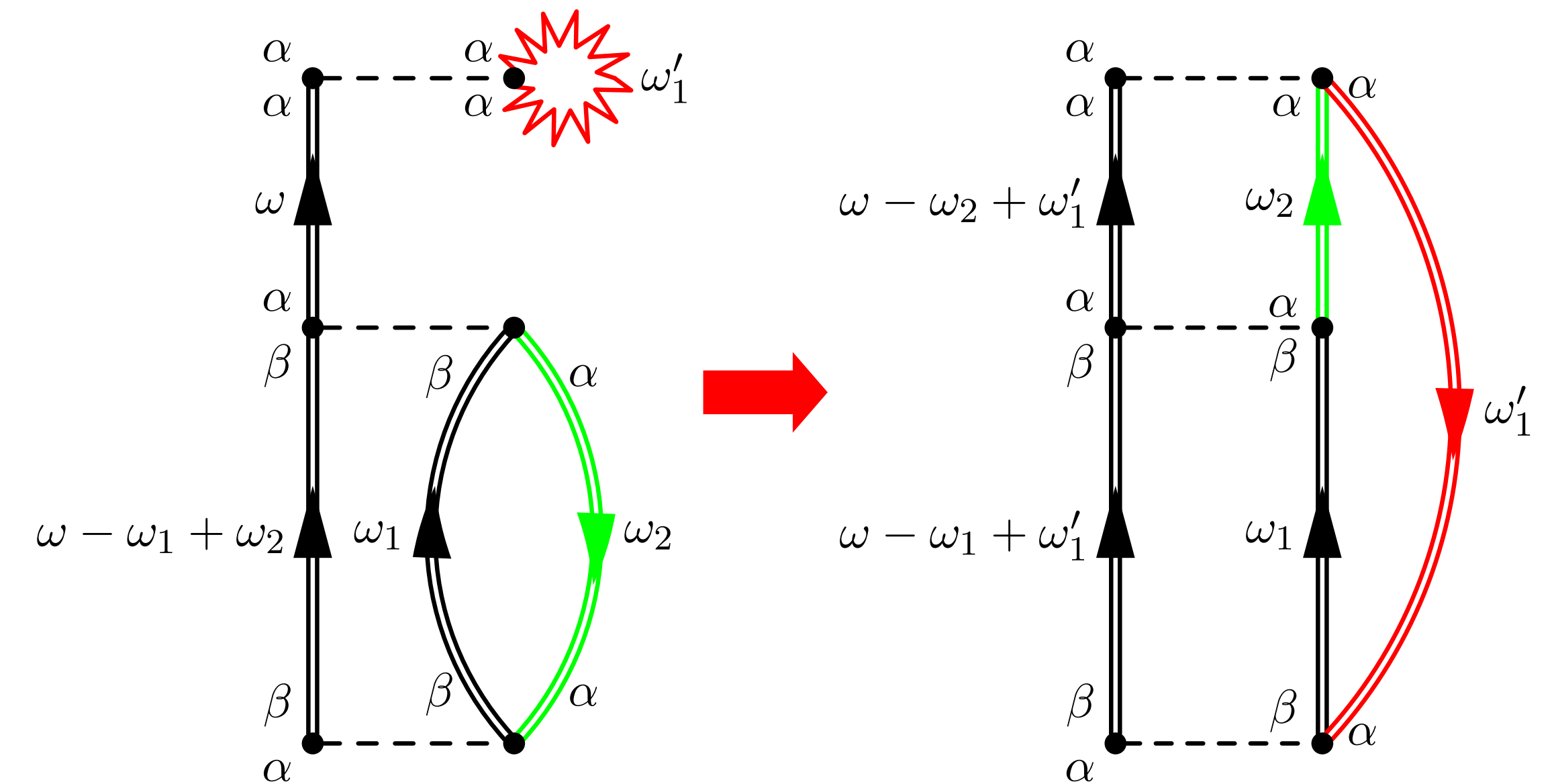⑤ *Reconnect*

S. Brolli (Masters thesis)

Add Loop & Remove Loop:

ω_1' is drawn from the probability distribution $W_f(\omega_1')$.

$$q_{AL} = \frac{|g|}{4\pi} \frac{1}{W_f(\omega_1')} e^{-k\omega_1'^2} |G_\alpha(\omega)| \frac{W_o(3)}{W_o(2)}$$
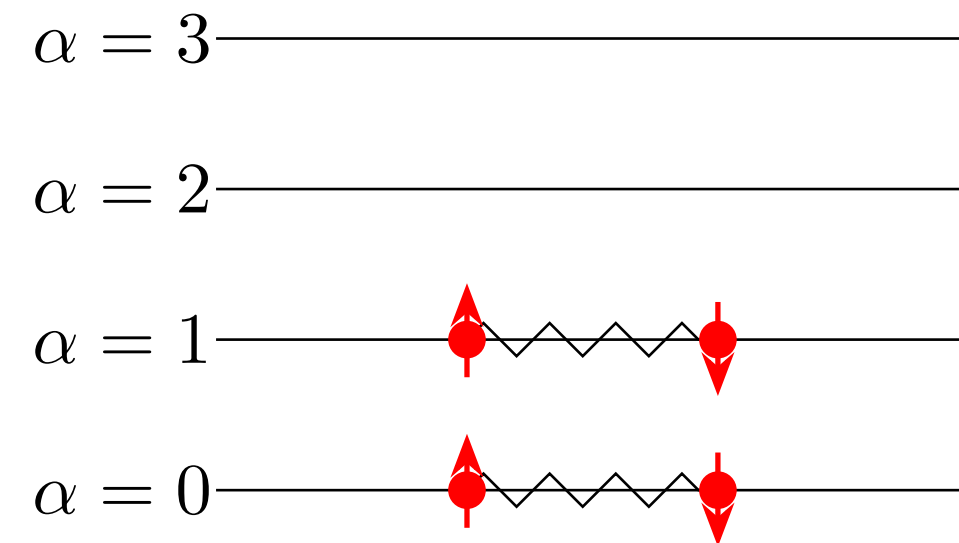
Reconnect:

The unphysical propagators are turned into physical ones when reconnected.

UNIVERSITÀ DEGLI STUDI DI MILANO
DIPARTIMENTO DI FISICA

INFN
MILANO

Richardson pairing model with D states, half filled:

$$H = \xi \sum_{\alpha=0}^{D-1} \sum_{\sigma=+,-} \alpha c_{\alpha\sigma}^{\dagger} c_{\alpha\sigma} \; - \; \frac{g}{2} \sum_{\alpha,\beta=0}^{D-1} c_{\alpha+}^{\dagger} c_{\alpha-}^{\dagger} c_{\beta-} c_{\beta+}$$

$\alpha = 3$ ————————————

$\alpha = 2$ ————————————

$\alpha = 1$ ——————⟋⟍⟋⟍——————

$\alpha = 0$ ——————⟋⟍⟋⟍——————

$$\Sigma_{\alpha\beta}^{\star}(\omega) = \Sigma_{\alpha\beta}^{(\infty)} + \sum_{i,j} \mathbf{M}_{\alpha,i}^{\dagger} \left(\frac{1}{E - (\mathbf{K}^{>} + \mathbf{C}) + i\Gamma} \right)_{i,j} \mathbf{M}_{j,\beta}$$

$$+ \sum_{r,s} \mathbf{N}_{\alpha,r} \left(\frac{1}{E - (\mathbf{K}^{<} + \mathbf{D}) - i\Gamma} \right)_{r,s} \mathbf{N}_{s,\beta}^{\dagger}$$
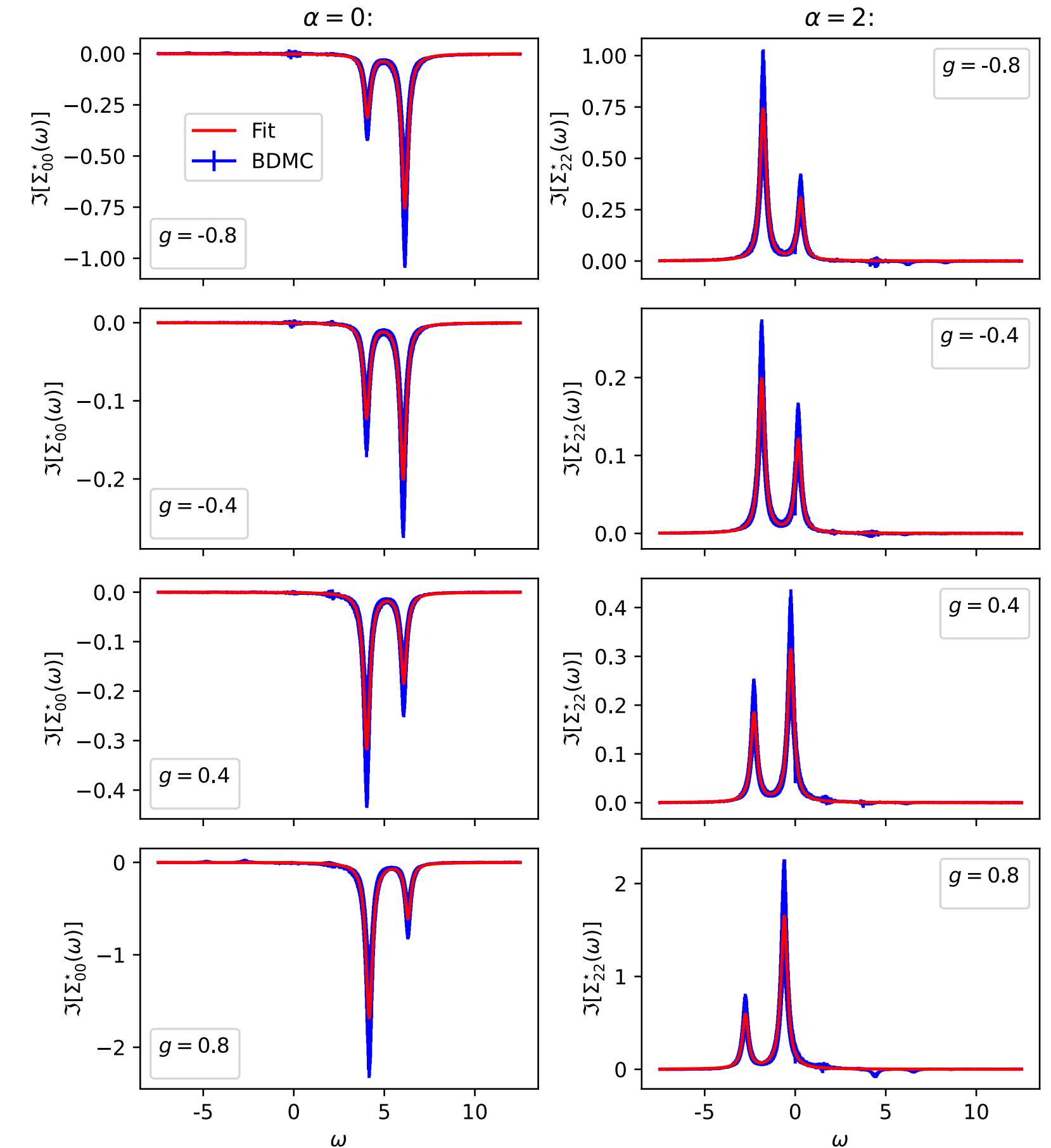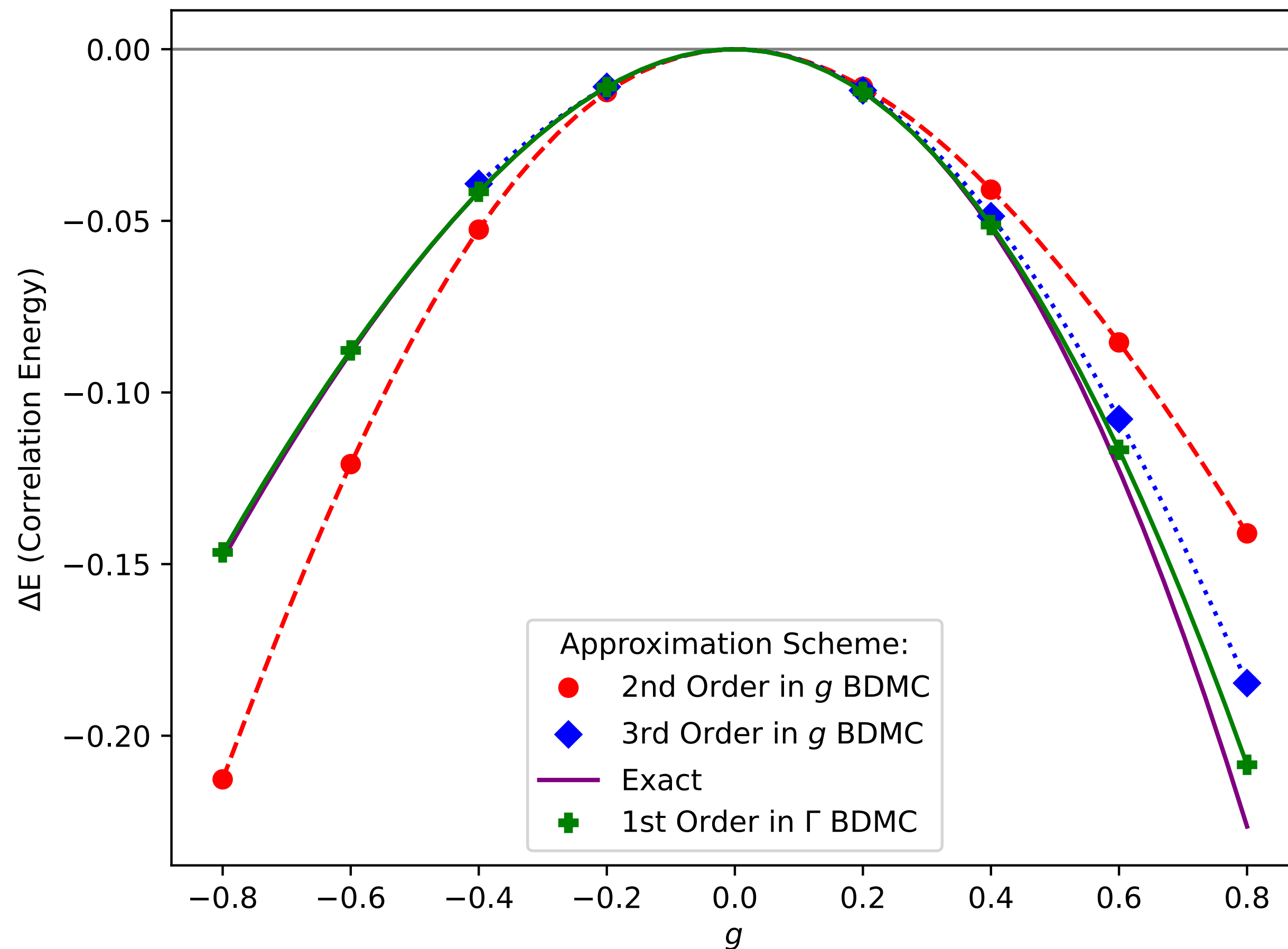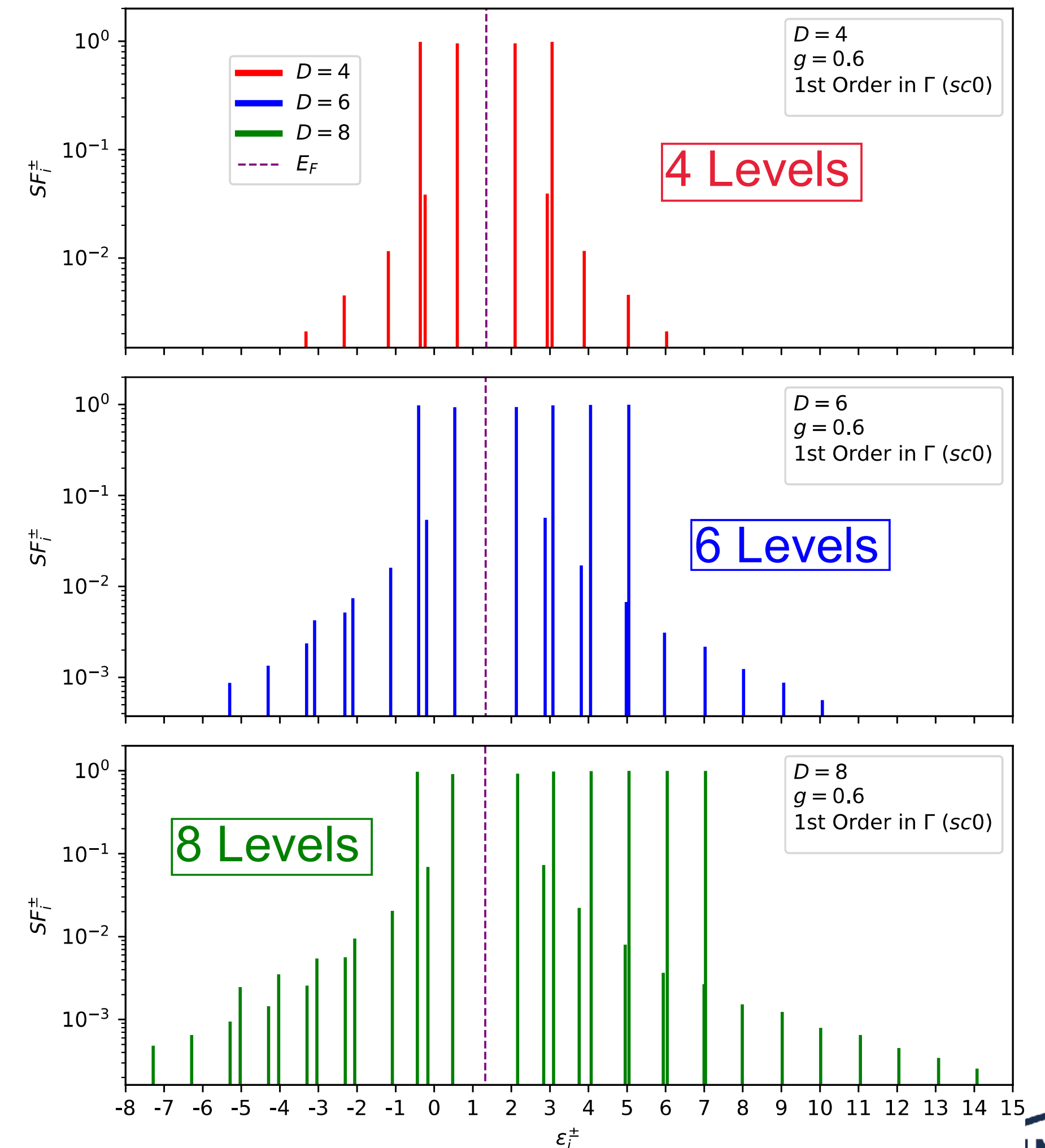

Figure 4.1: Components $\alpha = 0$ and $\alpha = 2$ of the imaginary part of the self-energy for different values of the coupling g. The blue line is the results obtained with the BDMC simulation, while the red line is the best fit as a sum of two Lorentzians. The results for the two values of $\alpha = 0, 2$ are displayed respectively on the left and on the right of the graph. The error bars are calculated as explained in the main text.

UNIVERSITÀ DEGLI STUDI DI MILANO

DIPARTIMENTO DI FISICA

INFN
MILANO

Reorganization in terms of ladders (Γ)

Correlation energy $\Delta E = E - E_{HF}$ as a function of interaction strength (g):

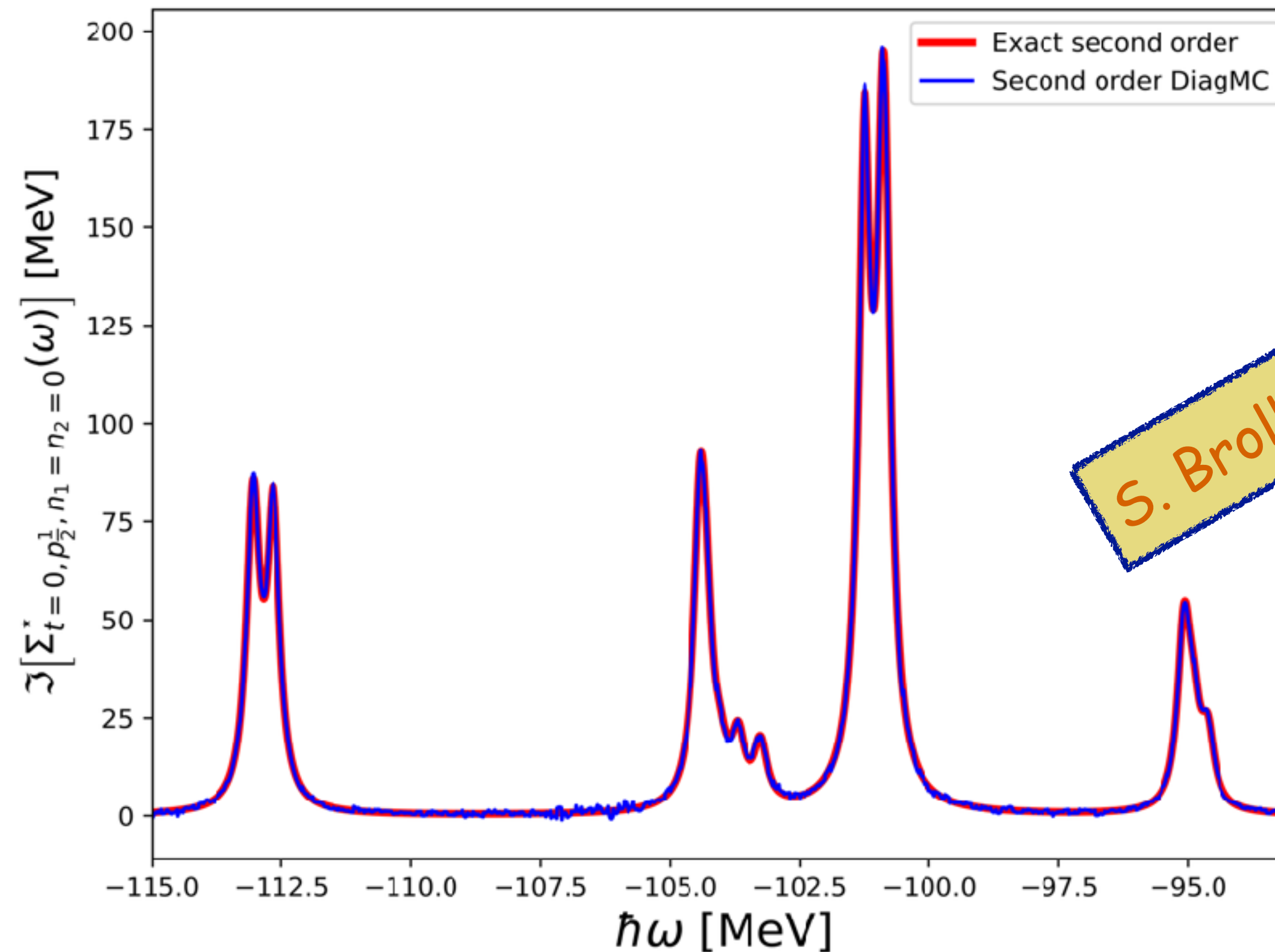Spectroscopic function for different dimensions of the model space (D):

S. Brolli, CB, Vigezzi, in preparation

Approximation Scheme:

- ●   2nd Order in g BDMC
- ◆   3rd Order in g BDMC
- ——   Exact
- ✚   1st Order in Γ BDMC

DiagMC is being extended to treat realistic microscopic nuclear Hamiltonians.

Example of DiagMC neutron $p_{1/2}$ self-energy partial wave at 2nd order in harmonic oscillator space

with dimension N_{max}= max $\{2n+l\}$=2 in ^{16}O.

Imaginary part of the

neutron p $_{1/2}$ hole

self-energy in ^{16}O.

S. Brolli & CB — very preliminary !!!

UNIVERSITÀ DEGLI STUDI DI MILANO

DIPARTIMENTO DI FISICA

INFN
MILANO

Summary

→ HAL QCD share characteristic with low energy EFT interactions — though they are different.

→ HAL QCD forces allow studying (un)physical quark masses and improve in Y-N description.

→ SCGF Gorkov/ADC(3) computations with ChEFT — reliable and evolving to large masses

→ Occurrence of a charge bubble in 46Ar (second case "known")

→ Diagrammatic Monte Carlo is a promising method to go forward on high precision simulations.

And thanks to my collaborators (over the years...):

G. Colò, E. Vigezzi, **S. Brolli**

M. Vorabbi, **P. Arthuis**

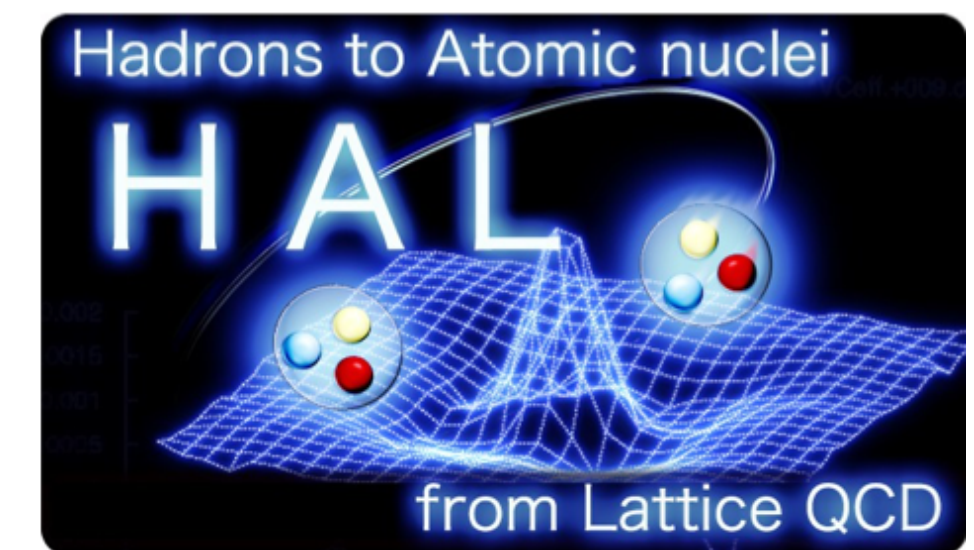V. Somà, T. Duguet, **A. Scalesi**

P. Navrártil

C. Giusti, P. Finelli

A. Idini

UNIVERSITÀ DEGLI STUDI DI MILANO

DIPARTIMENTO DI FISICA

Backup slides

SCGF computations of infinite matter

F. Marino (PhD Thesis)

Nuclear Density Functional from Ab Initio Theory

Nuclear energy density functionals grounded in *ab initio* calculations

F. Marino [1,2,*] C. Barbieri [1,2] A. Carbone,[3] G. Colò [1,2] A. Lovato [4,5] F. Pederiva,[6,5] X. Roca-Maza [1,2]
and E. Vigezzi [2]

[1]*Dipartimento di Fisica "Aldo Pontremoli," Università degli Studi di Milano, 20133 Milano, Italy*
[2]*Istituto Nazionale di Fisica Nucleare, Sezione di Milano, 20133 Milano, Italy*
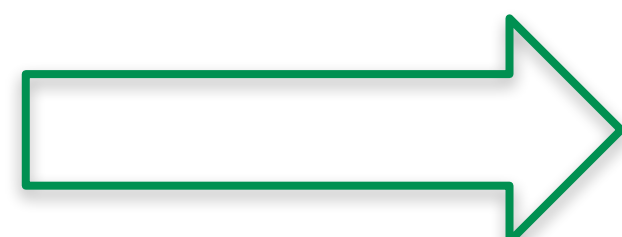[3]*Istituto Nazionale di Fisica Nucleare–CNAF, Viale Carlo Berti Pichat 6/2, 40127 Bologna, Italy*

DFT is in principle exact – but the energy density functional (EDF) is not known

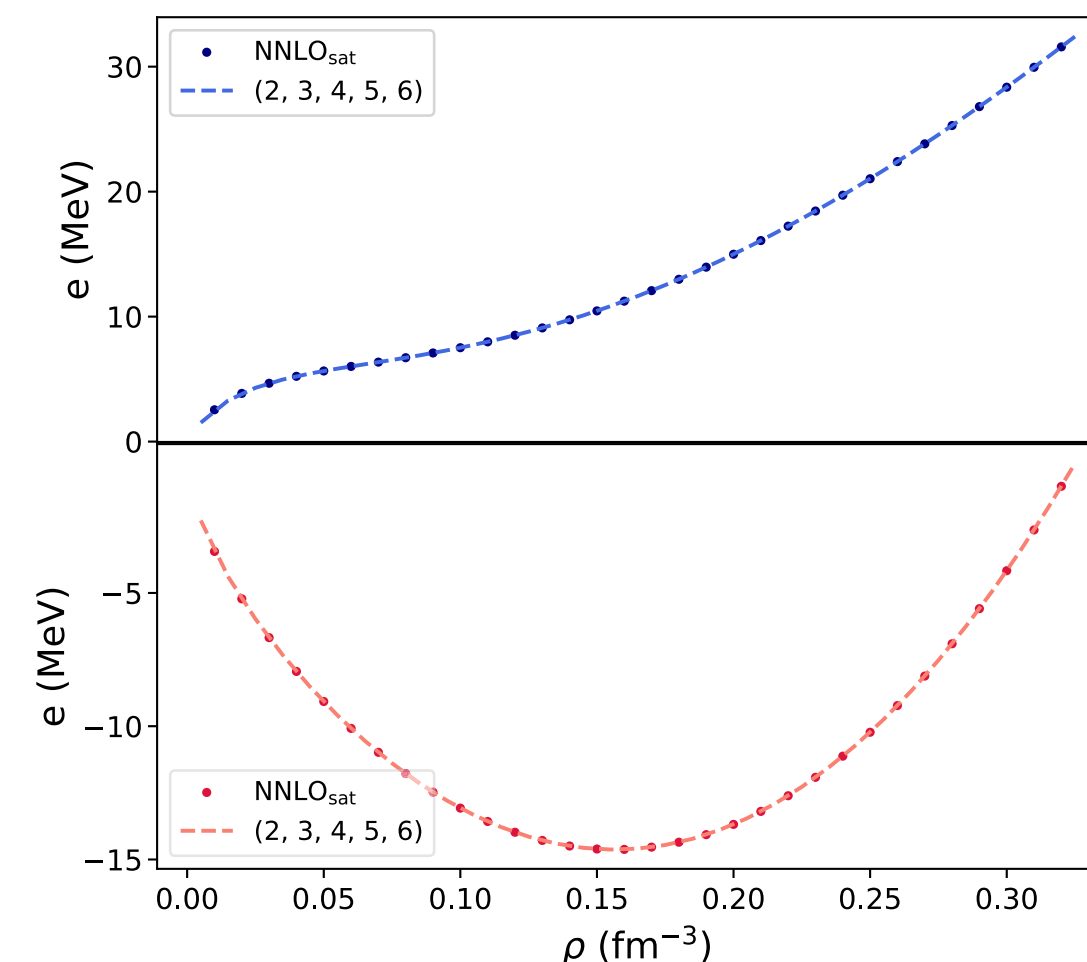For nuclear physics this is even more demanding: need to link the EDF to theories rooted in QCD!

Machine-learn DFT functional on the nuclear equation of state

Jacob's ladder

+ approximate GA

Benchmark in finite systems

$$E = \int d\mathbf{r}\, \mathcal{E}(\mathbf{r}) = E_{\text{kin}} + E_{\text{pot}} + E_{\text{Coul}}$$

$$E_{\text{GA}} = E_{\text{LDA}} + E_{\text{surf}}$$

$$E_{\text{surf}} = \int d\mathbf{r} \left[\sum_{t=0,1} C_t^\Delta \rho_t \Delta \rho_t \right.$$
$$\left. - \frac{W_0}{2} \left(\rho \nabla \cdot \mathbf{J} + \sum_q \rho_q \nabla \cdot \mathbf{J}_q \right) \right]$$

UNIVERSITÀ DEGLI STUDI DI MILANO
DIPARTIMENTO DI FISICA

INFN
MILANO

*Machine-learn DFT functional
on the nuclear equation of state*

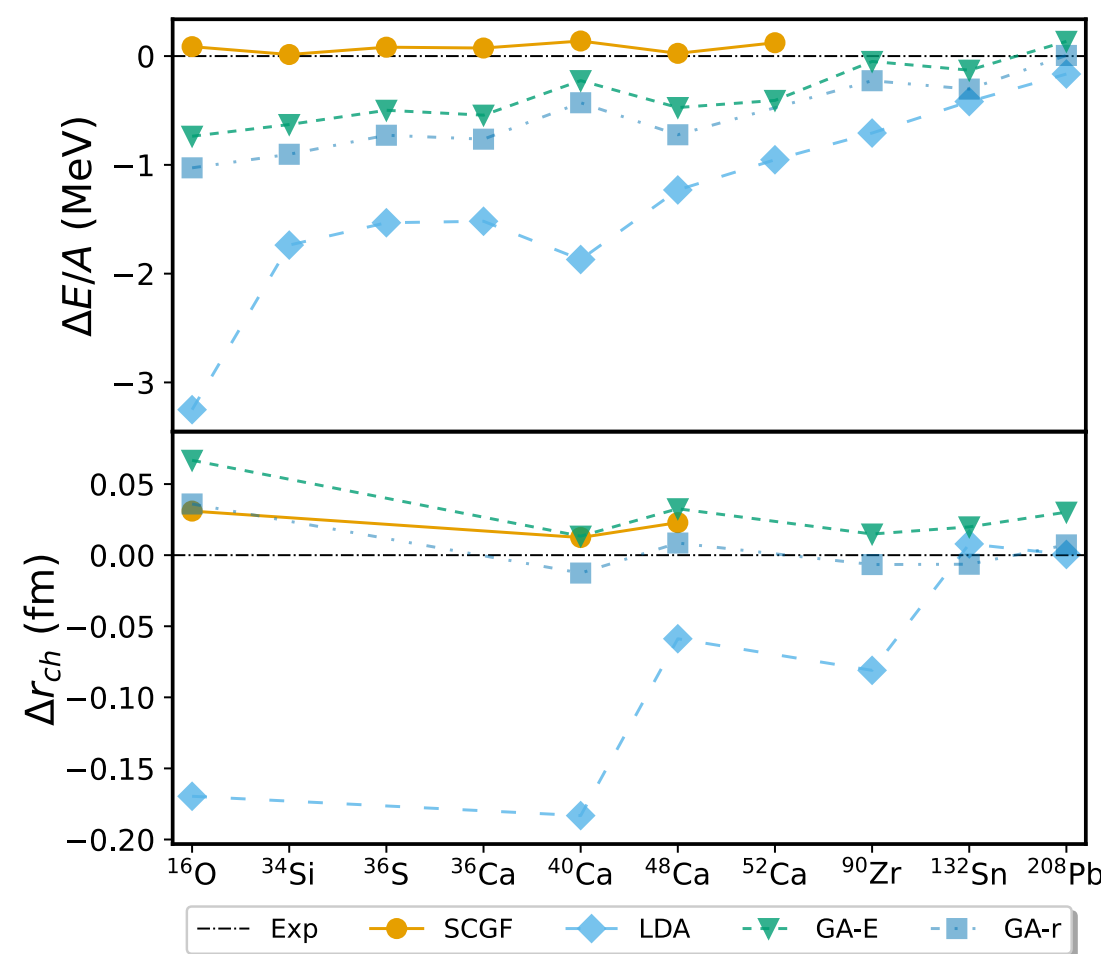*Jacob's ladder*
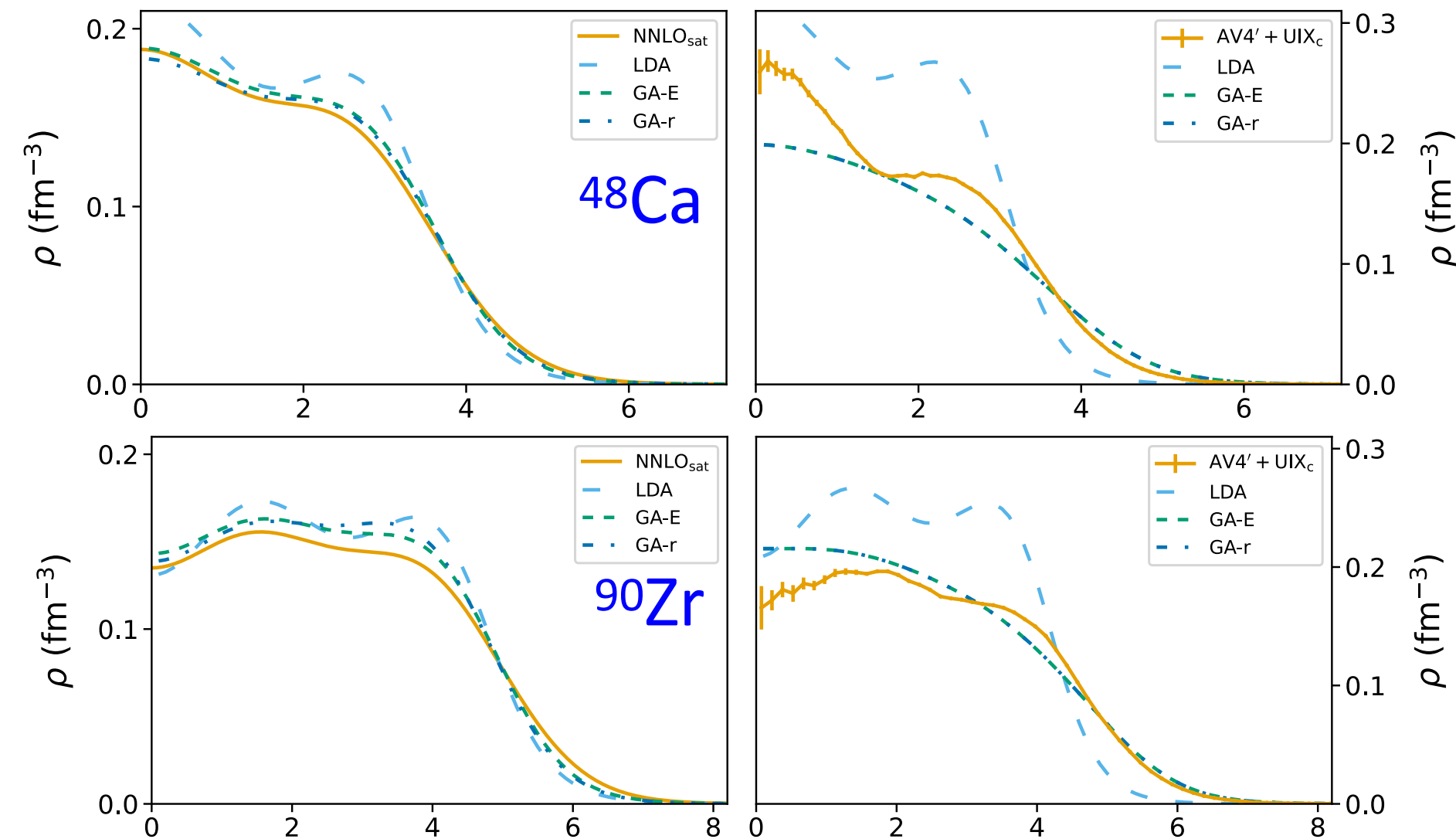
→

+ approximate GA

<u>Benchmark</u> in finite systems

Gradient terms are important (but they seem to work!):

SCGF/NNLO-sat :

AFDMC/AV4' :

^{48}Ca

^{90}Zr

Need to extract gradient information from non-uniform matter

—>

External (monocromatic) perturbation:

$$v(\mathbf{x}) = v_q e^{i\mathbf{q}\cdot\mathbf{x}} + c.c. = 2v_q \cos(\mathbf{q}\cdot\mathbf{x})$$

$$\delta\rho(\mathbf{x}) = 2\rho_q \cos(\mathbf{q}\cdot\mathbf{x})$$

UNIVERSITÀ DEGLI STUDI DI MILANO
DIPARTIMENTO DI FISICA

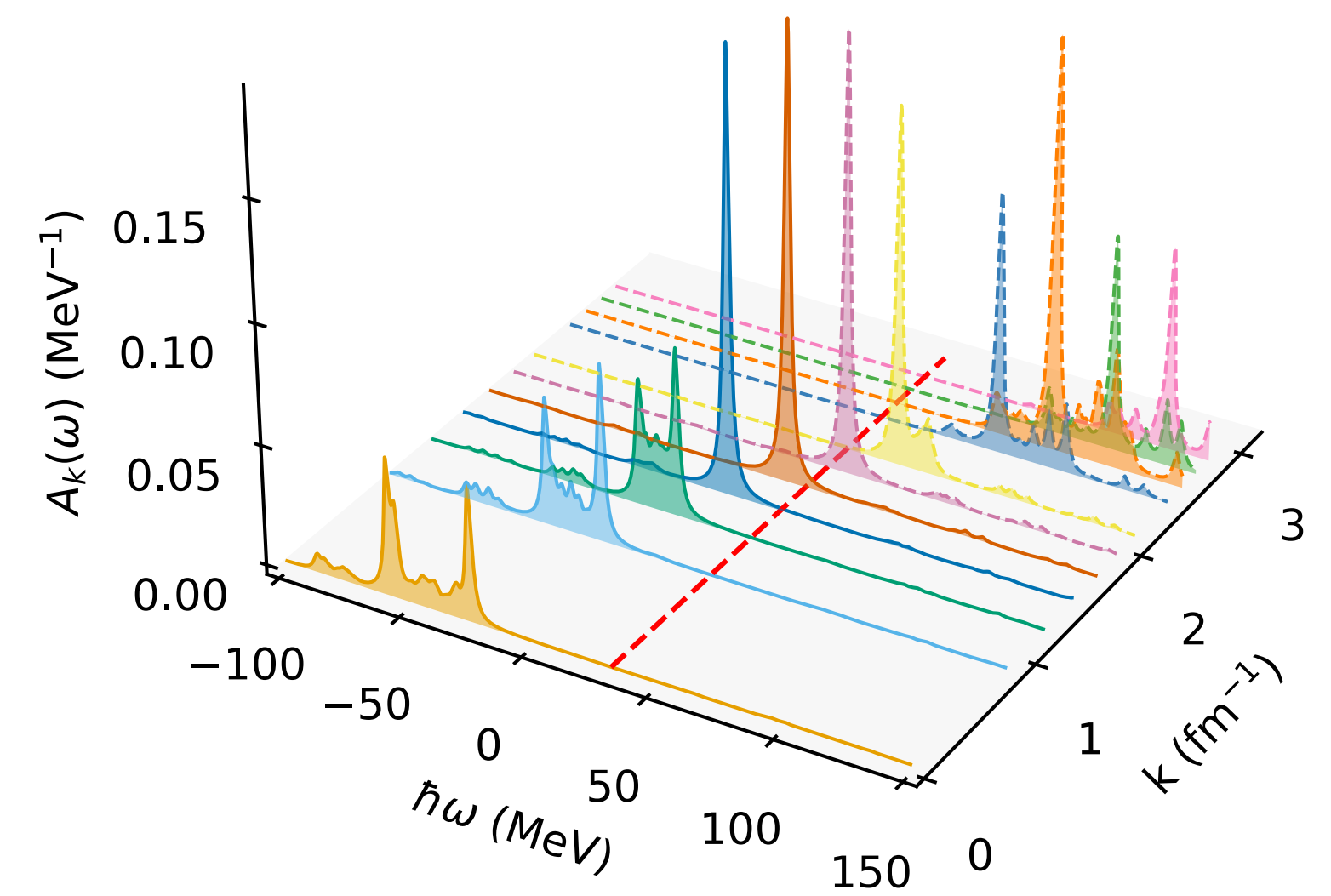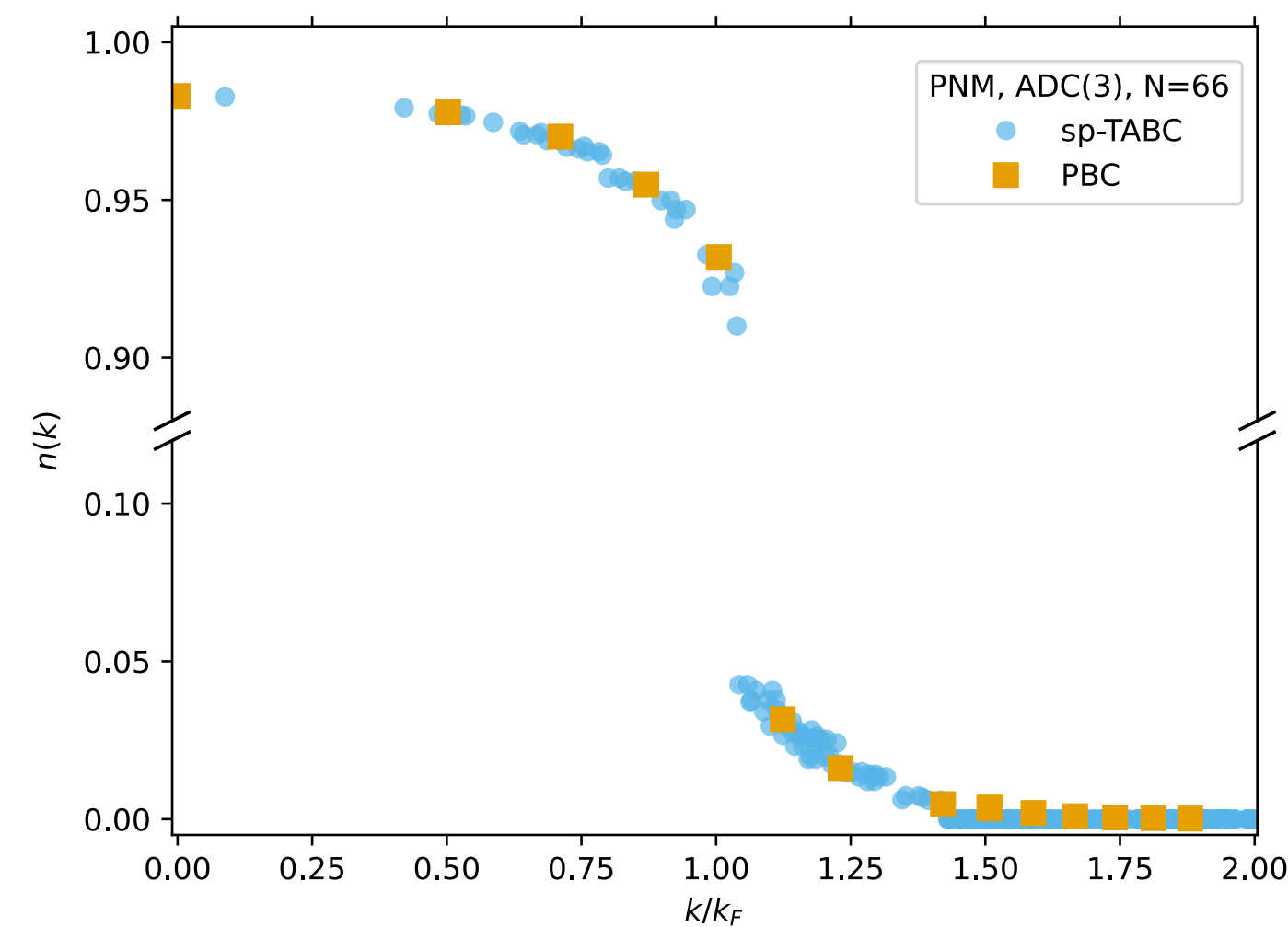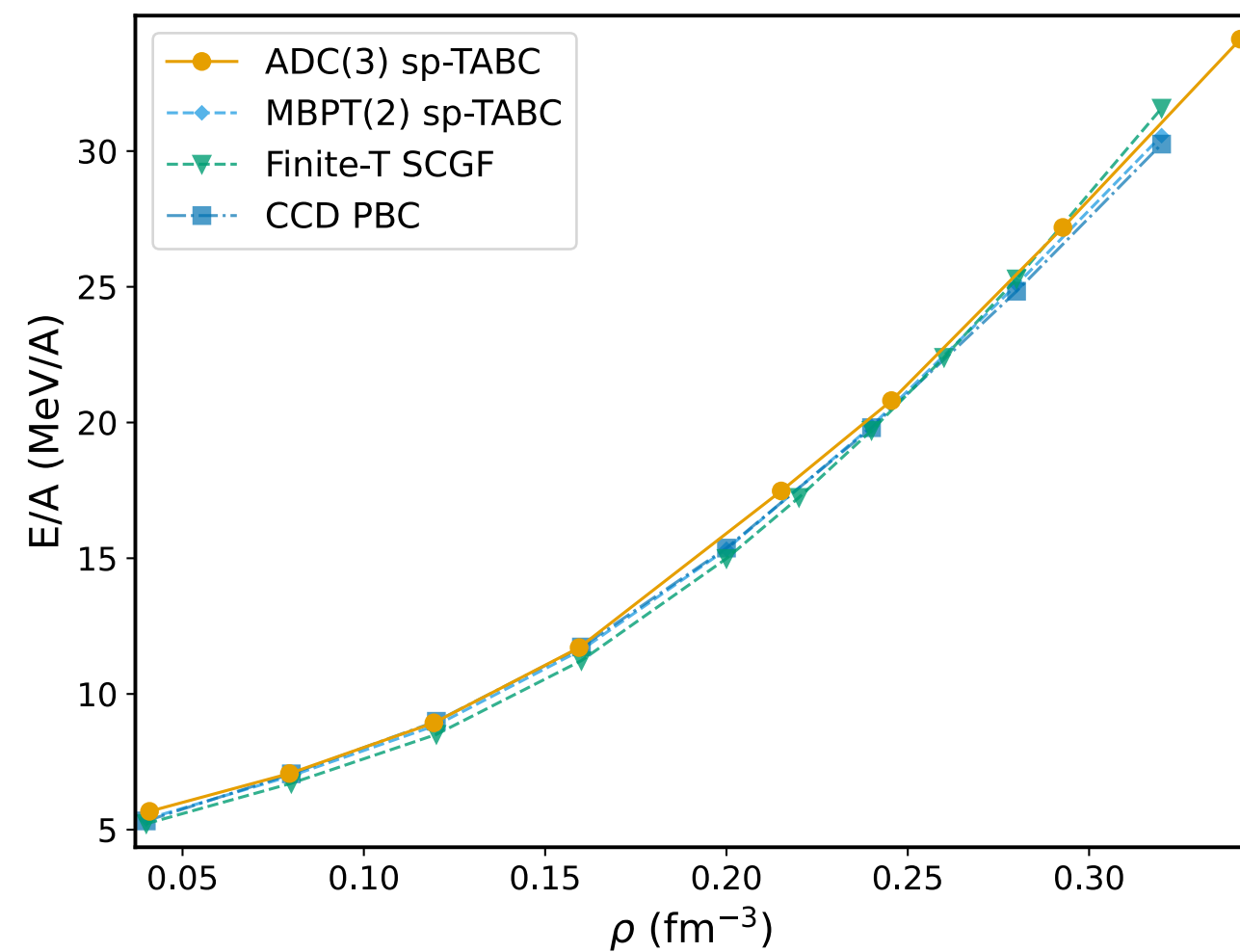INFN MILANO

ADC(3) computations for infinite matter

Finite size box (of length L) with periodic boundary conditions:

$$\rho = \frac{A}{L^3} \qquad p_F = \sqrt[3]{\frac{6\pi^2 \rho}{v_d}}$$

$$\phi(x+L, y, z) = \phi(x, y, z)$$

$$\cdots$$

A=66,   2+3 NF (NNLOsat)

$$\widehat{H} = \sum_{\alpha} \varepsilon_{\alpha}^0 \, a_{\alpha}^{\dagger} a_{\alpha} - \sum_{\alpha\beta} U_{\alpha\beta} \, a_{\alpha}^{\dagger} a_{\beta} + \frac{1}{4} \sum_{\substack{\alpha\gamma \\ \beta\delta}} V_{\alpha\gamma,\beta\delta} \, a_{\alpha}^{\dagger} a_{\gamma}^{\dagger} a_{\delta} a_{\beta} + \frac{1}{36} \sum_{\substack{\alpha\gamma\epsilon \\ \beta\delta\eta}} W_{\alpha\gamma\epsilon,\beta\delta\eta} \, a_{\alpha}^{\dagger} a_{\gamma}^{\dagger} a_{\epsilon}^{\dagger} a_{\eta} a_{\delta} a_{\beta} \, .$$

ADC(3) self energy:

$$\Sigma_{\alpha\beta}^{(\star)}(\omega) = -U_{\alpha\beta} \; + \; \Sigma_{\alpha\beta}^{(\infty)} \; + \; M_{\alpha,r}^{\dagger} \left[\frac{1}{\omega - [E^> + C]_{r,r'} + i\eta} \right]_{r,r'} M_{r',\beta}$$

$$+ N_{\alpha,s} \left[\frac{1}{\omega - (E^< + D) - i\eta} \right]_{s,s'} N_{s',\beta}^{\dagger}$$

F. Marino, CB et al., **in preparation**